MASTER'S THESIS ASSIGNMENT

I. Personal and study details

Student's name:	**Szekely Jakub**	Personal ID number:	**473522**
Faculty / Institute:	**Faculty of Mechanical Engineering**		
Department / Institute:	**Department of Aerospace Engineering**		
Study program:	**Aerospace Engineering**		
Specialisation:	**Aircraft and UASs**		

II. Master's thesis details

Master's thesis title in English:

A fixed-wing UAV design

Master's thesis title in Czech:

Návrh bezpilotního prostředku s pevným křídlem

Guidelines:

Bibliography / sources:

Dle pokynů vedoucího

Name and workplace of master's thesis supervisor:

Ing. Jiří Brabec, Ph.D. Department of Aerospace Engineering FME

Name and workplace of second master's thesis supervisor or consultant:

Date of master's thesis assignment: **26.04.2024** Deadline for master's thesis submission: **24.05.2024**

Assignment valid until: ______________

Ing. Jiří Brabec, Ph.D. Supervisor's signature	Ing. Milan Dvořák, Ph.D. Head of department's signature	doc. Ing. Miroslav Španiel, CSc. Dean's signature

III. Assignment receipt

The student acknowledges that the master's thesis is an individual work. The student must produce his thesis without the assistance of others, with the exception of provided consultations. Within the master's thesis, the author must state the names of consultants and include a list of references.

.

Date of assignment receipt — Student's signature

Master's thesis

FIXED-WING UAV DESIGN

Bc. Jakub Szekely

Faculty of Mechanical Engineering
Department of Aerospace engineering
Supervisor: Ing. Jiří Brabec, Ph.D.
May 24, 2024

Citation of this thesis: Szekely Jakub. *Fixed-wing UAV design.* Master's thesis. Czech Technical University in Prague, Faculty of Mechanical Engineering, 2024.

Contents

List of Figures

List of Tables

I would like to first and foremost thank my mother for her immense support during my studies and also my supervisor for the amount of time and effort he was willing to give me.

Declaration

I declare that I have prepared my thesis independently under the supervision of my thesis supervisor and that I have listed all information sources used.

In Prague on May 24, 2024

Abstract

This thesis explores possibility of replacing smaller industry multi-copters by fixed wing drones motivated by higher endurance. First exploring the users needs and requirements for such drone. Estimating probable weight and performance and creating concepts with aims on STOL and VTOL propulsion. In the end creating preliminary design of the best suited concept with performance calculations.

Keywords UAS, VTOL, STOL, endurance, drone, fixed wing

Abstrakt

Tato diplomová práce se zabývá možností nahradit menší průmyslové multikoptéry drony s pevným křídlem s cílem zvýšení výdrže. Nejdříve byly specifikovány nároky na navrhovaný dron. Na jejich základech vznikly první odhady rozměrů a první koncepty s důrazem na STOL a VTOL. Na základě vybraného konceptu vznikl i předběžný návrh s výpočty výkonů.

Klíčová slova UAS, VTOL, STOL, výdrž, dron, pevné křídlo

List of abbreviations

A_H	Horizontal stabiliser volume coefficient
A_V	Vertical stabiliser volume coefficient
s	Wing Area
s_h	Horizontal Stabiliser Area
s_v	Vertical Stabiliser Area
b_r	Chord length at wing root
b_t	Chord length of wing tip
b_{MAC}	Chord length of Mean Aerodynamic Chord
l	Wing Span
l_h	Arm between wing and horizontal stabiliser (b_{MAC} quarter points)
l_H	Horizontal stabiliser span
l_v	Span/height of Vertical Stabiliser
C_l	Coefficient of lift of an airfoil
C_{l_α}	Lift slope usually in [1/rad]
C_L	Coefficient of lift of a wing
C_d	Coefficient of drag of an airfoil
C_D	Coefficient of drag of an wing or other 3D object
Re	Reynolds number
AR	Aspect Ratio (Interchangeable with λ)
α_{inc_w}	Angle of Wing Incidence
α_{inc_h}	Angle of Horizontal stab. Incidence
α	Angle of Attack
η_w	Wing Taper Ratio
η_h	Horizontal Stabiliser Taper Ratio
λ	Aspect Ratio
λ_h	Horizontal stabiliser Aspect Ratio

AoA	Angle of Attack (Interchangeable with α)
UAV	Unmanned Aerial Vehicle
UAS	Unmanned Aerial System
BL	Butt Line
CAS	Finite Automaton
QFD	Quality Function Deployment
ESC	Electronic Speed Controller
FS	Fuselage Station
ISA	International Standard Atmosphere
LLS	Linear Line Theory
HZS	Hasičský záchranářský sbor (Firefighting department)
LPS	Labelled Prüfer Sequence
NFA	Nondeterministic Finite Automaton
NPS	Numbered Prüfer Sequence
MTOM	Maximum Take-Off Mass (replaced MTOW - Maximum Take-Off Weight)
MF	Mass Fraction
MRA	Multi Regression Analysis
RTK	Real-time Kinematic Positioning
T/W	Thrust to Weight ratio
XPath	XML Path Language
s	Wing Area
VTOL	Vertical Take-Off and Landing
STOL	Short Take-Off and Landing
SME	Subject Matter Expert
WL	Watter Line
TOL	Take-Off and Landing

Introduction

0.1 Motivation for this work

With the increasing usage of drones, UAVs and UASs (these terms will be used interchangeably) of different sizes, types and capabilities by different operators there arose a question about where is the line between the application of only multicopters and fixed wing UASs. Both variants have some strong advantages and disadvantages which will be discussed later, but the main focus is on the improvement of endurance by utilising fixed wing in all modes aside from take off and landing.

Drones in the commercial sphere tend to be lighter, cheaper, mass produced and oriented towards capturing photo imagery of different types and also to LIDAR or Radar scans, compared to heavier, more rugged military drones with higher payload capability. Military drones have a long history and have been part of militaries since the second half of Cold War. As such they started as fixed wing systems [1]. While commercial drones, in their mass utilisation as we know them now, are relatively new thing highly dependent on technological advances in electronics and batteries. With the rise in electronics miniaturisation and in computing power, the use of quadcopter configuration become the norm [2]. However as the demands for payload rose, also the weight increased. With multi-copters needing to be able to lift their own weight a solution for higher endurance and/or payload capability would not be possible by just simply using bigger batteries or higher powered propulsion system. The idea for this topic came to light with a research of small military drones and heavier multi-copters where an overlap of payload weight and performed missions appeared.

For some applications an ability to hover is a must, for some it might be beneficial or possibly of no value at all. To identify these fields, some research was done of the missions fixed wing and multi-copter drones perform and where there might be a possible crossover. Also as there is a trend that the cheaper the commercial drones are, the bigger the market they (usually) reach. As

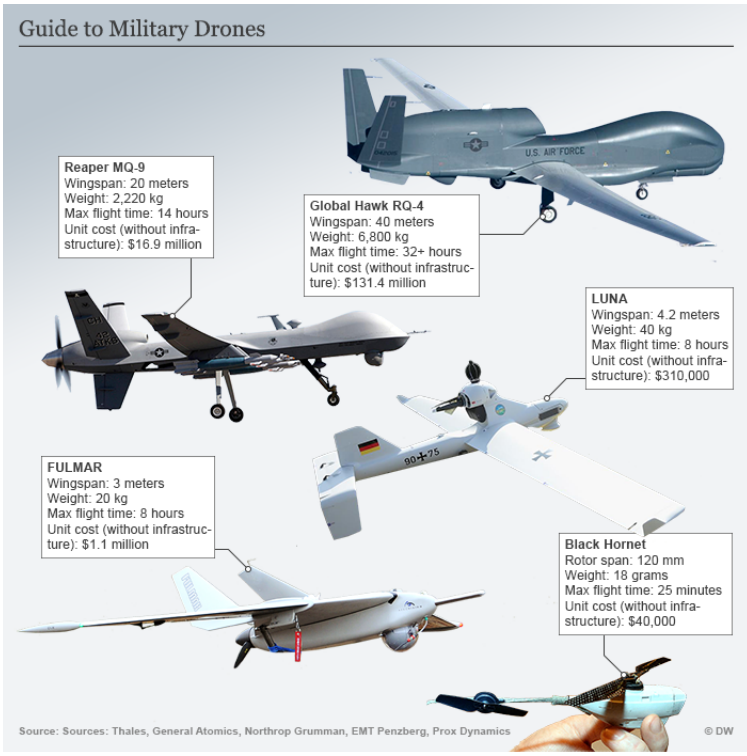

Figure 1 Overview of typical military drones [1]

seen with the sales of drones like DJi Mini series. For this reason the purpose of this work was to identify the smallest (lowest Maximum Take Off Mass - MTOM) possible drone with fixed wings that might find a wide commercial success.

Based on these facts the work begins by assuming that for drones used primarily for the creation of entertainment content such as videos and photos, a fixed wing drone would be impractical due to the inability of hover for an extended period of time or any hover (if a non VTOL drone), inability to work indoors and due to higher risk of operations in urban areas under the Open Category of EASA (more on certification later). Big part of the problem would be the constant movement of the drone and its possibly much higher energy on impact during collision. The ease of transportation also plays a huge role in their usability. In the military sphere a lot of the details are unknown and also a lot of the requirements are very specific as well as user cases. From these presumptions focus will be put on to heavier freely soled multi-copters aimed for industry or first responders (police, firefighters and paramedics/para-rescue) use cases.

Product	Company	Price	Locale	Flight Time/ Payload	Camera/ Operation Range/ Features	Image	Reference
AR Drone 2.0	Parrot	$249	France	12 min/ 100g.	Built-in 720p Cameras 200m/ Supports multiple controlling devices		[73]
Bebop 2	Parrot	$799	France	22 min/ 20g.	Stabilised 1080p Cameras 180° vision HD 2000m/		[74]
Iris+	3D Robotics	$599	US	22 min/ 400g.	GoPro Camera/ 1000m/		[75]
Solo	3D Robotics	$919	US	25 min/ 420g.	GoPro Camera/ 805m/ Powered by twin computers Ballistic parachute system		[76]
HEXO+	Squadrone System	$999	US	15 min/ 200g.	GoPro Camera/ 100m/ 2-second battery swap		[77]
Phantom 4	DJI	$1,399	China	28 min/ 300g.	Built-in1080p Camera, 4K resolution video/ 5000m Automatically avoid obstacles.		[78]
Inspire 1 Pro	DJI	$3,899	China	18 min/ 1700g.	Built-in1080p Camera, 4K resolution video/ 2000m/ Independent camera controller		[79]
MATRICE 100	DJI	$3,299	China	40 min/ 1000g.	External camera stabilization gimbal/ 5000m/		[65]
QR X900	Walkera	$4,399	China	25 min/ 3000g.	External camera stabilization gimbal/ 1000m/ Parechute protection device		[80]
Typhoon H	Yuneec	$1,299	China	25 min/ 600g.	Built-in1080p Camera/ 800m/ Integrated autonomous flight models		[81]

Figure 2 Overview of typical commercial drones [2]

0.2 Aim of the thesis

The purpose of this thesis is to create a concept and a preliminary design of a fixed wing drone that could achieve commercial success based on its design features and parameters based on the account of currently available multi-copter drones. Before the concept design can commence a series of requirements and some research needs to be done. To create a set of specifications (demands and wishes) a market research needs to be done. As this thesis is not a market or economy based thesis all the needed work before the designing process itself is done from the view of an engineer with a biased vision for a product. Which means a market needs are defined by locating a multi-copter competitor and assuming it can be outperformed by a new fixed wing design. The first assumption needs to be evaluated by basic calculations and then a definition of requirements can begin. Based on these, a multitude of concept designs can be created.

Chapter 1
Requirements Specification

The outcome of this chapter is intended to set the boundaries for further chapters and all the designing work done in them.

As the biggest advantages of the fixed wing drone are endurance and subsequently range and payload capacity, the drones can perform only the missions in which potential users see the benefits in using such drones. Currently the number of (potential) users is quickly expanding as well as the variety of missions they are becoming viable for. To get a first look at these possible missions lets inspect the lightest multi-copters not oriented at producing audiovisual production.

1.1 Direct competitors

As the most utilized competitors were selected lightest industry DJi drones, as they are the biggest producer of civilian drones. According to [3] 70% of the quadcopter market is dominated by DJi. Even if industry drones sales are dwarfed by their consumer level ones, they are in their respective sector just as popular.

1.1.1 Industry aimed DJi UAS

For industrial use, the company offers drones from the Enterprise category, namely Matrice 30, 300 RTK and 350 RTK. These are drones with masses (MTOM) from 4kg (Matrice 30 (1.1)) to 9.2kg (Matrice 350 RTK (1.2)) where 300/350 are just slightly different variants (newer iteration) of one type. A comparison of their basic parameters and those relevant for future evaluation are shown in the table below: All of the drones above come, besides their own cargo box and ground station, also with a battery box for charging multiple batteries. This shows that the manufacturer is aware of the lacking endurance

Table 1.1 Technical parameters of DJi Matrice 30/300/350 [4]

Parameter	Matrice 30(T)	Matrice 300	Matrice 350
Battery type	IFB	IFB TB60	IFB TB65
Time [min]	38,5	55	55
Range (track) [km]	53,13	56,1	56,1
MTOM [g]	3998	9200	9200
Single Bat. Weight [g]	685	1350	1350
Normal TOW [g]	3770	6300	6470
Energy [Wh]	131,6	274	263,2
Capacity [mAh]	5880	5935	5880
Voltage [V]	26,1	52,8	52,8
Hor. Speed (cruise) [m/s]	23	17	17
Ver. Speed [m/s]	5,5	4,5	4,5
Service Ceiling [m]	5000	5000	5000
Range CE [km]	8	8	8
Certification (EASA)	Case 2	Case 3	Case 3
Payload [g]	-	930	960

Figure 1.1 DJi M30 [4]

of the drones and knows that operator will need to land and replace batteries multiple times per mission.

1.1.1.1 M30

The lighter of the selected drones is in design closer to the consumer drones as it doesn't have interchangeable payload and its landing gear is still located on its arms with motors and propellers. Besides the ease of transport and price, the M30 also falls into a lower certification category. Total price for this system is around 11 000€.

■ **Figure 1.2** DJi M350 [4]

1.1.1.2 M300/350

The heavier drones allow for mounting payload on many different positions via unified (DJi specific) mounting point. They also have RTK (Real-time Kinematic Positioning) which helps with lowering the error from GPS. This drone also comes with necessary accessories for battery charging. To skip ahead a little bit, this drone will be the main competitor for the conceptual design specified in this thesis. The total price of the drone kit without payload is usually around 13346€at the time of writing. Payload can be a simple TV camera with cost in lower thousands of dollars or a thermal camera for over ten thousand dollars.

After subtracting these number 1.2 from the kit price we get the final price of the drone of 8848€. Other parts like replacement propellers or transport box are still part of this cost.

■ **Table 1.2** Cost of sub-components in M350 Kit

Name	Price [€]
1x Battery WB37	69€
2x Battery TB65	844€
Battery Charging Station	1241€
Control Station DJi RC Plus	1500€

1.2 Missions sets

The variety of missions is wide, but in principle they can be divided into three categories according to the UAV flight profile.

The first category is a preplanned flight with a minimum number of in-flight changes, where the aircraft spends most of the time in cruise mode with occasional hovering (in our case ”loiter”) at set waypoints. The next type of mission is one where the aircraft spends most of its time in a hover/loiter. The last category are missions where operationally it is necessary to switch between long-use en route cruise/flight mode and hover/loiter mode.

1.2.1 Civil

The designed drone is mainly aimed at the civilian sector as data for it are easily accessible and it's a more demanding market with bigger variety of missions.

1.2.1.1 First responders

This relatively new term covers the police force, the firefighters and paramedics. These units can utilise a long endurance UAV with bigger payload for overwatch over the emergency saturation, for long search and rescue operations or for mapping of natural or other disasters. In extreme situations the payload of such drone can be switched out for medicine transported at longer distances.

1.2.1.2 Infrastructure

These missions include checking infrastructure or hard-to-reach industrial complexes and can be done in routine manner or prior to expansion or after some sort of accident. Infrastructure is a very wide term so some examples can be refineries, pipelines, road networks, bridges and especially power plant inspections such as solar panels or wind turbines, but that's not all.

1.2.1.3 Mapping and agriculture

Under mapping can fall 3D modeling by LIDAR or by other methods using sensors with reasonable weight, for example multi-spectral cameras. Those can also be used in agriculture for monitoring of growth and health of crops.

1.2.2 Military

The planned drone should be capable of performing some military tasks.

1.2.2.1 Border patrol

Inspecting the border or locating disturbance based on other inputs are both missions where operators benefit from a longer endurance drone with longer range.

1.2.2.2 Maritime use

Either inspection of anything suspicious on the surface or just a monitoring over the horizon.

1.2.2.3 Direct reconnaissance

Missions where a location is inspected with the aim to locate and follow possible targets.

1.3 Payload

Unfortunately, there is not yet a uniform, or at least recognized by much of the industry, mounting system for mounting gimbals or payloads directly. In searching for ready-made solutions for the most demanding missions, mostly gimbals with camera/thermal/laser rangefinder etc. with 1 [kg] and above have been found. Large number of standalone camera solutions and a smaller number of gimbals were found. However, going back to the manufacturer DJi, they offer a standalone gimbal solution for their drones in addition to a complete solution and also release a PSDK (Payload Software Development Kit) with which users with specific payloads can design and integrate their specific payloads themselves. From the perspective of a potential competitor, it would be worth exploring the possibility of using DJi's PSDK to create a compatible environment and physical storage so that a payload designed for the M300/M350 can be installed on the proposed drone. This however can be a motivation for another thesis and as is later explored from communication with actual operators a completely open-source software system would be much preferable and also probably easier to design.

1.4 Certification

As the drone design is done under a European university and mainly aimed at civilian operators the certification basis will be taken from EASA.

1.4.1 EASA

For a proposed drone to be competitive it must fall into the same certification category or "better". By better is meant a category that is less restrictive to the end user. Since the missions will be identical to those of the M30/300/350, the needed risk of operating them must aimed to be the same. The certification basis for the M30 is C2 and for the M300/350 it is C3 as seen in the info-graphic below 1.3.

1.4.1.1 Open Category - C2 and C3 [5]

First to understand the certification categories from EASA for small UAS systems [5]. On figure 1.4 is the primary segregation. This is done based on the risk level which is mostly defined by SAIL number (which is calculated based on EASAs risk assessment matrix), which is solely based on the operations. As such drone can fall into Open Category for one mission and to Specific category for other. As this is based on the user the focus will for now be at the definitions in Open category. According to the certification, drones in C 3 must have two flight modes, (S and P), which determine the speed at which the drone can move. The P mode, cruise, is indicated in the table 3.4. From

UAS with C-Class Markings

Class	Designed By	Type Category	Model	Commercial Name	Low Speed Mode	Noise Level (db)
C0	DJI	Multi-rotor	MT2SD, MT2SDCE	DJI Mini 2 SE	N/A	N/A
C0	DJI	Multi-rotor	MT3PDCE, MT3PD, MT3M3VDB	DJI Mini 3, Mini 3 Pro	N/A	N/A
C0	DJI	Multi-rotor	MT4MFVD	Mini 4 Pro FLy More Combo	N/A	N/A
C1	DJI	Multi-rotor	EB3WBC	DJI AIR 3	N/A	81
C1	DJI	Multi-rotor	L2AA, L2PA, L2C	DJI MAVIC 3 V2.0, Cine V2.0, Classic	N/A	83
C2 C6	AgEagle	Fixed-wing	SENSEFLY EBEE X, GEO, AG, TAC PUBLIC SAFETY	SENSEFLY eBee	No	N/A
C2	DJI	Multi-rotor	M30 RTK EU, M30T RTK EU	M30 EU, M30T EU	Yes	90
C2	DJI	Multi-rotor	M3E-EU, M3T-EU, M3M-EU	DJI MAVIC 3E EU, 3T EU, 3M EU	Yes	82
C3 C5 Through kit developed by Flyingeye	DJI	Multi-rotor	M350 RTK	Matrice 350 RTK	N/A	97
C3	Quantum System	Fixed-wing	R10	Trinity F90+	N/A	N/A
C3	Wingtra	Fixed-wing	Wingtraone Gen II	WingtraOne	N/A	N/A
C6	Delair	Fixed-wing	UX11-AG-C6, IR-C6, RGB-C6, AG-LE, IR-LE, RGB-LE	Delair UX 11 Camera AG, IR, RGB; Longue Elongation Camera AG, IR, RGB	N/A	N/A

Figure 1.3 Class of competitor UAS under EASA [5]

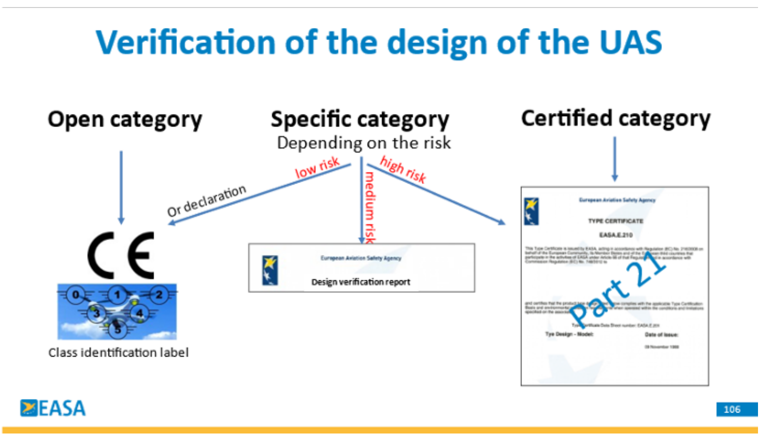

Figure 1.4 First categorization of UAS under EASA [6]

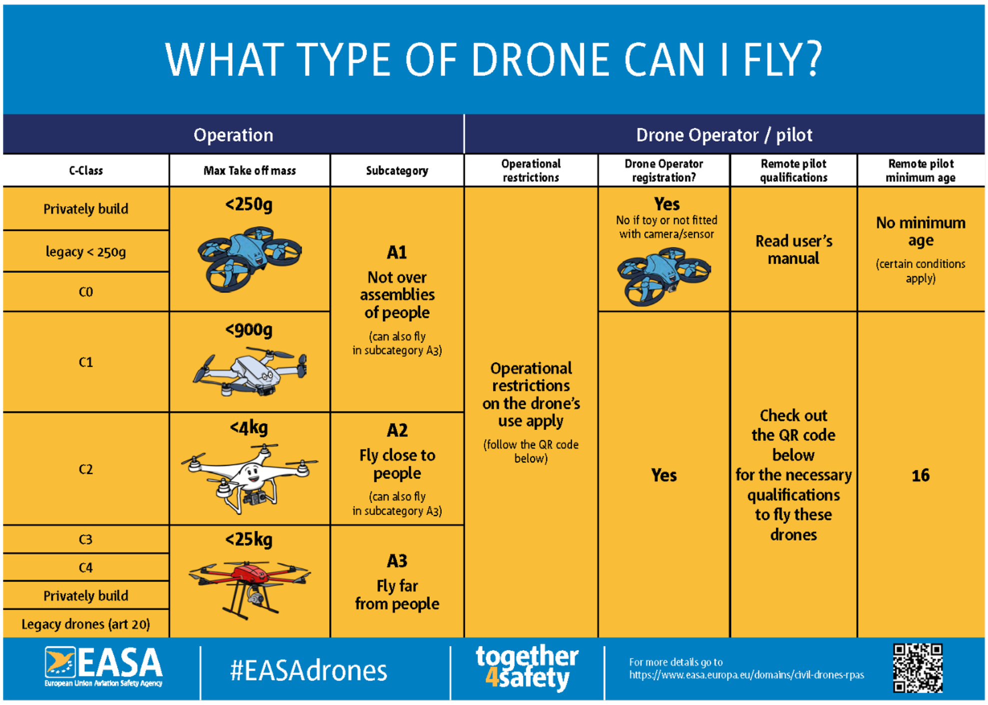

Figure 1.5 C-Classes of Open Category [5]

figure 1.5 its apparent that the lower the category the more the operator can get closer to urban areas or people and perform missions with higher risk. This mostly corresponds to the weight of the drone but there is also a difference between C3 and C4. Drones with one dimension bigger than 3 [m] fall under C4 or higher.

1.4.2 Conclusion

In order to conclude what certification basis will be used (eg. what MTOM limit will be active for the design). It is needed to do basic calculations and assumptions if we are able to built a 4 [g] UAS (C2) with 1 [kg] payload, required endurance and wing span under 3 [m]. If not a C3/C4 will be selected which for the manufacturer mainly means MTOM under 25kg, which should not be limiting for this design. Other design specific requirement by the EASA is the installation of a ADSB style system like DroneTag Mini.

1.5 First Weight Estimation

Feasibility study of C2 certification was first done by very rough calculations and consolidated by looking at other already done desing or research work.

The first method of verification was through the linear dependence by values in [7], although the paper is mostly about the design of canister loiter munitions, for a preliminary conservative design, using their approach should be sufficient. The values are based on drones with less than two hours of endurance, and therefore the resulting mass should be expected to be even higher. To estimate the mass of the $MTOM$, we invert their equation .

$$W_p = 0,1573 \cdot MTOM + 0,2118\ [kg] \tag{1.1}$$

$$MTOM = \frac{1 - 0,2118}{0,1573} = 5,01\ [kg]$$

In another study [**anarticle**] specialising only in the propulsion of unmanned vehicles, using both internal combustion and electric motors, the effect of the mass of the payload for a 4 [kg] drone on endurance was analysed. The results can be seen in 1.6. For a payload of 1 [kg], the endurance would be only 0,79 hours (47 minutes).

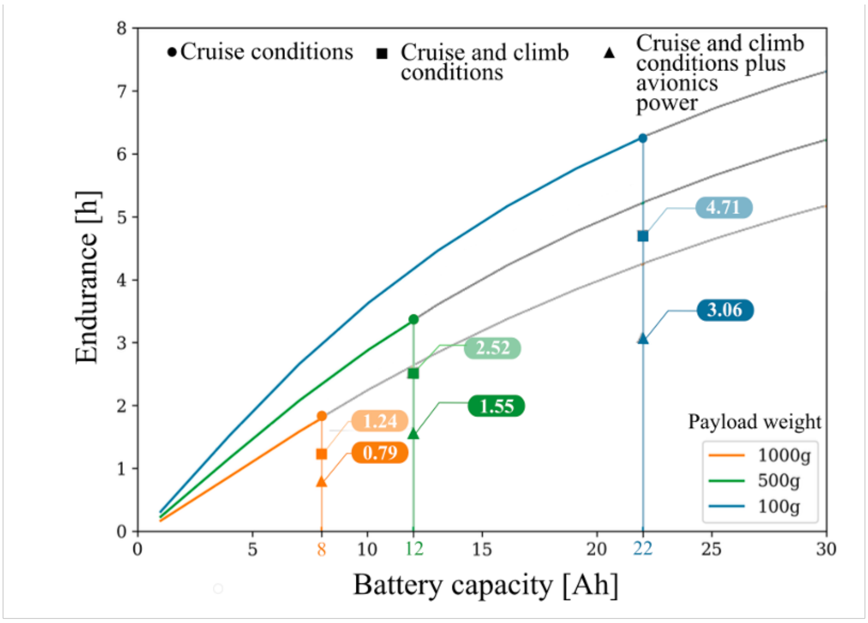

Figure 1.6 Relation between endurance and payload weight [7]

1.5.1 Certification Basis

Based on the rough calculation and studies it is clear that a 4 [kg] MTOM is unachievable with our planned requirements. This is further consolidated in the research of drones and payloads.

Figure 1.7 Use of FPV drone for detailed and rapid inspection (authors archive)

1.6 UAS Users inputs

To get a better idea of the needs of possible operators multiple agencies and companies were contacted with questions concerning their use of drones. Only companies operating industry level drones were contacted.

1.6.1 Firefighters - Czech General Staff Drone Unit

After contacting the General Staff of Firefighter in Czech republic, author was invited by Mr. Jiří Studnička to join him in exercise of first responders and ask him questions there.

The theme of the exercise was a collapse of a building with multiple people trapped inside. One of the units taking part in this exercise was ”drone unit” from General staff and regional unit. These operate DJi Mavics as seen in picture here1.8, Matrice M30/300 but also FPV drones seen here 1.7(all multicopters). During this practical exercise a single operator operated multiple drones. Usually one or more drones were on station around the building providing overwatch for the commander and other decision making personnel. While these drones had set object to observe the operator switched to another drone, either FPV or drone with thermal imaging camera and piloted the selected drone to fulfil the new set of tasks. Multiple video feeds were then mixed similarly as a hockey or football match stream 1.9 and sent to a commanders operation room.

Questions regarding the requirements for the new possible system were

Figure 1.8 Use of DJi Mavic for over-watch and monitoring (authors archive)

Figure 1.9 Transport van with specialised cargo shelves and video feed mixing station (authors archive)

made concerning the endurance, Take-Off and Landing demands, trans-portability, payload expectations, speed (resistance to wind), and some other details as IP expectations (operational environment). As drones were a completely new capability often their limitations were not realised, but after going to detail in other possible missions constructive replies were given.

Priorities were then given to endurance, sensor flexibility and size and to ease of operations as main pillars. Use in bad weather and higher IP standards were preferable and comparable price to a drone with similar sensor capacity a must. On the other side the transport size or the need to operate in small places (and imitate hover by loiter) did not seem important, however a concern was raised over a constantly maneuvering drone directly above or close by to people.

Originally was a plan to use House of Quality approach and connect customer needs with engineering requirements. However due to time constrains just a very simple version of QFD matrix was constructed without relations between engineering parameters.

1.6.2 Other users

From other contacted operators of DJi M30/300/350 (or similar) the questions about what to improve were usually about system logic or payload capability as most civil operators do not have experience with fixed wing drones and their whole operations logic is created with multi-copter limitations in mind.

As most of the other operators willing to communicate were drone schools or contractors their missions were inseparable from their operated drones as contractors were called for abilities of their quad-copter drones and drone "pilot" schools were teaching for operations on such drones. Willingness of contractors to discuss specific mission was very low, but based on few information they would appreciate longer endurance in *some* missions and the cruise flight mode is not a problem for *some* missions however always without the sacrifice of vertical take-off and landing. There were plans by this operator to use a VTOL fixed wing drone, but due to the several times higher price point, compared to a multi-copter with similar payload, it was not used. Also one of the frequent comments about the chosen competition was the ecosystem of DJi as it was compared to Apple with its closed software or even hardware (as it uses its own special mounting points), which makes it hard to use specific payload or modify the drone for more specific missions.

1.6.3 Conclusion

Some of the conclusions drawn from the operators were that in this category of drone (and related price range of such equipment) a transport vehicle is selected (or modified) for the drone and not the other way around, so transportable is more of a wish than a demand as it doesn't need to fit any specific trunk size.

Endurance is viewed as a huge benefit but a sizable fixed wing maneuvering drone would be viewed as a bigger distraction and hazard if operating close to first responders or urban areas. Overall the lower would be the difference in operations from a multi-copter to the designed drone the higher the will of the operators to use them.

- Endurance - to show a considerable advantage a 4x of the normal operating time should be considered which is based on operators 45 minutes or less
- Hover or the ability to observe object from single point - will be augmented by slow loiter flight regime with maximised payload view angles (to observation of objects on the same plane as is the UAS) for undisputed view while circling
- Transport - dimensions will be minimised but not in the cost of endurance ”hover”
- Simplicity and price - number of pieces minimised
- Demand on operator - autonomous flight regime with VTOL or STOL (hand launch and belly landing) capability
- Payload - at least 1 [kg] with easy to modified mounting point for high variety of payloads
- Fully Autonomous operations - not considered as they are also done only with specialised multi-copters

1.7 Requirements description

To quantify previously stated ideas, feature requirements and required parameters it is worth creating a table of parameters the resulted preliminary design could be compared to. These parameters are written down in following table

Table 1.3 Set of requirements

Parameter	Value	Wish or Demand
Price	10000€	Wish
Endurance	180 [min].	Demand
MTOM	Under 25 Kg	Demand
Cruise speed v_{cruise}	17 [m/s]	Demand
Transportation	In box 100x50x40 [cm]	Wish
Payload weight	At least 1 [kg]	Demand
Structure	Rugged (at least IP 55)	Wish
Take-Off and Landing space	5 [m2]	Demand
Camera angles (same level)	360 [°]	Wish

Chapter 2
Research

To understand where there is already overlap you can find in table 2.1 all the drones found in the first set of research which also worked as feasibility study. Other fields that were researched at this point were also payload which was needed to understand not only the needed weight the drone can carry, but also the power consumption of such payload (or systems related to it) which will have a great impact on the initial sizing.

2.1 Comparable UAS

Besides using googling the biggest source of UAS was Janes [8] and recommendation on where to look from operators. In total 33 drones were compared. None of the drones surpassed all the previously set requirements and as such it confirmed the worth of exploring this design. The closest designs to the requirements were then used in the Statistics. Drones under 15 [kg] with fixed wings for cruise flight regime and payload at least 800 [g] were collected.

All the other information collected with the drones is in the excel spread sheet attachment (DP Szekely). This research was done to understand the correlation between sizes of drones and their payload capacity and endurance and primarily to see what type of methods for landing and take off are successfully used with these drones. The parameters collected (if available) were name, company, country of origin, MTOM, normal operating weight, Payload, max. horizontal cruise speed, wing span, length, endurance, battery (only few drones had data about this available), take-off/landing method, range, civil/military (often indistinguishable) and price.

2.1.1 Data

In table 2.1 you can see the average values of tracked parameters which were available with the most drone types are easiest for comparison. For example

Table 2.1 Researched drones [8] [9] [10] [11] [12]

Name	Company	Country
Caburé	Nostromo Defensa	Argentina
Kasper	Aerosystema	Belarus
Horus FT-100	FT Sistemas	Brazil
CH-802	CASC	China
CH-901	CASC	China
Dragon VTOL	Sparkle	China
EOS	Threod Systems	Estonia
ASF 20	Aero Surveillance	France
Tracker	Tracker	France
Biodrone	Alcore	France
Spy Ranger	Thales	France
Aladin	EMT	Germany
Spybird	BlueBird	Israel
Skylark I LEX	Elbit Systems	Israel
Bird Eye 650	IAI	Israel
Micro Falcon	Innocon	Israel
FlyEye	WB Electronics	Poland
AR1 Blue Ray	Tekever	Portugal
Puma LE	AeroVironment	USA
Dragonfish Standard	Autelrobotics	China
Heliplane LRS 240	Drone Volt	France
Volanti	Carbonix	Australia
Trinity Pro	Quantum Systems	Germany
One Gen II	Wingtra	Switzerland
EOS C VTOL	Threod Systems	Estonia
VA23	T-Drones	China
VA25	T-Drones	China
Raefly VT240	CUAV	China
Raefly VT260	CUAV	China
AYK-250	Foxtech	China
Loong 2160	Foxtech	China
BABY SHARK 260	Foxtech	China
BABY SHARK 260 PRO	Foxtech	China

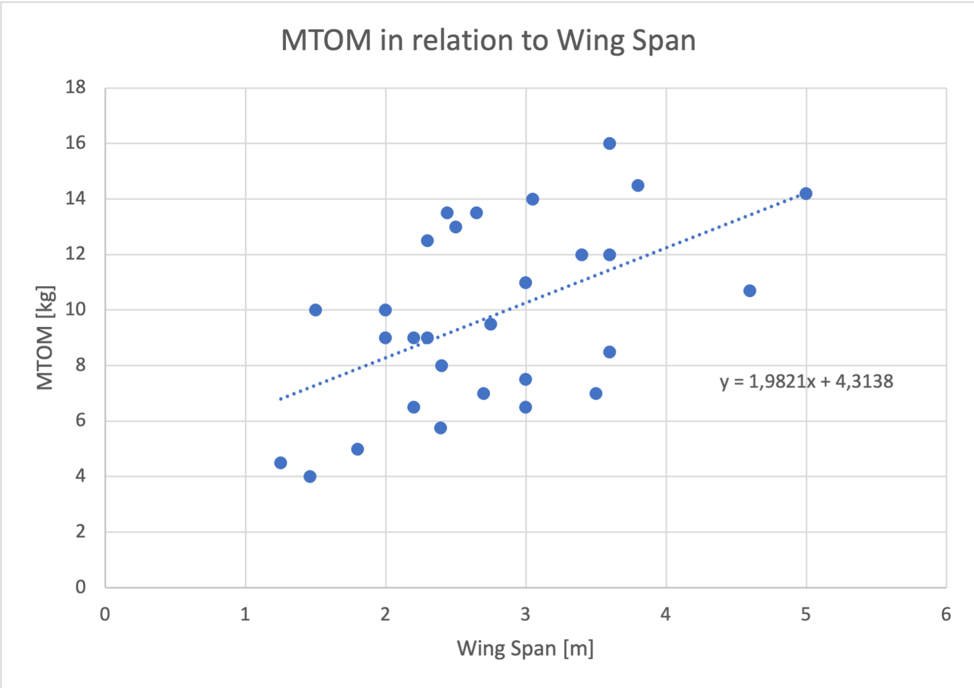

Figure 2.1 Correlation between MTOM and wingspan in first wide research

some values like range were largely dependent on the way the manufacturer specified as information. If it was based on the longest possible communication with ground station it might have been also limited by regulations etc.. The most interesting tendencies are visualised in figures 2.1 and 2.2. The average

Table 2.2 Researched drones

Parameter	Average value
MTOM	9,78 [kg]
max. payload	1,53 [kg]
max. cruise speed	74,4 [km/h]
wing span	2,76 [m]
length	1,5 [m]
endurance	152 [min.]

endurance in the table 2.2 might seem surprising as it is very close to the requirements. This is thanks to a multiple military high endurance drones used in the research with price tags not feasible for civil operators and also with specialised take-off assistance, which also will not be feasible for this design.

With minor differences drones could have been categorized by landing and take-off to categories as visualised for Take-Off 2.3 and Landing2.4. ”Hand

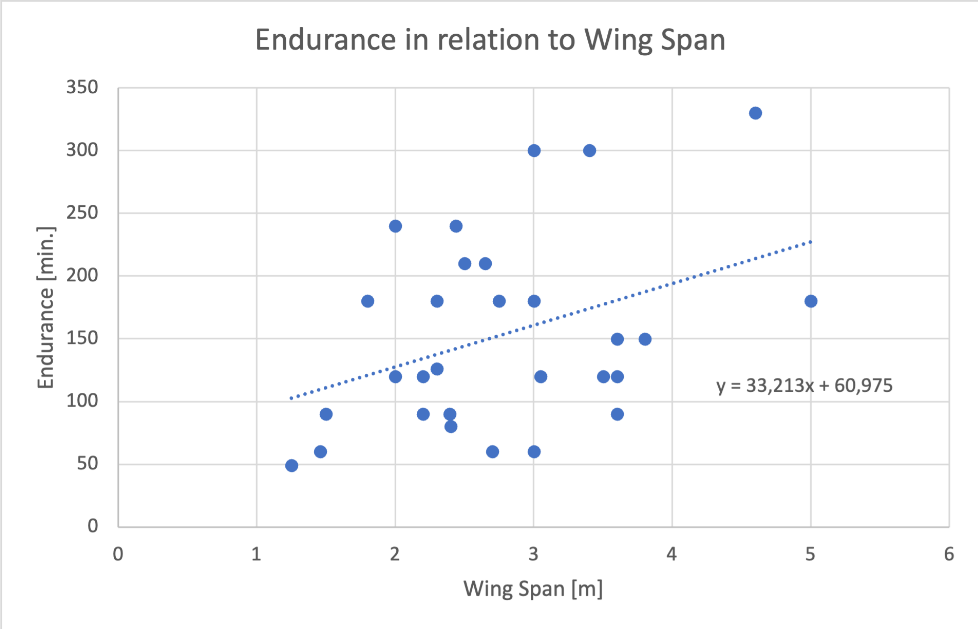

Figure 2.2 Correlation between endurance and wingspan in first wide research

only" means a hand launch when drone is tossed either by its fuselage/mid-section or by the wingtip. "Hand + Device" are drones that can be launched either by hand or by device which can be anything from bungee chord/sling or catapult. As all such devices require extra space (high operational change to multicopters) there was no need for further separation.

For landing a belly landing is category containing any landing where aircraft doesn't use any sophisticated landing mechanism or thrust conversion for minimising forward speeds and thus just performs a controlled crash. Some companies describe it as deep stall landing, belly landing etc. but they all come in contact with ground by their fuselage at high AoA. Some use Parachute or Parachute optionally with belly landing being the other option and those are the last two types. Some military drones for maritime operations also fell in the relevant category for this research but due to their sometimes very specific landing and take-off methods were not used in this research.

Small number of drones, 4 to be specific, had also specified weight of airframe and MTOM without batteries. All those drones are from the same Chinese company CUAS without specified endurance of the drones. However from their promo videos and website we can see what batteries they use and what avionics and type of propulsion (propeller, electric motor and ESC) they use, based on which it was possible to get following mass fractions 2.3.

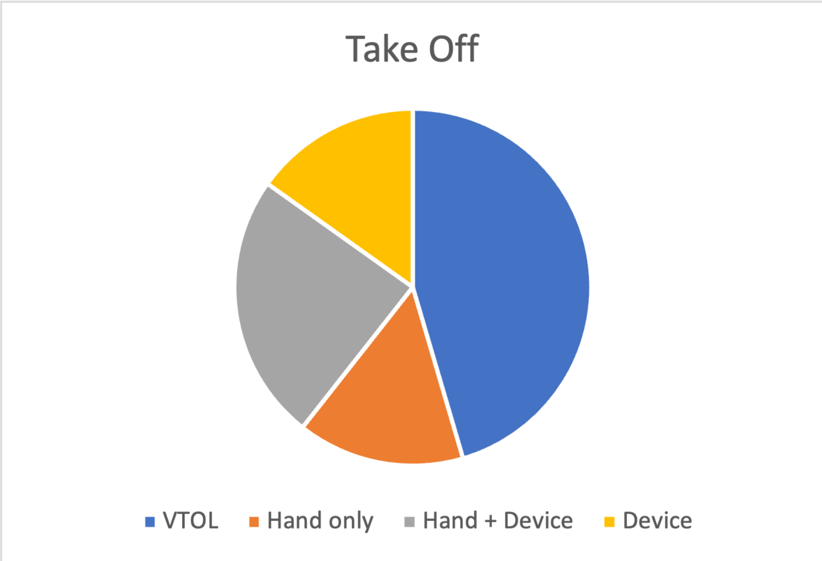

Figure 2.3 Different methods of take-off

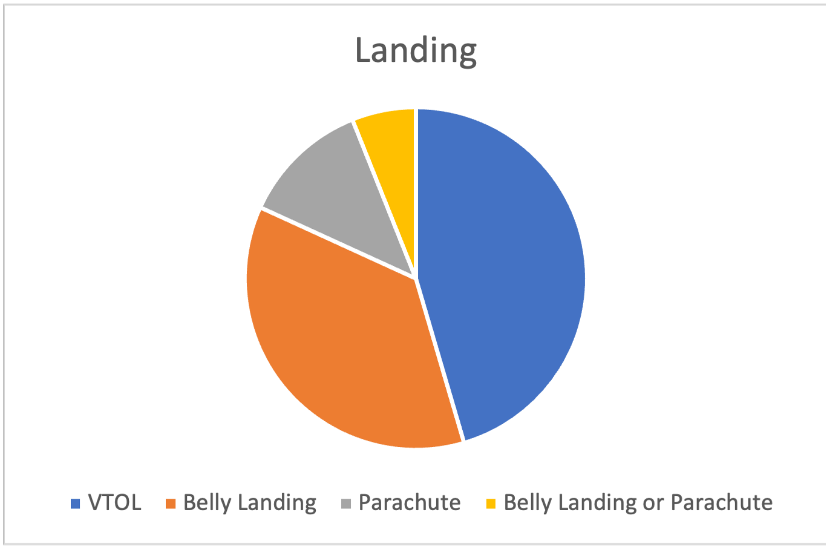

Figure 2.4 Different methods of landing

Table 2.3 Mass Fractions

Parameter (fraction by MTOM)	Avarage	Min.	Max.
$MF_{Equip.+Airframe}$	0,469	0,431	0,493
$MF_{Equip.}$	0,284	0,223	0,35
$MF_{Airframe}$	0,195	0,125	0,269
$MF_{Batteries}$	0,384	0,343	0,411

Figure 2.5 HD-45 (left) [13], YellowScan Mapper+ [14] (bottom right), RedEdge-P [15] (top right)

2.1.2 Conclusion

Based on research it is worth to explore both variants of Take-Off and Landing - VTOL and STOL (hand launched under high angle and belly landing).

2.2 Payload research

To fulfill all the possible missions the designed UAS must be able to carry and support large variety of payloads. From LIDAR (YellowScan Mapper+), Multi-spectral cameras (MicaSense RedEdge-P) to Thermal or IR cameras (HD-45-LV-CZ) all were inspected to make sure their integration will be possible 2.5. However the only parameters concerning concept air frame design are the payload consumption, weight and dimensions.

Table 2.4 Example of available drone payload

Name	Weight [g]	Avg. P. Consumption [W]
Z10TIR	800	9,6
MicaSense RedEdge-P	350	7
D-STAMP-HD	860	11
YellowScan Mapper+	1100	19
Gimbal 10z Embention	1000	15
HD40-XV	840	15
HD-45-LV-CZ	1280	15

Last payload is much heavier than the expected (required) payload weight however is on the limit that might be possible and as such its size will be used as reference for designing the drone.

Chapter 3

Statistics and First Sizing

To specify main geometries and propulsion configuration it is first needed to estimate the MTOM and that is best done through calculating the needed capacity of batteries. For that purpose we first needed guesstimate the probable MTOM and geometries from statistics to calculate the energy consumption and based on that the batteries. All measured parameters are added to the Appendix A.

3.1 Statistics

From the research a number of drones closest to our requirements were selected. From available pictures rough geometries were measured in CAD (Fusion 360) and some proportional parameters were calculated.

3.1.1 Selected models

3.1.1.1 Puma LE

Puma LE 3.1 made by company AeroViroment [16] is a classic military style reconnaissance drone used on the front lines by smaller units. This variant of Puma is designed for Longer Endurance (LE). As such it has much larger wing span and MTOM.

As a STOL aircraft an interesting decision was made not to provide any extra separation or slides for the belly landing but to retract the payload inside the fuselage. This UAS was also the only one with surpassing specified endurance.

3.1.1.2 Dragonfish Standard

Dragonfish Standard was recommended to research by one of the interviewed operators and is a representative of one of the most common configuration with

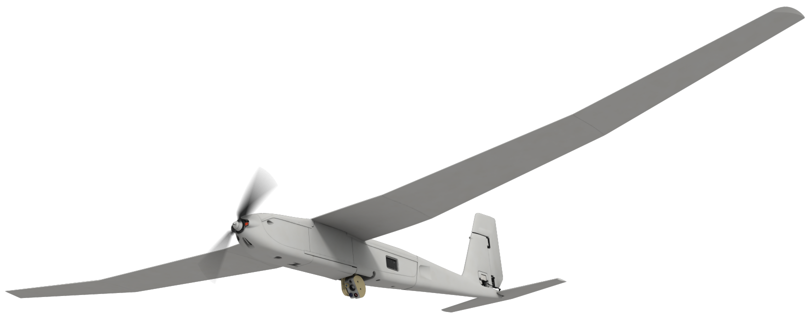

Figure 3.1 Puma LE [17]

Chinese small VTOL drones. It uses separate motors for Take Off/Landing and forward flight, thus carrying dead weight in all flight regimes.

3.1.1.3 EOS and EOS C VTOL

With the military drones there appeared to be theme of manufacturers noticing the limitations of non VTOL operations and as such started to provide versions of their drones with extra propulsion is just for VTOL that is unused during other flight regimes.

3.1.1.4 SpyRanger

Military purpose built drone SpyRanger by Thales is one of the drones surpassing the required endurance, however it is also a drone launched from catapult and with fixed payload.

3.1.1.5 Heliplane LRS240

Heliplane is drone very similar to DragonFish in using separate propulsion for Take-Off/Landing and cruise, but its closer in its design to the EOS C VTOL as its positions it 4 VTOL motors on special arms in roughly 1/3 of its semi span. This is a more typical configuration for these types of drones as it usually symbolises that the VTOL capability was an afterthought and is an interesting design choice for a brand new design.

3.1.1.6 Trinity Pro

Probably the biggest influence for the following VTOL concept design was the Triniti Pro 3.6 however with much lower endurance and payload capabilities

Figure 3.2 DragonFish Standard [10]

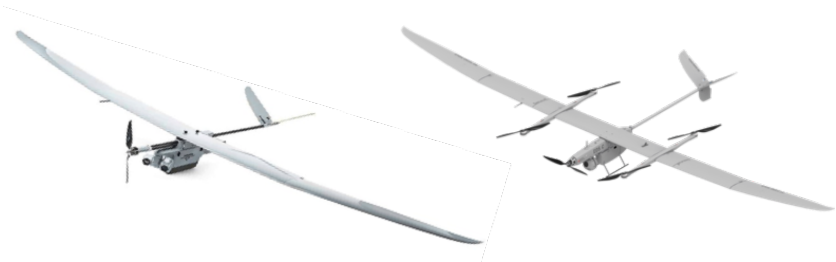

Figure 3.3 EOS (left) and EOS C VTOL (right) [18]

Figure 3.4 SpyRanger [19]

Figure 3.5 Heliplane LRS240 [20]

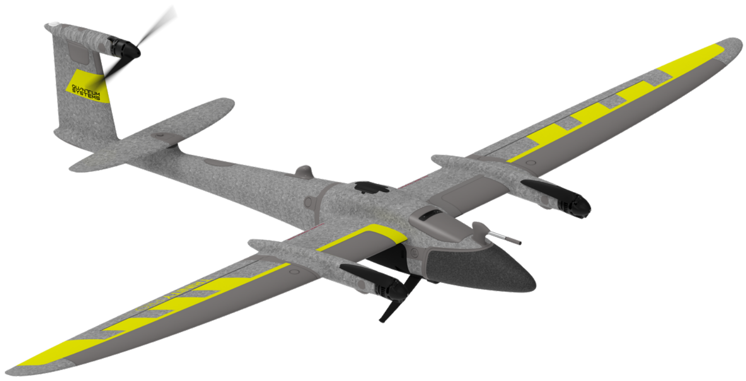

Figure 3.6 Trinity Pro [21]

than specified in Requirements. This drone rotates all of its three propellers and electric motors after take off from vertical position to horizontal as a classical convertiplane. What caught my attention were the fold-able propellers on the two bigger wing positioned electric motors. This systems probably allows the drone to perform horizontal flight at much efficiency as it uses its smaller electric motor for that regime.

3.1.2 Geometries and MRA

As usually there were no clear images of the drones from the side, the estimation/sizing of vertical stabiliser will be made based on the rest of the design. For Puma LE was not even any clear top down view so a modified (stretched) picture was used and thus data for this type need to be taken with grain of salt. Values in Estimation column with decimal points are often calculated from other estimated values (using common equations) in said column or modified by following MRA. Those were created based on logarithmic values as per [22].

Table 3.1 Results of the statistics

Name	Units	Avg.	**Estimation**
Wingspan l	m	3,4277	3,5
Length	m	1,6057	1,5
Wing Area s	m^2	0,7732	0,817
Hor. Stab. Area s_h	m^2	0,0912	0,098
Hor. Stab. Arm l_h	m	0.9551	-
Propeller Diameter	m	0,3556	-
Hor. Stab. Volume coeff. A	-	0,5412	0,45
λ	-	15,8257	15
Wing Root Chord b_r	m	0,2688	-
Wing Tip Chord b_t	m	0,1299	-
Mean Aerodynamic Chord	m	0,2127	0,23
η_{wing}	-	0,5013	0,5
Hor. S. b_r	m	0,1736	-
Hor. S. b_t	m	0,1005	-
η_h	-	0,6029	0,6
Number of engines	-	2,8571	-
Payload	kg	1129,0	1
Endurance	$min.$	153,7	180
MTOM	kg	9,8786	10,45
VTOL	-	57%	-
$\frac{S_h}{S}$	-	0,1257	0,12
$\frac{l_h}{b_{MAC}}$	-	4,5179	-

As is the practice taught at CTU in Prague Aerospace department the geometry is based on statistics. As such the averages were slightly modified in the way that should get the design closer to wanted parameters - mainly endurance. After selecting main parameters like Aspect Ratio, wing surface etc. from statistical averages a multitude of Multiple Regression Analysis were performed 3.2 in MS Excel. These helped iterate the most important values for next (second) sizing based on batteries. After obtaining the coefficients estimated parameters from statistics or requirements were used. MRA were used to estimate value of Depended variable based on two Independent ones.

These resulting values were averaged and inputted back into the guesstimating in 3.1.

Table 3.2 Multiple Regressions Analysis

Ind. Variable	Ind.Variable	Dep. Variable	Value
Endurance	Payload/MTOM	Wing span	4,01 [m]
Wing loading	Endurance	Wing span	2,88 [m]
Endurance	Aspect Ratio	Wing span	3,58 [m]
Endurance	Aspect Ratio	MTOM	10,62 [kg]
Wing span	Aspect Ratio	MTOM	10,29 [kg]

3.2 Propulsion efficiency and battery research

To estimate the size of needed batteries we need to take into consideration not only the physical geometrical properties creating drag but also the energy losses that come with the propulsion method and also at the end the specific energy of the selected batteries.

3.2.1 Batteries

As any flying system running on batteries, its performance its heavily dependant on the specific energy of the used batteries. As such a limited research was done to explore the options of ready made battery packs and battery cells or pouches.

Table 3.3 Battery packs

Name	[Wh]	[g]	[Wh/Kg]	[$]
Lipo-11000-12S-Pack-3	488,4	2530	193	799,9
LiIon-11200-12S4P 43.2v	483,84	2304	210	959,9
Tattu TA-30C-12000-6S1P-EC5	266,4	1532	173,89	268,99
Tattu TA-25C-30000-6S1P-AS150	666	3673	181,32	532,99
Tattu 22000mAh	488,4	2460	198,54	446,29
Overlander 7s	569,8	3096	184,04	373,02
T-Drones Ares	666	2570	259,14	619
Diamond HV [9]	948	3600	263,33	889

Some battery packs from this research are directly used in some of the VTOL drones researched (T-Drones and CUAV) so even if there could be some scepticism concerning the use of Li-ion batteries ability to work under much higher loads needed for VTOL operations, compared to Li-Po, based on these drones using such batteries, we can assume it is achievable even with off the shelf packs and that is what matters at concept and preliminary design study.

As cells and paunches are not made for end user but for industry use (by manufacturers etc.) they offer much higher Specific Energy e, but not all their parameters are publicly available as well as price per unit.

Table 3.4 Battery Pauches and Cells (data per cell/pauch)

Name	E $[Wh]$	m $[g]$	e $[Wh/kg]$
Kokam UHE SLPB065070180	44,2	170	260
EaglePicher SLC-203	46,15	156	300
EaglePicher SLC-202	8,17	33	250
Amprius Drones-Long Endurance	13,2	31,7	416
3,6V Samsung 18650	7,9	44,5	178
Amprius E485795C	18,9	62	304,27

Most of the cell and paunches collected here were, thanks to their high specific energy, even specified as for UAS. Energy is calculated from specified Ampere hours times the highest continues voltage.

As you can see an overlap emerges at around $e = 250$ $[Wh/kg]$ as its a lower boundary for high specific energy pouches/cells and upper limit for already made packs. Selecting this value thus should be realistic and designing or selecting batteries with this parameter possible. For simplicity it is assumed a new battery pack will be designed for this drone and for sizing internal space inside the drone the EaglePicher SLC-202 will be used with size per pouch being 50 x 56 x 7 [mm].

3.2.2 Propeller efficiency

Propeller efficiency was assumed from experimental data provided by Ing. Jiří Walter (attachment vrtule-14x85-mereni-4.xlsx) that were part of his thesis [23] and by academical papers [24] [25]. First one was to assume efficiency for VTOL (hover) and the second one was as an aid for the locating the speeds at which should be propellers the most efficient. Even [24] uses mostly propellers with higher pitch their data for non VTOL regime are still interesting as seen in their graphs3.7, where we can see where we should expect (at which velocities) the highest efficiency. With lower pitch we can expect the maximum to move to lower velocity values.

From Ing. Walters work were created these figures 3.10 and . As the biggest unknown was the efficiency for stationary free stream velocity efficiencies were calculated for the lowest possible velocity. These however do not capture good absolute data for such speed and as such were used and should be used only as visualisation on how the efficiency and progresses based on power settings or thrust (or revolutions per minute) respectively.

From figure 3.10 the 3rd order polynomial trend-line will be used in preliminary design flight performance.

For the immediately following weight estimation a fixed value was assumed for propeller efficiency for VTOL and cruise and loiter, as it is expected a proper selection of propulsion combination would need specific experimental data and would be optimised for the loiter flight regime. As such propeller

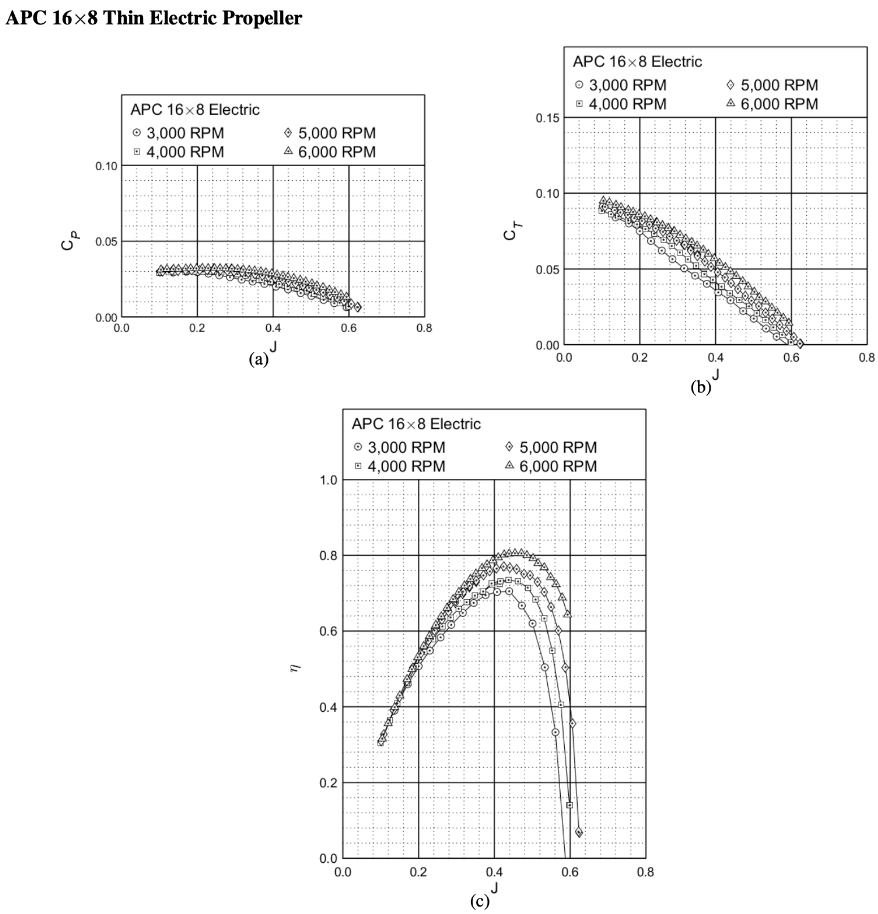

Figure 3.7 Performance of the APC 16×8 Thin Electric propeller: (a) thrust coefficient, (b) power coefficient, (c) efficiency.[24]

efficiency for loiter was assumed as $\eta_{loiter} = 0,6\ [-]$, for cruise and STOL as $\eta_{cruise} = 0,5\ [-]$ and for VTOL $\eta_{VTOL} = 0,15\ [-]$. The VTOL value at first seemed unrealistically low, but based on this paper and figure 3.10 it should be roughly the right value.

3.2.3 Electric motors

At propulsion configuration will be done a deeper dive into the electric motors considered and subsequently selected. However at this point just a rough estimation of the efficiency was done. From spec sheets of electric motors like AXI ([26] we can see some reaching efficiencies even above 80%. Even if further experimentally (not in this thesis) tested propulsion configuration is expected an electric motor efficiency of 70% will be used ($\eta_{el.motor} = 0,7\ [-]$).

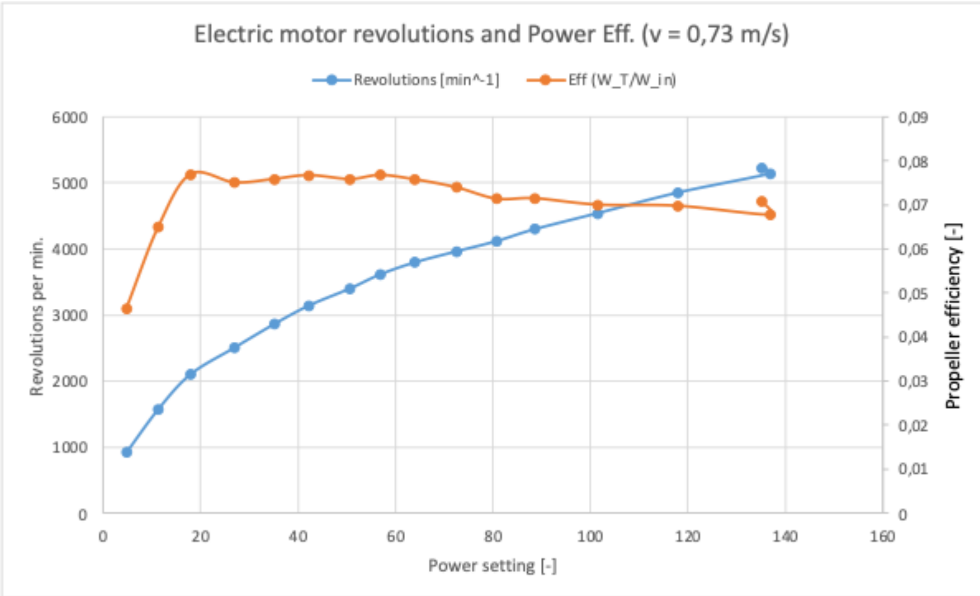

Figure 3.8 Thrust and Efficiency in relation to Free Stream Velocity and its prediction

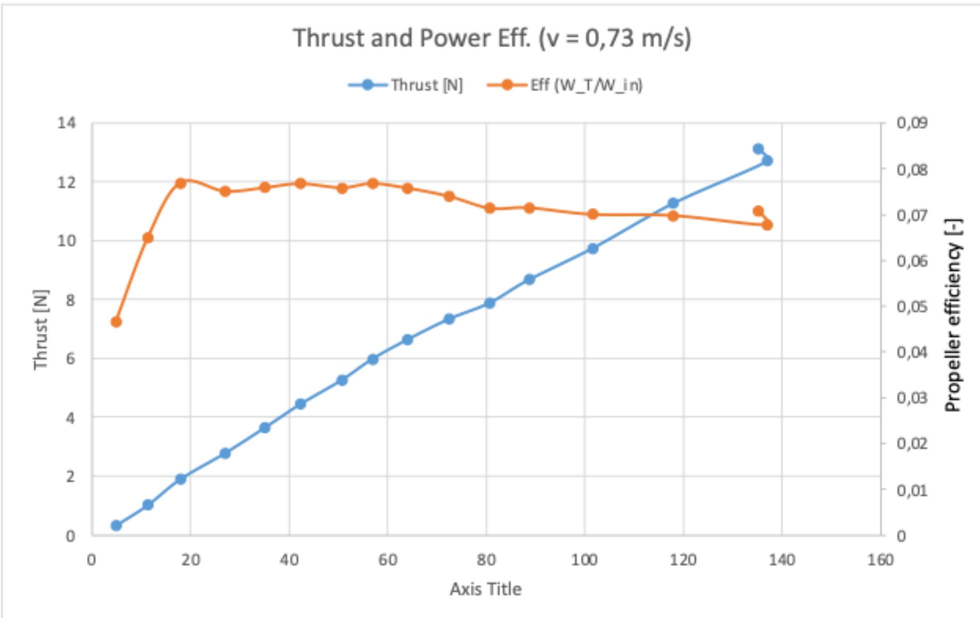

Figure 3.9 Thrust and Efficiency in relation to Free Stream Velocity and its prediction

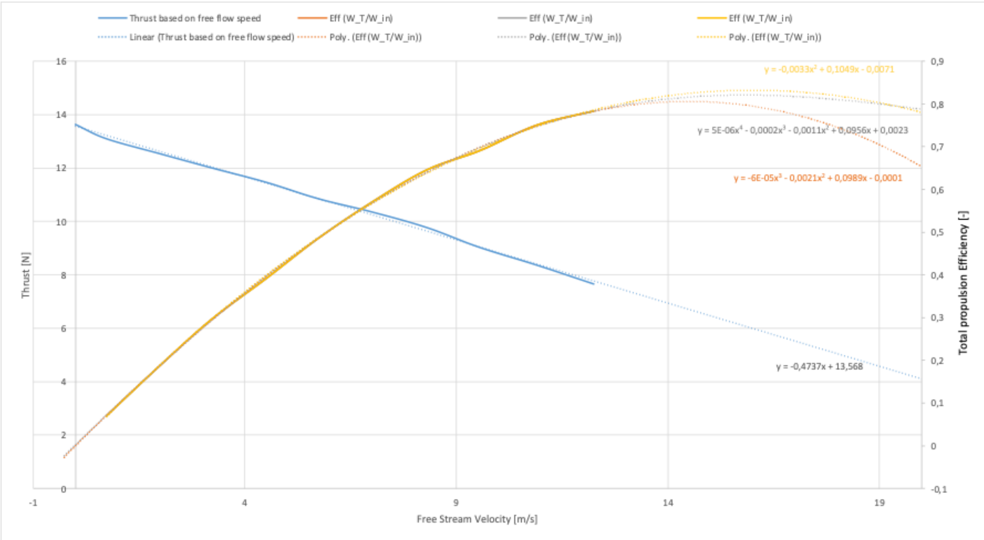

Figure 3.10 Thrust and Efficiency in relation to Free Stream Velocity and its prediction

3.3 Mission definition

Based on missions from research we can imagine two types of missions that will be described as A and B, where in A most of the time is spend in loiter, observing a single or smaller number of points for longer time, and B where the mission might be mapping and more time is spend in cruise as more ground needs to be covered. It is accounted for a travel to the mission/points and back as if all the distance covered was directly from the operator. As for the conceptual design a STOL and VTOL variants will be covered with the take-off and landing regimes widely differing and will be specified separately and not counted in the total endurance (which in normal multi-copters is).

Table 3.5 Mission specification - horizontal flight regimes

Phase	A	B
Cruise [min.]	165	30
Loiter [min.]	15	150

Both missions are inspected as if the difference is significant a cruise or loiter regime might be redefined.

3.3.1 Avionics

Even if using in house designed AHRS with off-shelf IMU and GPS for first reference (and maybe even a demonstrator) an off the shelf complete avionics package will be used. One of the most known autopilot systems for autonomous

UAS is open source Ardupilot and for its build hardware on the basis of Pixhawk like The Cube Orange and X7+ Pro. As the most advanced with least extra input the X7+ Pro will be used in future estimation together with GPS antenna, Pitot tube and the reserve FPV camera. In its spec-sheet an energy consumption of 10 [W]. Another system with higher consumption is RTK (for example CUAV C-RTK 9Ps) which consumes another 5 [W] and is needed for all the mapping missions. Other systems either do not have consumption mentioned or its significantly lower (other sensors). For the purpose of the other systems and servomotors its assumed a shared consumption of another 10 [W]. Under that field falls even the EASA required responder DroneTag Mini which for example should consume only 0,25 [W] on average.

Table 3.6 Example of off the shelf drone avionics

Name	Weight [g]	Power Consumpt. [W]
Veronte Autopilot 1x - ADS-B V4.8	210	10
Pixhawk 6C Holybro (just board)	35	15
Auterion Skynode X	188	15
X7+ (Pro)	105	10

3.4 Second Weight Estimation - Battery Weight

3.4.1 Fixed Energy Consumption

To estimate the battery weight we need to estimate how much energy we need. That is determined by the amount energy consumed by the propulsion system, payload and other systems essential for the mission as avionics. The total fixed consumption is as follows:

$$P_{cons_{fixed}} = E_{avionics} + E_{payload} + E_{other} \tag{3.1}$$

$$P_{cons_{fixed}} = 15 + 15 + 10 = 40\ [W] \tag{3.2}$$

To calculate the consumption of the propulsion system during all stages of imagined missions its needed to do some assumptions. Mostly the assumption of needed thrust and based on that needed power during Take-Off, Cruise, Loiter and Landing. Besides geometries assumed from Statistics coefficient of drag C_D is critical.

3.4.2 Geometry and Aerodynamic Performance Estimation

To estimate the probable minimal drag coefficient $C_{D_{min}}$ for VTOL and STOL configuration an inspiration was drawn from [27] and the final aerodynamic parameters for this sizing are in table 3.7 where the wing surface area s was calculated with the help of wing span l and aspect ratio λ

$$s = \frac{l^2}{\lambda} = \frac{3.5^2}{15} = 0,8167\ [m^2] \tag{3.3}$$

Table 3.7 Assumed minimal drag coefficients and other physical values used

Name	Value	Units
$C_{D_{min}}$ for STOL	0,025	[-]
$C_{D_{min}}$ for VTOL	0,0275	[-]
g	9,81	$[m/s^2]$
ν_{ISA}	$1,460 \cdot 10^{-5}$	$[m^2/s]$
h_{cruise}	100	$[m]$

Important value that will also be used later is wing loading

$$\frac{W}{S} = \frac{MTOM \cdot g}{s} = 125,528\ [N/m^2] \tag{3.4}$$

Sometimes will be used lift as $L = MTOM \cdot g = 102,515\ [N]$ Value for VTOL was guessed as higher due to probable placement of extra nacelles on wings compared to STOL.

Now the symmetrical polar was designed accordingly for AoA from -5 to 15 [°] in Matlab R2024a (will be used for all other calculations if not specified differently and will be placed in attachment called DP Szekely.m). The lift slope was assumed as ideal $C_{l_\alpha} = \frac{1}{2 \cdot \pi}$.

$$C_L = C_{L_\alpha} \cdot AoA \tag{3.5}$$

Which is visualised in polar 3.11 with relation to drag coefficient C_D.

From the required achievable cruise speed we can calculate first the lift coefficient and the needed thrust T and power P for these regimes.

$$C_{L_{cruise}} = \frac{L}{\frac{1}{2} \cdot v_{cruise}^2 \cdot s \cdot \rho} \tag{3.6}$$

$$C_{L_{cruise}} = \frac{102,515}{\frac{1}{2} \cdot 17^2 \cdot 0,817 \cdot 1,225} = 0,709\ [-]$$

For creating the drag polar e (Oswald efficiency number) and subsequently K needs to be calculated.

$$e = 1,78 \cdot (1 - 0,045 \cdot \lambda^{0,68}) - 0,64 \tag{3.7}$$

$$e = 1,78 \cdot (1 - 0,045 \cdot 15^{0,68}) - 0,64 = 0,6349\ [-]$$

And then

$$K = \frac{1}{\lambda \cdot \pi \cdot e} \tag{3.8}$$

$$K = \frac{1}{15 \cdot 3,14 \cdot 0,6349} = 0,0334\ [-]$$

In the original idea of this thesis was even a plan for optimisation of wing geometry based on aspect ratio, however this was due to the time constraints left out, but can be a motivation for future thesis.

By adding to estimated minimal drag a lift induced drag we can get this quick thrust estimation from following equations:

$$C_{D_{cruise}} = C_{D_{min}} + K \cdot (C^2_{L_{cruise}}) \tag{3.9}$$

So for $STOL$ it would be:

$$C_{D_{cruise}} = 0,025 + 0,0334 \cdot (0,709^2) = 0,0418\ [-]$$

and VTOL $C_{D_{cruise}} = 0,0443\ [-]$.

From this it is possible to estimate the thrust for cruise equation 3.10. However it would be better to estimate cruise based flight regime with minimal thrust T_{min}(and loiter on flight regime with minimal needed power P_{min}) especially if the v_{cruise} is lower, making also v_{loiter} lower which is more beneficial to requirements than to match v_cruise from requirements perfectly. This can be said only if the difference too large and as such flight at required v_{cruise} highly uneconomical.

$$T_{cruise} = \frac{1}{2} \cdot \rho \cdot v^2_{cruise} \cdot S \cdot C_{D_{cruise}}\ [N] \tag{3.10}$$

So for $STOL$ it would be:

$$T_{cruise} = \frac{1}{2} \cdot 1,225 \cdot 17^2 \cdot 0,817 \cdot 0,0418 = 6,0438\ [N]$$

the same way for VTOL $T_{cruise} = 6,405\ [N]$. For polar a coefficient of drag is calculated for each coefficient of lift value same way as in equation 3.9.

Some interesting parameters we can estimate from the symmetrical polar is glide ratio which is the maximal $\frac{C_L}{C_D}$ ratio. For STOL $max\frac{C_L}{C_D} = 12,159$ and VTOL $max\frac{C_L}{C_D} = 11,868$ which are quite low values especially for high aspect ratio aircraft.

3.4.3 Flight Regime Specification

In this part an energy consumption is specified per flight regime as it is specified in [28].

3.4.3.1 STOL and VTOL

Even if these regimes should be proportionally only very small part of the mission due to their energy consumption, as the UAS needs to climb and gain speed, are significant. From the parameters of the competitor drones is assumed a minimal vertical speed during climb as $v_{asc.} = 2,5\ [m/s]$ and the ideal forward speed for climb as

$$v_{climb} = 0,8 \cdot v_{cruise} = 0,8 \cdot 17 = 13,6\ [m/s] \tag{3.11}$$

First, lets define the STOL operations. For short landing assume stall belly landing which would take shorter time than short take-off and climb out but will consume same energy (will be assumed) as the aircraft will have the largest drag during the deep stall. Possibly a slightly over conservative approach, but as STOL is not as different to horizontal flight regime as VTOL it should not play significant role in final comparison.

To calculate the needed thrust for the climb we need to first calculate the dynamic pressure ρ for the v_{climb} (Take off and Landing - TOL).

$$q_{TOL} = \frac{1}{2} \cdot v_{climb}^2 \cdot \rho \tag{3.12}$$

Where $\rho = 1,255\ [kg/m^3]$ is fluid mass density as defined for 0 [m] altitude for ISA.

$$q_{TOL} = \frac{1}{2} \cdot 13,6^2 \cdot 1,225 = 113,288\ [kg/m \cdot s^2]$$

An expected operating altitude that needs to be reached during take-off was estimated as $h_{cruise} = 100\ [m]$, which an conservative estimation as normal operations can be expected to be done in much lower altitudes or without the need to reach this height during take-off.

For $STOL$ the thrust with $C_{D_{climb}}$ relevant to the needed $C_{L_{climb}}$ for v_{climb}. Due to the constrains for STOL operations lets put higher expectations on it and double the direct vertical climb speed $v_{asc.}$.

$$T_{STOL} = \left(\frac{v_{asc.} \cdot 2}{v_{climb}} + \frac{q_{climb}}{\frac{W}{S}} \cdot C_{D_{climb}} - \frac{K}{q_{climb}} \cdot \frac{W}{S} \right) \cdot MTOM \cdot g \tag{3.13}$$

$$T_{STOL} = \left(\frac{2,5 \cdot 2}{13,6} + \frac{113,288}{125,528} \cdot 0,0660 - \frac{0,0334}{113,288} \cdot 125,528 \right) \cdot 10,45 \cdot 9,81$$
$$= 39,99\ [N]$$

and subsequently the power.

$$P_{STOL} = \frac{T_{STOL} \cdot v_{climb}}{\eta_{el.motor} \cdot \eta_{prop.}} \tag{3.14}$$

$$P_{STOL} = \frac{39,99 \cdot 13,6}{0,7 \cdot 0,5} = 1554,3\ [W]$$

For $VTOL$ the needed and used thrust is estimated to be $T/W = 1,5\ [-]$. Normally it is recommended to have T/W above 2 for rotor-crafts, however here it is not designed to spend significant amounts of time in hover and us such a lower efficiency (closer to max thrust setting) should be acceptable as well as the first MTOM should be (and by following calculations is) conservative and the final T/W will be higher. Lets assume it will be possible to achieve the $v_{asc.}$ with this T/W.

$$P_{VTOL} = \frac{MTOM \cdot g \cdot \cdot v_{asc.}}{\eta_{el.motor} \cdot \eta_{prop.}} \tag{3.15}$$

$$P_{VTOL} = \frac{10,45 \cdot 9,81 \cdot 1,5 \cdot 2,5}{0,7 \cdot 0,5} = 3661,2\ [W]$$

Now follows estimation of the time spend in these regimes. For descend its estimated we use the same energy, but due to the needed caution for landing the expected descend speed for VTOL and STOL being $v_{desc.VTOL} = 2\ [m/s]$ and $v_{desc.STOL} = 1\ [m/s]$. Times for these regimes is then calculated as

$$t = \frac{h_{cruise}}{v} \tag{3.16}$$

For example the time for STOL climb would be

$$t = \frac{100}{2,5 \cdot 2} = 20\ [s]$$

3.4.3.2 Loiter

The loiter regime will be the main regime this drone will be designed for and as it should be a regime with the longest endurance, it must be also the regime with lowest power consumption usually called P_{min} flight regime and is defined in [28]. Coefficients of drag and lift are defined as

$$min\left(\frac{C_D}{C_L^{3/2}}\right) \tag{3.17}$$

Based on the lowest value position a $C_{D_{P_{min}}}$ is defined for both configurations.

Directly the $C_{L_{P_{min}}}$ can be calculated by following equation:

$$C_{L_{P_{min}}} = \sqrt{3 \cdot \pi} \cdot \sqrt{\lambda \cdot e \cdot C_{D_{min}}} \tag{3.18}$$

For STOL configuration it would be:

$$C_{L_{P_{min}}} = \sqrt{3 \cdot \pi} \cdot \sqrt{15 \cdot 0,635 \cdot 0,025} = 1,4980\ [-]$$

Which is quite high, but as it is first estimation of a symmetrical polar it can be expected and P_{min} are usually very close to the critical C_L. For the VTOL it is then $C_{L_{P_{min}}} = 1,571\ [-]$.

Based on coefficient of lift it is possible to calculate loiter speed v_{loiter}

First v_{loiter} needs to be calculated for each configuration:

$$v_{loiter} = \sqrt{\frac{2 \cdot g \cdot MTOM}{\rho \cdot s \cdot \sqrt{3 \cdot \pi \cdot e \cdot \lambda \cdot C_{D_{min}}}}} \tag{3.19}$$

So for STOL it equals to:

$$v_{loiter} = \sqrt{\frac{2 \cdot 9,81 \cdot 10,45}{1,225 \cdot 0,817 \cdot \sqrt{3 \cdot pi \cdot 0.635 \cdot 15 \cdot 0.025}}}$$

$$v_{cruise} = 11,697\ [m/s]$$

And for VTOL $v_{loiter} = 11,421\ [m/s]$.
Now P_{min} is defined in [28] as:

$$P_{min_{ideal}} = min\left(\frac{C_{D_{min}}}{C_L^{\frac{3}{2}}}\right) \cdot \sqrt{\frac{2 \cdot (MTOM \cdot g)^3}{\rho \cdot s}} \tag{3.20}$$

Which is without propulsion efficiencies so the total P_{min} is:

$$P_{min} = \frac{P_{min_{ideal}}}{\eta_{prop} \cdot \eta_{elmotor}} \tag{3.21}$$

And for STOL it equals to

$$P_{min_{ideal}} = 0,0545 \cdot \sqrt{\frac{2 \cdot (10,45 \cdot 9,81)^3}{1,225 \cdot 0,817}} = 80,047\ [W]$$

And to

$$P_{min} = \frac{80,047}{0,6 \cdot 0,7} = 190,588\ [W]$$

VTOL configuration consumes in loiter $P_{min} = 195,184\ [W]$

3.4.3.3 Cruise

Will be defined as a regime based on lowest needed thrust, which is also a regime with low power consumption but a relatively high speed compared to loiter.

First v_{cruise} needs to be calculated for each configuration:

$$v_{cruise} = \sqrt{\frac{2 \cdot g \cdot MTOM}{\rho \cdot s \cdot \sqrt{\pi \cdot e \cdot \lambda \cdot C_{D_{min}}}}} \tag{3.22}$$

So for STOL it equals to:

$$v_{cruise} = \sqrt{\frac{2 \cdot 9,81 \cdot 10,45}{1,225 \cdot 0,817 \cdot \sqrt{pi \cdot 0.635 \cdot 15 \cdot 0.025}}}$$

$$v_{cruise} = 15,394\ [m/s]$$

And using 3.22 for VTOL $v_{cruise} = 15,031\ [m/s]$. Both estimated cruise speed are under 2 $[m/s]$ from the required cruise speed which will be considered as small enough difference considering the way propulsion efficiency progressed in experimental data 3.10 3.9.

The Thrust estimation itself is based on following equation also derived from [28]

$$T_{min} = \frac{MTOM \cdot g}{K_{max}} \tag{3.23}$$

where K_{max} is Glide Ratio (also GR) and is assumed as

$$K_{max} = max\frac{C_L}{C_D} \tag{3.24}$$

so for STOL are inputted these data

$$T_{min} = \frac{10,45 \cdot 9,81}{17,297} = 5,927\ [N]$$

Power needed for cruise flight regime is then calculated as per equation 3.14. Resulting values are in table 3.8.

Table 3.8 Needed power per regime in [W]

Regime	STOL	VTOL
Take Off and Landing	1554,3	3661,2
Cruise	260,668	266,954
Loiter	190,588	195,184

3.4.4 Battery Weight

In the table 3.8 we see the power needed for each regime multiplying those values by the time the drones spends in it (in hours) and adding them together results in the total power consumed by the drone in Watt hours [Wh] and from this value it is possible to calculate the weight of the battery.

Using the times specified in 3.16 and 3.5 it is possible to calculate total energy consumption per configuration per mission by following equation:

$$E_{tot} = P_{TO} \cdot t_{TO} + P_{crui.} \cdot t_{crui.} + P_{loi.} \cdot t_{loi.} + P_{Land} \cdot t_{Land} + P_{fix.} \cdot t_{tot} \tag{3.25}$$

So for example for STOL in Mission A the total power consumption would be (time in hours):

$$E_{tot} = 1554,3 \cdot 0,0056 + 260,668 \cdot 2,75 + 190,588 \cdot 0,25 + 1554,3 \cdot 0.0278 + 40 \cdot 3,033$$

$$E_{tot} = 937,627\ [Wh]$$

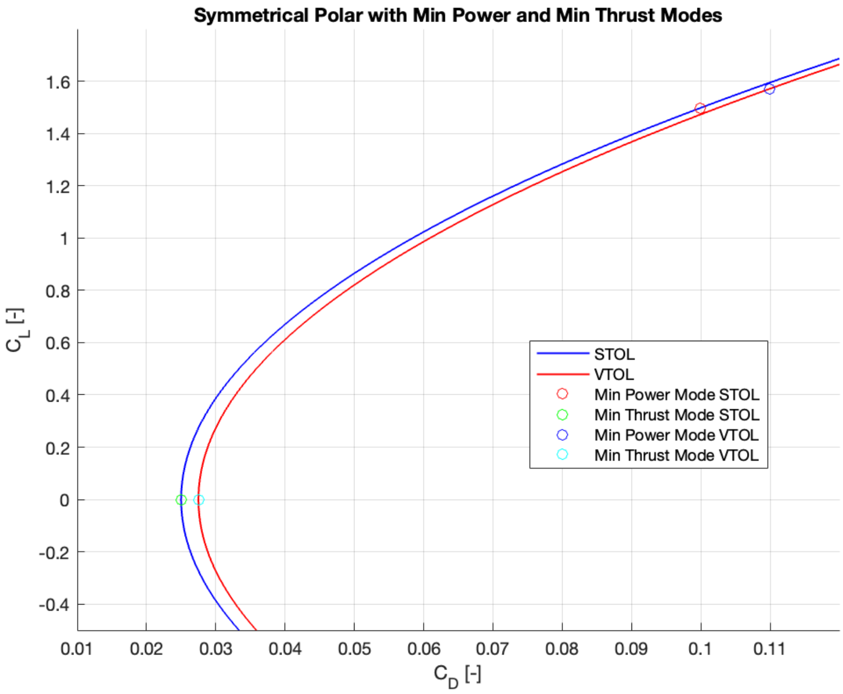

Figure 3.11 Symmetric Polar with flight regimes

Table 3.9 Energy consumption [Wh]

Mission	STOL	VTOL
A	937,627	995,449
B	779,947	833,967

Results for other configurations and Missions are in table .

Battery weight can then be estimated with the help of the assumed energy density.

$$m_{battery} = \frac{E_{tot}}{e} \; [kg] \tag{3.26}$$

Using the $e = 250 \; [Wh/kg]$ results in values in 3.10.

Table 3.10 Battery Weight [kg]

Mission	STOL	VTOL
A	3,751	3,982
B	3,120	3,336

For Mass Fraction calculations higher values per configuration will used (From Mission A).

3.4.5 Mass Fractions

Based on the estimated weight of batteries it is now possible to estimate new MTOM custom for each configuration. Mass Fractions are one of the classical approaches for first weight estimations [29].

As the MF are taken from VTOL drones a minimal mass fraction STOL will be used, as we can expect STOL will have much lower mass fraction towards air-frame and equipment (mainly propulsion) due to its much lower complexity compared to VTOL (no nacelles, extra motors etc. for VTOL regime).

First it is possible to estimate the new MTOM from the battery weight using Mass Fractions from table 2.3. For estimating parts of the aircraft the known mass needs to be just correctly multiplied or divided by the Mass Fraction. Example of MTOM estimation for STOL:

$$MTOM_{MF} = \frac{m_{battery}}{MF_{batteries}} \tag{3.27}$$

$$MTOM_{MF} = \frac{3,751}{0,384} = 8,960 \; [kg] \tag{3.28}$$

Rest of the estimate values is in the table. Due to the less complex nature of the STOL the minimal MF values were used in calculating the empty weight and the weight of equipment, where the equipment is the avionics and propulsion etc. and empty weight is air-frame weight plus the equipment. Also there was not any information about the payload weight for these drones and as such the payload weight is, after all MF are utilised for creating table 3.11, as:

$$m_{payload_{MF}} = MTOM_{MF} - m_{empty} - m_{battery} \tag{3.29}$$

Table 3.11 Mass Fraction Estimations [kg]

Weight type	STOL	VTOL
MTOM	9,767	10,369
m_{frame}	1,905	2,022
m_{empty}	4,210	4,863
$m_{equipment}$	2,178	2,945
$m_{payload}$	1,807	1,524

From this table you can see that the values do not add up perfectly as they are a combination from multiple drones, but they provide precise enough clue for the weight proportions of parts of the aircraft. With the much higher payload capacity (+50% and +80% respectively) it is possible to assume that utilising this MTOM for future calculation will provide some reserve in the way of thrust, endurance or the payload weight itself. It is also interesting how close is the first estimation from statistics (and MRA) and estimation based on Mass Fractions.

Chapter 4

Concept Definition

After finalising the weight estimation a conceptual study of the aerodynamic design and propulsion definition follows. From these more accurate data of weight estimation of all aircraft parts can be done as well as equipment (propulsion, avionics, controls etc.) and its position. From all the approximated part sizes a more accurate drag coefficient can be estimated. After getting Center of Gravity (CG) for each configuration a stability study and horizontal stabiliser sizing will be done.

4.1 Conceptual Aerodynamic Design

Before it is possible to choose airfoil a Reynolds number needs to be calculated as there is a huge performance gap between airfoils designed for low and high Reynolds number - *Re* (or Mach numbers etc.).

Figure 4.1 Concept design of STOL and VTOL configuration

4.1.1 Airfoil

To get relevant *Re* the Mean Aerodynamic Chord length needs to be calculated which is calculated from the root 4.1 and wing tip chord length. *eta* in following equations symbolises Taper Ratio. Lets start with root chord

$$b_r = \frac{2 \cdot s}{l} \cdot \frac{1}{1 + \eta_{wing}} \tag{4.1}$$

For values estimated from statistics

$$b_r = \frac{2 \cdot 0,817}{3,5} \cdot \frac{1}{1 + 0,5} = 0,311\ [m]$$

Now tip chord

$$b_t = b_r \cdot \eta_{wing} \tag{4.2}$$

$$b_t = 0,311 \cdot 0,5 = 0,156\ [m]$$

After these calculations it is possible to determine the b_{MAC}

$$b_{MAC} = \frac{2}{3} \cdot \left(b_r + b_t - \frac{b_r \cdot b_t}{b_r + b_t} \right) \tag{4.3}$$

Which equals to

$$b_{MAC} = \frac{2}{3} \cdot \left(0,311 + 0,156 - \frac{0,156 \cdot 0,156}{0,311 + 0,156} \right) = 0,242\ [-]$$

With all the information for *Re*

$$Re = \frac{v \cdot b_{MAC}}{\nu_{ISA}} \tag{4.4}$$

As the primary flight regime for the drones is loiter speed from battery weight estimation calculated here 3.22 is used. As the difference is very little between STOL and VTOL values used in equations in this section, there will be unusually calculated values for both configuration and instead just VTOL will be used as it will be assumed as the worse case.

$$Re_{MAC} = \frac{11,421 \cdot 0,242}{1,460 \cdot 10^{-5}} = 193860\ [-] \tag{4.5}$$

These are very low Reynolds numbers. For these numbers airfoils normally used (or historicaly) for gliders were recommended such as the Eppler and Wortmann series. Also the same as in equation 4.5 were calculated Re number for b_t and b_r to create an analysis with realistic range of Re number. The following airfoils were tested in software XFLR 5.

- Eppler 193
- Eppler 1200

- Eppler 387
- Eppler 68
- Wortman FX-63-145 (137)

Also other airfoils from these two series were analysed with their performance based on their graphs on Airfoil Tools [30] or on quick analysis in XFLR5, but were usually disregarded due to their problematic polars at Reynolds number close to the Re_{MAC}. Besides Re also Mach number M must be calculated. Speed of sound $a = 343$ $[m/s]$ for 20 $[°C]$ is used.

$$M = \frac{v}{a} = \frac{11,421}{343} \doteq 0,03\ [-] \tag{4.6}$$

For the analysis the setting used were accordingly to original XFOIL documentation [31]:

- $N - crit = 10$
- $T1$ as a polar type (constant speed and variable AoA)
- $M = 0,03\ [-]$ as Mach number

The $N - crit = 10$ $[-]$ selection was based on the table in [31] where values for the glider were 12-14, for motor gliders 11-13 and as this should have a wing close to motor gliders (for the high performance) the $N - crit$ was selected right under the motor glider, which falls in the category clean wind tunnels. Resulting comparison is in figure 4.2.

And XFLR generated graphs for the selected FX-63-145 4.3, which was selected for its $\frac{C_D}{C_L^{3/2}}$ values as well as the max lift performance. Biggest disadvantage of this airfoil is its high camber, which results in quite negative C_m and will result in bigger and heavier horizontal stabiliser.

To utilise data calculated in XFLR in the design of this drone, the results were done in $0,1$ $[^{\cdot}]$ step (for AoA) and imported to Excel, where a trend-line was created for most important coefficients as C_l, C_d and C_m.

Table 4.1 Important Values of FX63-145 for specific Re and M

Name	C_l $[-]$	C_d $[-]$	AoA $[°]$
$C_{l_{max}}$	1,525	0,0554	13,2
AoA_0	0,558	0,0160	0
$AoA_{Cl=0}$	0,006	0,0251	-4,8
$P_{min} = max\left(\frac{C_l}{C_d^{3/2}}\right)$	1,255	0,0203	6,7

Lift slope C_{l_α} $6,598$ $[1/rad]$

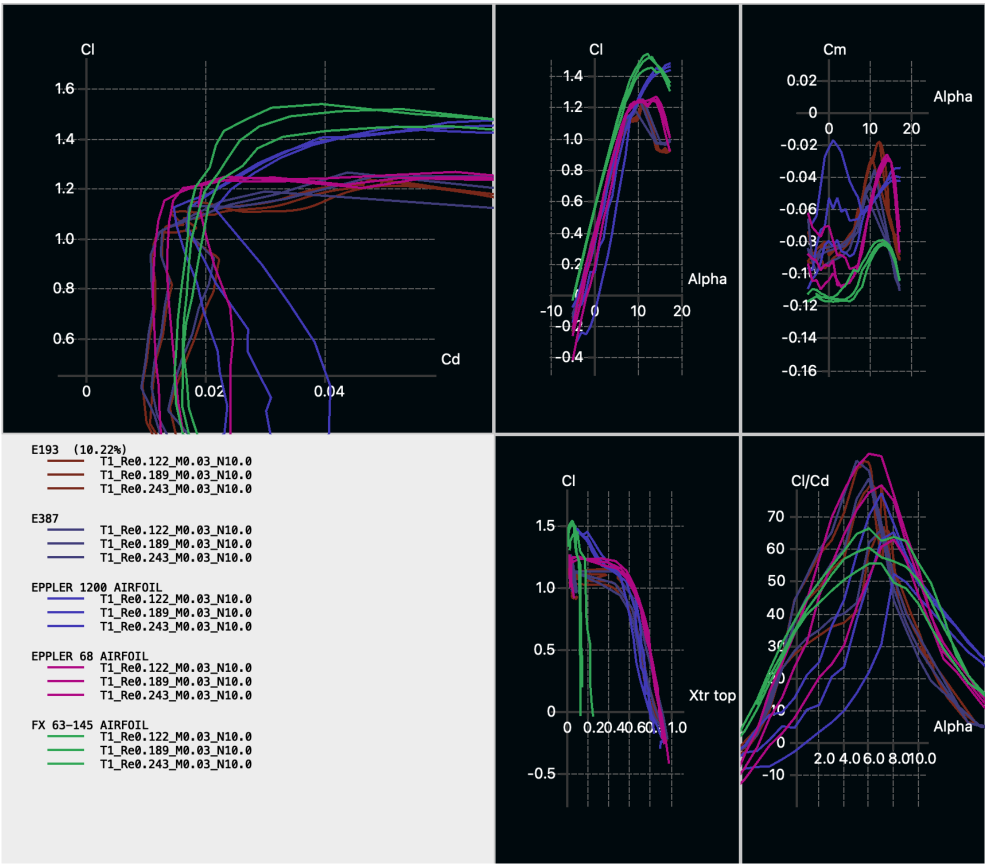

Figure 4.2 Comparison of best suited airfoils

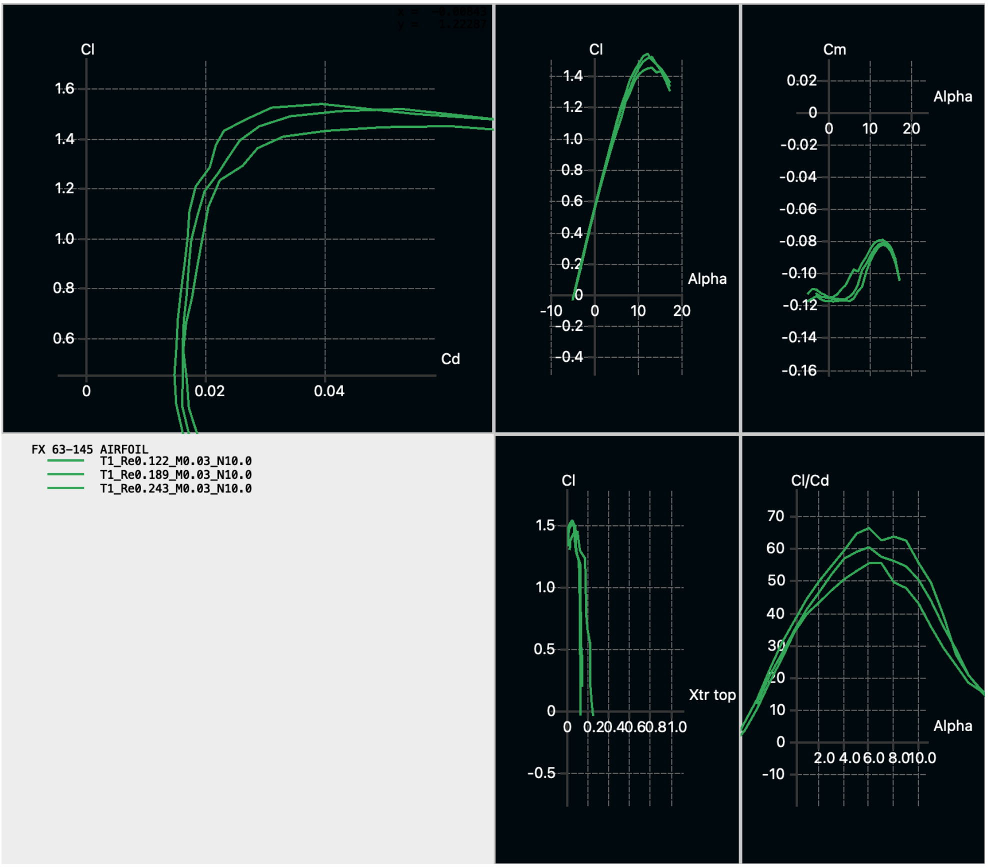

Figure 4.3 XFLR Analysis of FX-63-145

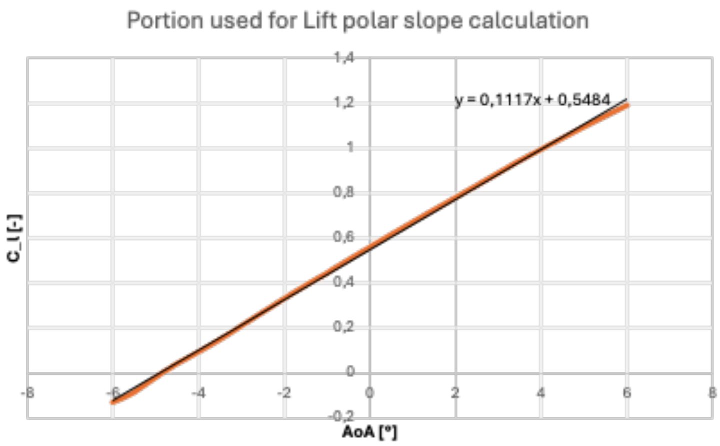

Figure 4.4 Isolated part of the FX63-145 lift polar used in estimating the lif slope for linear portion of the polar

4.1.2 Wing

First analytical estimation of C_L of the whole wing is done by following equation 4.7 where $K = 0.95$ $[-]$ for trapezoidal wing and maximal C_l are for $C_{l_{b_r}} = 1,542$ $[-]$ and for $C_{l_{b_t}} = 1,449$ $[-]$ (values from XFLR5).

$$C_{L_{max}} = \frac{C_{l_{b_t}} + C_{l_{b_r}}}{2} \cdot K = \frac{1,449 + 1,542}{2} \cdot 0,95 = 1,421 \; [] \tag{4.7}$$

Which is a first and very rough estimation of this coefficient. Lets now update the main geometries based on the more precise aerodynamic values. Lets keep AR the same as that can be a study of optimisation in Preliminary design. Recalculation of wing area s and wingspan l will now take place, as after all the weight and mission estimation/definition it is clear that the drone design will revolve around this regime. First the wing area

$$s = \frac{2 \cdot MTOM \cdot g}{C_{l_{P_{min}}} \cdot \rho \cdot v_{loiter}} = \frac{2 \cdot 10,369 \cdot 9,81}{1,255 \cdot 1,225 \cdot 11,421} = 0,989 \; [m^2] \tag{4.8}$$

Now the wingspan

$$l = \sqrt{\lambda \cdot s} = \sqrt{15 \cdot 0,989} = 3,851 \; [m] \tag{4.9}$$

Position of MAC on leading edge is [32] (assuming x is in the opposite of direction of flight and χ_{LE} which corresponds to $2,5$ $[degrees]$ as per symmetric leading and trailing edge by the axis running through middle points ($\chi_{1/2} = 0$ $[degrees]$ and previously selected geometry. Then for

$$x_{MAC} = \frac{0,5 \cdot l}{3} \cdot tan(\chi_{LE}) \cdot \left(\frac{b_r + 2 \cdot b_t}{b_t + b_r} \right) \tag{4.10}$$

And so

$$x_{MAC} = \frac{0,5 \cdot 3,851}{3} \cdot tan(2,5) \cdot \left(\frac{0,342 + 2 \cdot 0,171}{0,171 + 0,342} \right) = 0,0374 \; [m]$$

After these new values the chord lengths were recalculated accordingly by equations 4.1, 4.2 and 4.3. Now with the recalculated wing geometry a whole wing was modeled in XFLR5 and analysed.

In table 4.2 the values for $AoA_{Cl=0}$ were approximated (no point in calculating C_D) in the assumption the lift polar will have linear characteristic even at that point. Interesting thing to note is more than 100% increase in drag coefficient for P_{min} regime.

Before its used in further design it is a good practise to compare it with analytical methods most importantly the wing lift slope.

Also as the VTOL configuration is not limited by minimal speed, as there is not a certification requirement nor runway length there is no need for (positive) flaps that would augment the lift. Based for STOL, based on the limitation from [32], where the hand launched UAVs are described as being under

Table 4.2 Important Wing Values for $v = 11,42\ [m/s]$

Name	$C_L\ [-]$	$C_D\ [-]$	$AoA\ [°]$
$C_{l_{max}}$	1,476	0,0554	14,4
AoA_0	0,443	0,0202	0
$AoA_{Cl=0}$	0,006	-	-4,56
$P_{min} = max\left(\frac{C_l}{C_d^{3/2}}\right)$	1,141	0,0479	7,5

Lift slope C_{l_α}	$5,496\ [1/rad]$

$MTOM = 20\ [lbs]$ and wingspan under $l = 10\ [ft]$. Even if here designed drone has slightly larger wingspan, typical hand launched UAV does not have excess of power for rapid climbs, which our configuration is based around and as will be discovered in following sections will consist of multiple electric motors and propellers. However at this point it was noted a usage of negative simple flap would be beneficial for higher cruise speed and thus better performance in bad weather and strong winds and its use is planned for Preliminary Design, but due to the limitation of final thesis this flap description will stay as a starting point for another possible academic work.

4.1.2.1 Analytical

The wing lift slope is defined as [33]

$$C_{l_{\alpha_w}} = \frac{2 \cdot \pi \cdot \lambda}{2 + \left(\frac{\lambda^2 \cdot \beta}{k^2} \cdot (1 + \frac{tan^2(\chi_{1/2})}{\beta^2}) + 4\right)} \tag{4.11}$$

coefficients β and k needs to be calculated first from the Mach number

$$\beta = (1 - M^2)^{1/2} = (1 - 0,03^2)^{1/2} = 0,9994\ [-] \tag{4.12}$$

And for k a C_l adjusted for the correct Mach number is calculated just to follow the analytic approach through (separate batch analysis was done without the Mach number resulting in $C_{l_\alpha} = 6,59498$ - difference in thousandths).

$$C_{l_{\alpha_{w\ at\ M}}} = \frac{C_{l_\alpha}}{\sqrt{1 - M^2}} \tag{4.13}$$

After inputting all the needed values

$$C_{l_{\alpha_{w\ at\ M}}} = \frac{6,595}{\sqrt{1 - 0,03^2}} = 6,5987\ [1/rad] \tag{4.14}$$

And k is calculated by

$$k = \frac{C_{l_{\alpha_{w\ at\ M}}}}{2 \cdot \pi} = \frac{6,5987}{2 \cdot \pi} = 1,0502\ [-] \tag{4.15}$$

Now it is possible to calculate $C_{l_{\alpha w}}$ by equation 4.11

$$C_{l_{\alpha w}} = \frac{2 \cdot \pi \cdot 15}{2 + \left(\frac{15^2 \cdot 0{,}9994}{1{,}0502^2} \cdot (1 + \frac{tan^2(0)}{0{,}9994^2}) + 4\right)} = 5,742\ [1/rad] \tag{4.16}$$

4.1.2.2 XFLR5

For a previously described wing an LLT, wing planform and for fixed speed of $11,42\ [m/s]$ (v_{loiter}). More information in figure: Where also an expected flow separtion can be seen.

The resulting $C_{l_{\alpha w}} = 5,4962$ which result in difference between analytical and XFLR5 approach as

$$\Delta C_{l_{\alpha w}} = C_{l_{\alpha w_{Analy}}} - C_{l_{\alpha w_{XFLR}}} = 5,742 - 5,496 = 0,246\ [-] \tag{4.17}$$

Which is $4,3\%$ difference and as it is under 5% we can assume those values are similar enough and the use of only XFLR5 data should not lean far from the analytical approach. XFLR5 results are preferred compared for the number of values and possible approximation of all the main coefficient for the whole wing or its root or tip.

Lift slope of wing and fuselage needs to be adjusted for the fuselage diameter $d_f = 0,16\ [m]$.

$$C_{l_{\alpha wf}} = K_{wf} \cdot C_{l_{\alpha w}} \tag{4.18}$$

Coefficient adjusting the wing slope is calculated as

$$K_{wf} = 1 + 0,025 \cdot \frac{d_f}{l} - 0,25 \cdot \left(\frac{d_f}{l}\right)^2 = 1 + 0,025 \cdot \frac{0,16}{3,851} - 0,25 \cdot \left(\frac{d_f}{l}\right)^2 \tag{4.19}$$

$$= 1,0006\ [-]$$

So with the fuselage considered the lift slope is

$$C_{l_{\alpha wf}} = 1,0006 \cdot 5,496 = 5,4996\ [1/rad]$$

After this, it is possible to calculate the wing incidence, the angle between the root chord and the fuselage axis. Even if the primary regime is loiter the incidence will be set in such a way that fuselage should be leveled during cruise. If we calculate the needed C_L for v_{cruise} with the latest iteration of geometries in equation for C_l 3.4.2 the result will be $C_L = 0,566\ [-]$. Inverting the equation for calculating C_L for the linear part of lift polar defined as equation 4.20 based on figure 4.6.

$$C_{L_{lin}} = 0,0967 \cdot AoA + 0,4415 \tag{4.20}$$

We can calculate the incidence α_{inc_w} as

$$\alpha_{inc_w} = \frac{C_L - 0,4415}{0,0967} = 1,287\ [°]$$

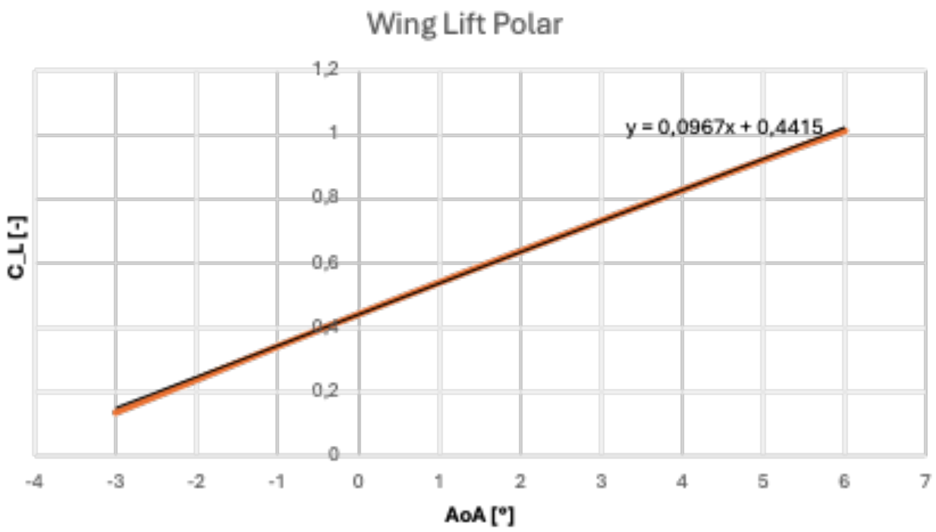

Figure 4.5 Isolated part of wing lift polar used in estimating the lift slope of the linear portion of the polar

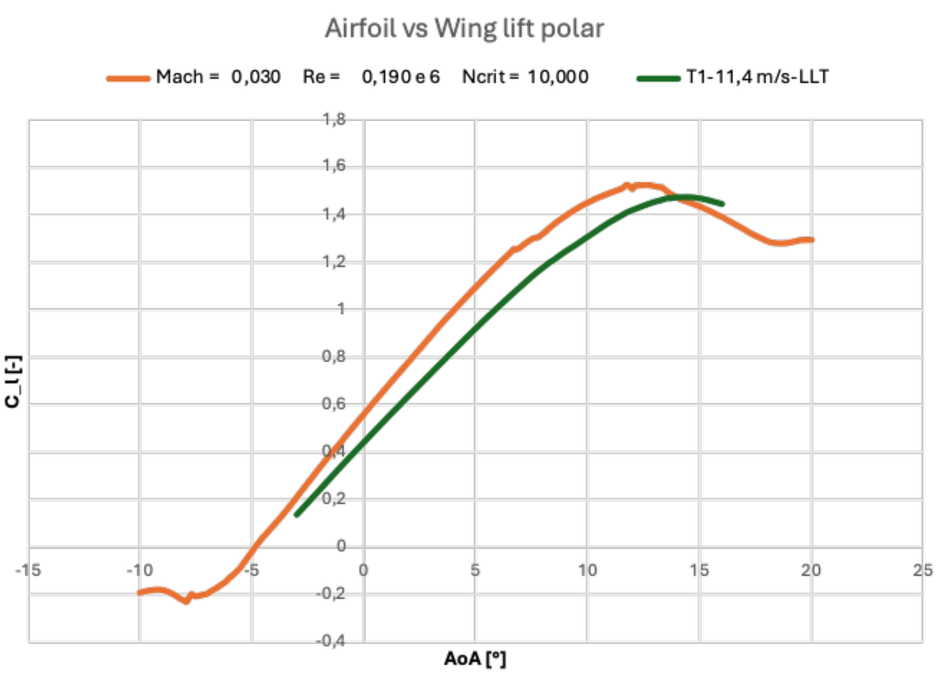

Figure 4.6 Comparison of Wing and Airfoil lift polar

The first estimation of Aerodynamic Center is as $1/4b_{MAC}$. Based on statistics and first sketches the following dimensions were estimated, although the horizontal stabiliser was calculated by 4.22. Following are some values concerning tail. For both horizontal and vertical was used airfoil $NACA$ 0012 with $C_{l_{h_\alpha}} = 3,0825$ $[1/rad]$.

- $b_f = 0,15$ $[m]$ Fuselage Width
- $h_f = 0,17$ $[m]$ Fuselage Height
- $l_{fn} = 0,26$ $[m]$ Fuselage Nose length
- $s_h = 0,122$ $[m]$ Horizontal stabiliser area 4.21
- $\lambda_h = 5$ $[-]$ Aspect Ratio
- $l_f = 1,35$ $[m]$ Fuselage length
- $t/c_m = 0,145$ $[-]$ Maximum wing thickness ratio
- $l_H = 0,770$ $[m]$ Span of the Horizontal Stabiliser 4.22
- $l_h = 0,951$ $[m]$ arm between $b_{MAC_{1/4}}$ and $b_{h_{MAC_{1/4}}}$
- $b_{t_h} = 0,116$ $[m]$ Tip Chord length (Hor. Stab.)
- $b_{r_h} = 0,193$ $[m]$ Root Chord length (Hor. Stab.)
- $t_{r_h} = 0,023$ $[m]$ Max. root chord thickness (Hor. Stab.)
- $\eta_h = 0,6$ $[-]$ Taper ratio (Hor. Stab.)

Aspect ratio should be lower than with the wing so a conservative number was selected [33]. Also later will be revealed why the arm l_h has such a specific number and won't aid with the horizontal stabiliser volume sizing as it also plays create role in weight and balance but most importantly the balance in thrust for VTOL propeller placement. Lower are some calculations needed for the values in the list above. Specifically for horizontal stabiliser area

$$s_h = s \cdot \frac{s_h}{s} = 0,989 \cdot 0,12 = 0,119\ [m^2] \tag{4.21}$$

and for horizontal stabiliser area

$$l_H = \sqrt{\lambda_h \cdot s_h} = \sqrt{5 \cdot 0,122} = 0,78\ [-] \tag{4.22}$$

Chord lengths are calculated the same way as for the wing 4.1 4.2. Vertical stabiliser would need either statistics, which there was very little available data (drawings or pictures) for or based around another feature. Due to the following design choice in the propulsion configuration, the height of the vertical stabiliser was estimated separately for STOL and VTOL and in the way that would allow mounting of a respective propeller on the tail while its center being on T-tails intersection. These values were then collected from this design

- $h_{v_{STOL}} = 0,218$ $[m]$ Height of vertical stabiliser for STOL
- $h_{v_{VTOL}} = 0,256$ $[m]$ Height of vertical stabiliser for VTOL
- $b_{r_h} = 0,192$ $[m]$ Root chord length (Vert. Stab.)
- $b_{t_h} = 0,172$ $[m]$ Tip chord length (Vert. Stab.)
- $t_{r_h} = 0,023$ $[m]$ Max. root chord thickness (Vert. Stab.)

4.2 Propulsion

One of the most important topics of the conceptual study is the propulsion for this drone as the two main concepts very mainly in this field and in features dependent on propulsion. From Mission definition it is known at which thrust (power setting) each configuration needs to be the most effective and at which it needs to be able to provide the total maximum thrust. Based on these requirement a combination of electric motors, propellers and ESC (Electric Speed Controllers) needs to be selected. For the ESC it is known from, the research and manufacturers tech sheets, that for our battery pack (or more accurately to battery pack with similarly energy capacity to our ideal battery pack) would need to be at least 60 $[A]$ for ”smaller” motors and 80 $[A]$ for ”bigger” ones.

4.2.1 Propulsion research

To have the best possible propulsion it is not enough to look at the efficiency of each propulsion part but also at their specific power (weight based power) and number of subsequent parts that needs to follow. Originally a wider research (in the sense of manufacturers) was planned, but the information provided by most manufactures was not sufficient. The two manufacturers providing sufficiently detailed technical specifications were manufactures SunnySky [34] and T-Motors [35]. Different parameters about 45 different electric motors were collected and some of their averages are in 4.3.

Also worth noting that in the spec. sheets was not estimated speed so it is assumed it is all static thrust. Here 4.7 4.8 are some trend-lines that can guide the configuration in more specific direction. In both of these we can see that the heavier the electric motor the higher the specific thrust. Based on this information it would be ideal to mount fewer engines and thus not experiment with abominations with number of motors in double digits.

Scatter in 4.7 is quite significant and as such the trend-line should be used very cautiously.

From the figure 4.8 it is possible to observe the thrust ratio between the maximal thrust and recommended thrust as $\frac{T_{Rec}}{T_{Max}} = 0,293$ $[-]$.

Table 4.3 Average values of researched electric motors

Name	Units	Average
Weight	g	188,180
Max Cont. Power	W	1165,267
Max F/Mass	N/g	0,265
Specific power	P/g	6139,034
Max F	N	51,745
Rec F	N	16,075
Price	USD	115,956
KV	rpm/V	571,444

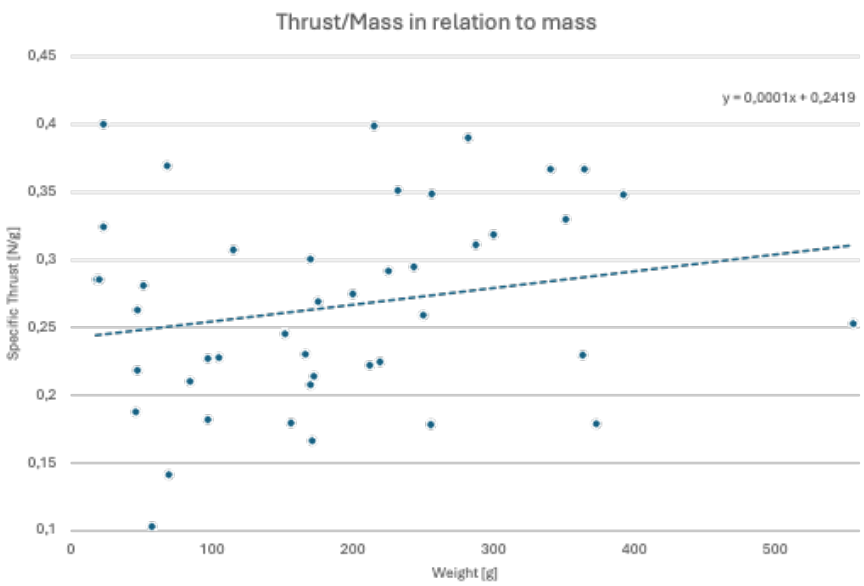

Figure 4.7 Specific Thrust (Thrust/Mass) in relation to Mass

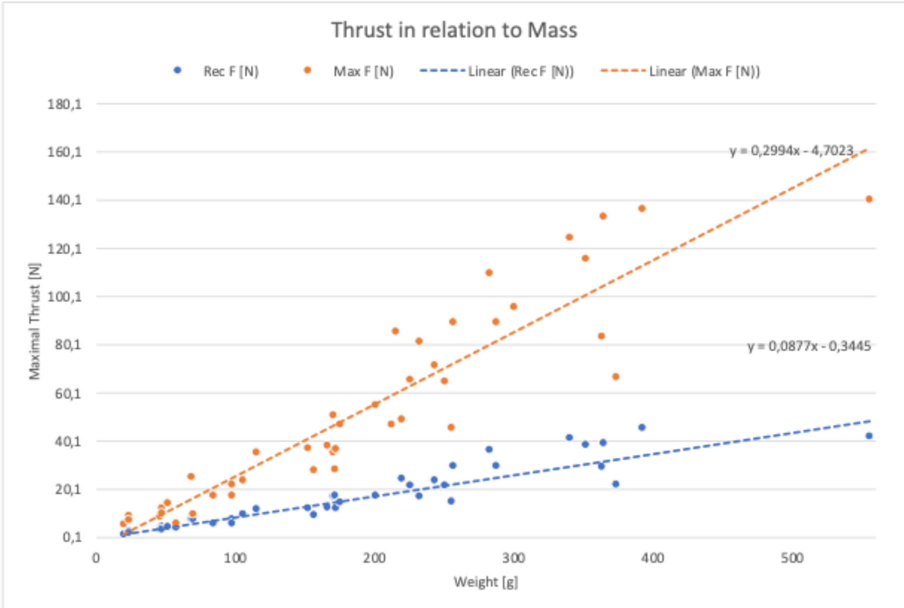

Figure 4.8 Thrust in relation to mass

4.2.2 Propulsion configuration

As the available data for motors was mostly in thrust the thrust values it is needed to satisfy are in table.

These thrust needs are satisfied by all the combinations in the graph. As just one electric motor wont suffice for both the take-off/landing and loiter as the difference is too great to have an electric motor with the highest efficiency at loiter and max. thrust at take-off at least two engines will be needed. For VTOL this number raises to three as two motors would be either problematic for stability, if both are the same size, or the bigger VTOL motor would have such a high torque that it would need a tail rotor similarly to conventional helicopters.

For the STOL was selected the 3rd configuration as is seen in the 4.9. Worth mentioning is the configuration with single motor, which would have abundance of power for loiter however it would allow for lighter air-frame as only only one position would need to be strengthen and enlarged for electric motor positioning.

The first two VTOL configurations, that are resulting in the lowest weights are two small motors (their combined recommended thrust would be enough for loiter) and one which would do most of the heavy lifting for VTOL. These are however problematic and just their positioning on air-frame would require unconventional wing and fuselage geometry. Combinations number 4, 7 and 8 are all mode with one engine type. Configuration 7 uses an electric motor with very high thrust to weight ratio and us such the initial weight seems

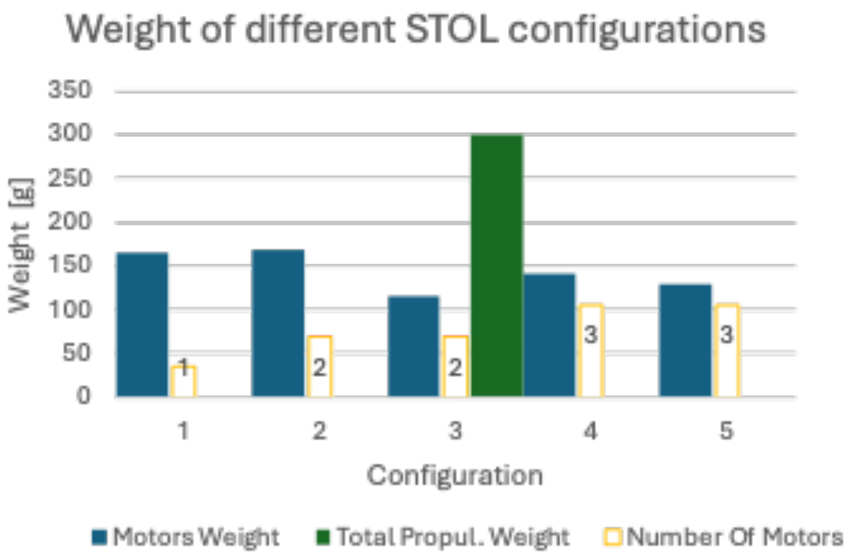

Figure 4.9 Different electric motor configurations and number of motors in them for them (STOL)

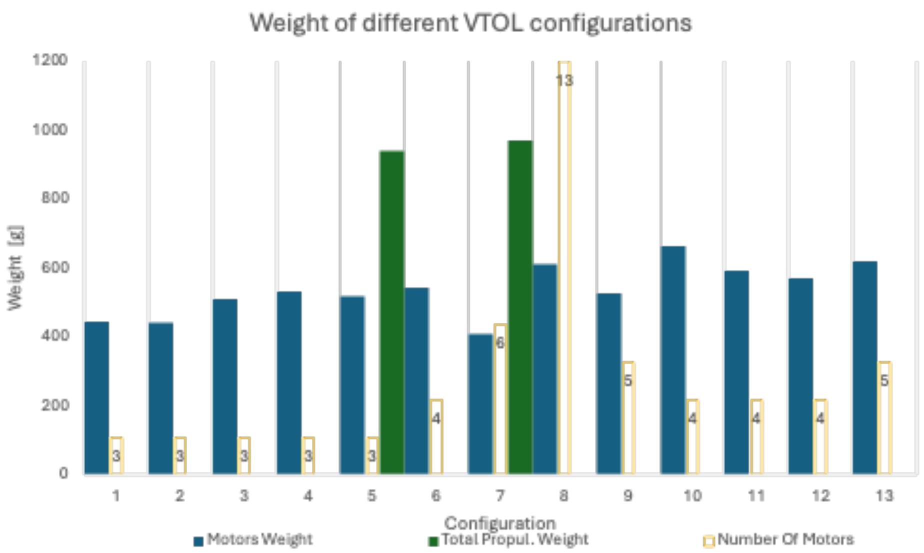

Figure 4.10 Different electric motor configurations and number of motors in them for them (VTOL)

quite promising. However each motor needs an ESC and the ones needed are $60 - 80$ $[A]$ the ESC itself weighs more than the motor. The lowest total weight then comes for the configuration number 5, which uses 2 heavy motors for VTOL and one for loiter. All the configurations are described in detail in the Excel spreadsheet attachment.

The resulting configurations are in the following table 4.6. In it it is possible to observe that the SunnySky V4006 was particularly popular choice as its recommended thrust was just 1-2 newtons above for the $P_m in$ and always had a small reserve during the numerous iterations the whole design went through.

Table 4.4 Selected electric motors for each concept configuration

Concept	Max. T [N]	Rec. T [N]	Motor name	No.	Mass [g]
VTOL	25,11	7,85	SunnySky V4006	1	68
	65,53	21,84	T-Motor MN505-S	2	225
STOL	25,11	7,85	SunnySky V4006	1	68
	12,36	4,415	SunnySky V2806	1	47

Other components accounted into the total (propulsion) weight were ESCs and propellers. Propulsion solution is in the table lower 4.5.

Table 4.5 Total propulsion weight

Config	VTOL		STOL	
	Name	Mass [g]	Name	Mass [g]
1st Propel.	(2x) 22x8 folding	60	CN15x5,5	21
2nd Propel.	CN15x5,5	21	CN12x5	17,5
ESC I.	80A 12S	110	60A 12S V1.2	73
ESC II.	60A 12S V1.2	73	60A 12S V1.2	73
Motors		518		115
Total		**952**		**299,5**

4.2.2.1 VTOL balance

For the correct balance during VTOL, the resulting thrust force must be at the same spot as the center of gravity of the whole aircraft. By manual iteration following positions were selected. As during VTOL maximal thrust (or close to it) is excepted, these forces were used in balancing. As a Fuselage Station (FS) 0 was selected a plane 500 $[mm]$ from the tip of the wing root chord leading edge.

Also a significant distance from the symmetry axis is used for each VTOL engine to ensure stability, particularly Butt Line $BL = 0,77$ $[m]$ was used for motor placement.

Table 4.6 Motor positioning on VTOL

Motor	Arm to FS 0 [m]
MN505	0,362
V4006	1,283

4.3 Weight Estimation and CG location

Before the Aerodynamic design can be finished a more precise position of the CG needs to be defined. For this reason a calculation of all the air-frame parts is done and also the positioning of all the needed equipment.

4.3.1 Parts weight estimation

First and the most important part is the wing. As the drone isn't a high performance one it would be naive to assume very low G loading as a drone with such a low MTOM and Wing loading will be heavily influenced by wind gust. As such the loading is selected as $n_{ult} = 5\ [-]$.

4.3.1.1 Wing

The wing CG is from statistic [36] usually between 38 − 42%. For this design a 40% is selected. The distance from $FS = O$ is

$$x_w = 0,4 \cdot b_r + 0,5 = 0,4 \cdot 0,3423 + 0,5 = 0,6369\ [m] \tag{4.23}$$

First approach is an approach developed by the Cessna corp. [36] for general aviation airplanes (low performance under 200 [kts]) with cantilever wing (not a strut-braced one)

$$m_{w_{cessna}} = 0,04674 \cdot MTOM^{0,397} \cdot s^{0,36} \cdot n_{ult}^{0,397} \cdot \lambda^{1,712} \tag{4.24}$$

All the inputs are in imperial units

$$m_{w_{cessna}} = (0,04674 \cdot (10,369 \cdot 2,2046)^{0,397} \cdot (s \cdot 10,764)^0, 36 \cdot n_{ult}^{0,397} \cdot \lambda^{1,712}) \cdot \frac{1}{2,2046}$$

$$m_{w_{cessna}} = 33,93\ [kg]$$

Which is not a realistic value.

Another approach for wing estimation is based on calculations from different US military branches. First one is USAF estimation [36] (for light and utility aircraft with speeds under 300 [kts].

$$m_{w_{USAF}} = 96,948 \left[\left(\left(\frac{MTOM \cdot n_{ult}}{10^5} \right)^{0,65} \cdot \frac{\lambda}{cos(\chi_{1/4})^{0,57}} \cdot \left(\frac{s}{100} \right)^{0,61} \right) \cdot \left(\frac{1+\eta_w}{2 \cdot t_{r_w}} \right)^{0,36} \cdot \sqrt{1 + \frac{v_h}{500}} \right]^{0,993} \tag{4.25}$$

where v_h is never exceed which was selected for this design as $v_h = 25\ [m/s]$ however in the equation it is used in knots. And the t_{r_w} is thickness to chord length ratio which is for FX63-145 $t_{r_w} = 0,145\ [-]$

$$m_w = 96,948 \left[\left(\left(\frac{10,369 \cdot 5}{10^5} \right)^{0,65} \cdot \frac{15}{cos(1,3)^{0,57}} \cdot \left(\frac{1,014}{100} \right)^{0,61} \right) \cdot \left(\frac{1+0,5}{2 \cdot 0,145} \right)^{0,36} \cdot \sqrt{1 + \frac{25 \cdot 1,9438}{500}} \right]^{0,993}$$

$$m_{w_{USAF}} = 1,263\ [kg]$$

From the Navy branch an equation for fighter and attack airplanes [36] was used, where K_w is coefficient differentiating between aircraft with wing sweep or without, for this design $K_w = 1\ [-]$

$$m_{w_{USN}} = \cdot \left[\left(\left(\frac{K_w \cdot n_{ult} \cdot MTOM}{t_{r_w}} \cdot \left(\frac{tan(\chi_{LE}) - 2 \cdot (1 - \eta_w)}{\lambda \cdot (1 + \eta_w)} \right)^2 + 1 \right) \cdot 10^{-6} \right)^{0,464} \right] \cdot$$

$$\cdot 19,29 \cdot ((1 + \eta_w) \cdot \lambda)^{0,7} \cdot s^{0,58} \tag{4.26}$$

As the inputted information as in the previous equations, besides mentioned coefficient, the result is

$$m_{w_{USN}} = 0,356\ [kg]$$

Which is also quite unrealistic. Based on composite gliders Gerard derived following equation [37] [32]:

$$m_{w_{Gliders}} = 0,0038 \cdot (n_{ult} \cdot MTOM)^{1,06} \cdot \lambda^{0,38} \cdot s^{1/4} \cdot (1 + \eta_w)^{0,21} \cdot t_{r_w}^{-0,14} \tag{4.27}$$

which is equal, for this design, to

$$m_{w_{Gliders}} = 0,0038 \cdot (5 \cdot 10,369)^{1,06} \cdot 15^{0,38} \cdot 1,014^{1/4} \cdot (1 + 0,5)^{0,21} \cdot 0,145^{-0,14}$$

$$m_{w_{Gliders}} = 1,001\ [kg]$$

As the most probable ones are USAF 4.3.1.1 and Gerard 4.29 so average between them will be used in future calculation.

4.3.1.2 Fuselage

From Roskam [36] a CG position of fuselage is estimated as $x_f = 0,727\ [m]$ from $FS = 0$. It is defined as fraction of fuselage length (selected fraction $0,40\ [-]$). First used will be the USAF method for light and utility aircraft under 300 [kts]

$$m_{f_{USAF}} = 200 \cdot \left[\left(\frac{MTOM \cdot n_{ult}}{10^5} \right)^{0,286} \cdot \left(\frac{l_f}{10} \right)^{0,857} \cdot \left(\frac{b_f + h_f}{10} \cdot \frac{KEAS}{100} \right)^{0,338} \right]^{1,1} \tag{4.28}$$

One of the specifics of this calculation is using cruise speed v_c in $KEAS$ (Knots Equivalent Air Speed) which is calculated by this equation 4.3.1.2 and where $1,94384$ is used to convert m/s to $knots$.

$$v_{c_{KEAS}} = \sqrt{\frac{\frac{1}{2}\cdot\rho\cdot v_c^2}{\rho}})\cdot 1.94384 = \sqrt{\frac{\frac{1}{2}\cdot 1,225\cdot 17^2}{1,225}})\cdot 1.94384 = 23,367\ [kts]$$

Also all the other values are in imperial units

$$m_{f_{USAF}} =$$

$$200\cdot\left[\left(\frac{10.37\cdot 2,2\cdot 5}{10^5}\right)^{0,286}\cdot\left(\frac{1,35\cdot 3,281}{10}\right)^{0,857}\cdot\left(\frac{0,15\cdot 3,281+0,17\cdot 3,281}{10}\cdot\frac{23,4}{100}\right)^{0,338}\right]^{1,1}$$

$$m_{f_{USAF}} = 0,538\ [kg]$$

From Gunndlach [32] (6.40) is fuselage estimated by following equation

$$m_{f_{Gundlach}} = 0,5257\cdot F_{MG}\cdot F_{NG}\cdot F_{Press}\cdot F_{VT}\cdot F_{Matl}\cdot l_f^{0,3796}\cdot(W_{Carried}\cdot n_{ult})^{0,4863}\cdot KEAS^2 \quad (4.29)$$

Where these values replaced variables:

- $F_{MG} = 1\ [-]$ as the landing gear is not on fuselage
- $F_{NG} = 1,04\ [-]$ as the nose (tail) gear will be on fuselage
- $F_{press} = 1\ [-]$ for unpressurised cabin
- $F_{VT} = 1\ [-]$ as vertical is not included
- $F_{Matl} = 2\ [-]$ as the material is yet unknown (fiber glass = 2, carbon fibre = 1)
- $W_{carried} = m_{payload} + m_{battery} + \frac{1}{2}\cdot m_{equipment} = 5,23\ [kg]$

And all was inputted in imperial units

$$m_{f_{Gundlach}} = 0,5257\cdot 1\cdot 1,04\cdot 1\cdot 1\cdot 2\cdot 4,429^{0,3796}\cdot(11,534\cdot 5)^{0,4863}\cdot 23,37^2 = 7564\ [lbs] = 3431\ [kg]$$

These results are completely off and will not be used. USAF result will be used for future calculations even if they seem a little too optimistic.

4.3.1.3 Empennage

From Gundlach [32] an equation was used for the whole empennage and from Roskam a USAF method that separately solves weight for vertical and horizontal stabiliser. First the whole approach

$$m_{empennage} = WA_{Emp}\cdot s_{Emp} \quad (4.30)$$

Where the the WA_{Emp} is the aerial weight in pounds per square feet, which is for tactical UAS recommended as $WA_{Emp} = 0,5\ [lb/ft^2]$. And the total empennage surface is estimated as

$$s_{Emp} = s_h + s_v = 1,45\ [ft^2] \tag{4.31}$$

Which results in

$$m_{empennage} = 0,5 \cdot 1,45 = 0,724\ [lbs] = 0,329\ [kg]$$

Calculated separately by USAF [36] the equation for horizontal stabiliser weight is

$$m_{h_{USAF}} = 127 \cdot \left[\left(\frac{MTOM \cdot n_{ult}}{10^5} \right)^{0,87} \cdot \left(\frac{s_h}{100} \right)^{1,2} \cdot 0,289 \cdot \left(\frac{l_h}{10} \right)^{0,458} \right] \tag{4.32}$$

Again everything in imperial units

$$m_{h_{USAF}} = 127 \cdot \left[\left(\frac{10,369 \cdot 2,2 \cdot 5}{10^5} \right)^{0,87} \cdot \left(\frac{0,122 \cdot 10,76}{100} \right)^{1,2} \cdot 0,289 \cdot \left(\frac{0,95 \cdot 3.28}{10} \right)^{0,458} \right]$$

$$m_{h_{USAF}} = 0,696\ [lbs] = 0,316\ [kg]$$

And for vertical tail section is by USAF method for airplanes with performance up to 300 [kts]

$$m_{v_{USAF}} = 98,5 \cdot \left[\left(\frac{MTOM \cdot n_{ult}}{10^5} \right)^{0,87} \cdot \left(\frac{s_v}{100} \right)^{1,2} \cdot 0,289 \sqrt{\frac{h_v}{0,12}} \right]^{0,458} \tag{4.33}$$

Again everything in imperial units

$$m_{v_{USAF}} = 98,5 \cdot \left[\left(\frac{10,369 \cdot 2,2 \cdot 5}{10^5} \right)^{0,87} \cdot \left(\frac{0,034 \cdot 10,76}{100} \right)^{1,2} \cdot 0,289 \cdot \sqrt{\frac{0.256 \cdot 3.28}{10}} \right]^{0,458}$$

$$m_{v_{USAF}} = 0,311\ [lbs] = 0,141\ [kg]$$

Comparison between the two approaches:

$$\Delta m_{Emp} = (m_{v_{USAF}} + m_{h_{USAF}}) - m_{emp_{Gundlach}} = (0,141 + 0,316) - 0,329 = 0,128\ [kg] \tag{4.34}$$

Or almost 39% increase between the methods. USAF is selected as more conservative approach and even if it might be heavier it is more in line of what can be generally expected.

4.3.1.4 Other

As nacelles and landing gear are a little bit more specific for this drone a fixed values was estimated for each feature based on experience and on research of part weights of landing gears from hobby markets for RC aircraft's. As calculations from Roskam [36] resulted in weight similar to the weight of the whole fuselage.

- $m_{n_{STOL}} = 0,015$ $[kg]$ Nacelles STOL - based on nacelle being only on tail in the intersection of vertical and horizontal stabilizer without any mechanisms
- $m_{n_{VTOL_w}} = 0,025$ $[kg]$ Nacelles STOL - nacelle being on tail in the intersection of vertical and horizontal stabilizer with convertiplane mechanisms
- $m_{n_{VTOL_t}} = 0,065$ $[kg]$ Nacelles STOL - nacelle being on with with convertiplane mechanisms for main VTOL motors

  For landing gear

- $m_{lg_{VTOL}} = 0,2$ $[kg]$ - as the landing gear needs to absorbed mostly vertical force during VTOL it can be relatively light (see landing gears on multicopters)
- $m_{lg_{STOL}} = 0,3$ $[kg]$ - this landing gear needs to withstand harsh belly landings and as such is estimated to be 50% heavier compared to VTOL

  Total weight of air-frame is sum of the calculated parts

$$m_{aiframe} = m_w + m_f + m_v + m_h + m_n + m_{lg} \tag{4.35}$$

Which for VTOL concept configuration is:

$$m_{aiframe_{VTOL}} = 1,132 + 0,538 + 0,141 + 0,316 + (2 \cdot 0,065 + 0,025) + 0,2$$

$$m_{aiframe_{VTOL}} = 2,481\ [kg]$$

And of the STOL is $m_{aiframe_{STOL}} = 2,302$ $[kg]$. Comparison of these air-frame weight with MF based ones in it table 4.7. The shown values are values by how much the detailed estimation was over the Mass Fraction one.

Table 4.7 Comparison of detailed weight estimation and Mass Fraction one

Configuration	Δ $[kg]$
VTOL	0,259
STOL	0,097

4.3.1.5 Equipment

The avionics package is assumed in [32] for tactical drones to weight 1 [lbs], based on in house calculation detailed in the table 4.8 the weight came out lower, however these calculations do not include any necessary cables, accessories, or possible modification that would definitely be needed for usage of off the shelf autopilot and even if a specifically designed autopilot would come to light, still it probably would not be that well weight optimised.

Other equipment that will be considered are parts of the propulsion that are specific for a configuration and are detailed in 4.5.

Table 4.8 Equipment shared between both configurations (*number differs for this one)

Name	Est. Weight [g]
Control + IMU	150
Antennas	15
Pitot tube	3
FPV camera	5
RTK	40
DroneTag Mini	37
Servomotors 17g	4 x 17
Servomotors 9g*	3 x 9
Sum	377

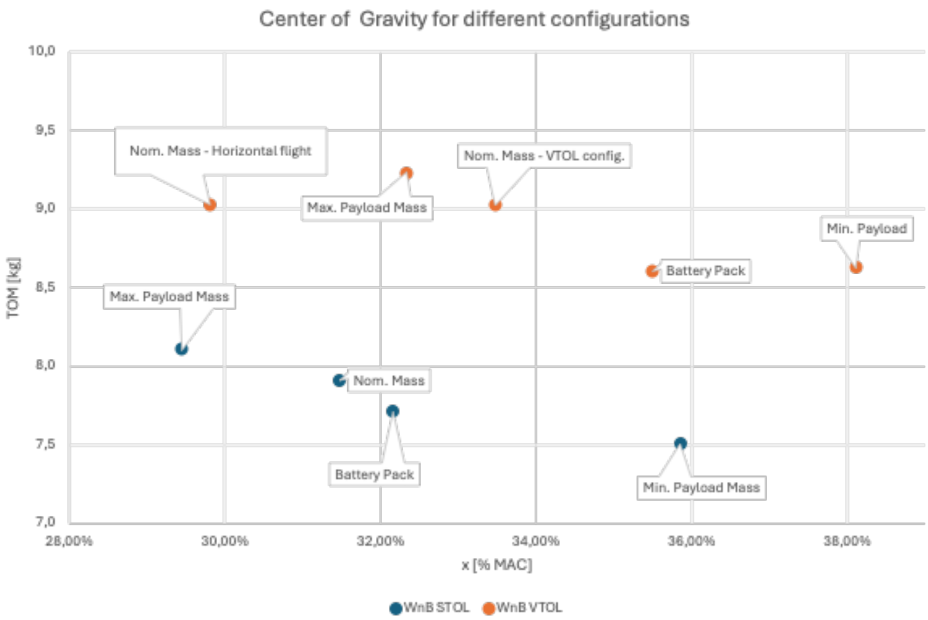

Figure 4.11 Weight and Balance of Concept designs

4.3.2 Center of Gravity

Based on concept design models and air-frame parts calculations a following weight configurations were considered

- Nominal weight (both STOL and VTOL) - estimated battery weights and 1 $[kg]$ payload
- Min. payload (both STOL and VTOL) - minimal estimated payload weight of 600 $[g]$
- Max. payload (both STOL and VTOL) - maximal theoretical payload
- Battery pack (both STOL and VTOL) - instead of designed battery a smaller off the shelf battery pack used
- VTOL - take-off and landing - CG of aircraft with motors positioned upwards

And their resulting position is in figure 4.11. From where the extremes used for horizontal stabiliser design are 4.9 and also the final weight distribution of the UAS is in graph 4.13 and their location in model is visualised in 4.12.

Unsurprisingly a less complex design allows for a lighter air-frame and propulsion and thus battery and payload takes even bigger part of the total MTOM.

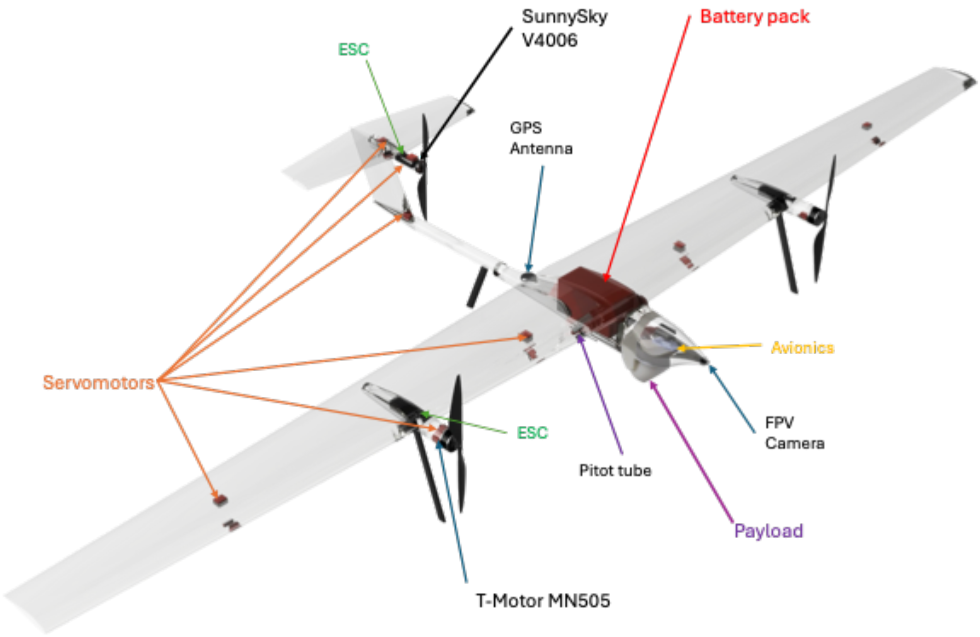

Figure 4.12 Transparent (air-frame from epoxy) VTOL Concept design with equipment location highlighted

Table 4.9 Limit CG positions

	Min. x_{cg}	Max. x_{cg}
STOL	29,45%	35,85%
VTOL	29,81%	38,11%

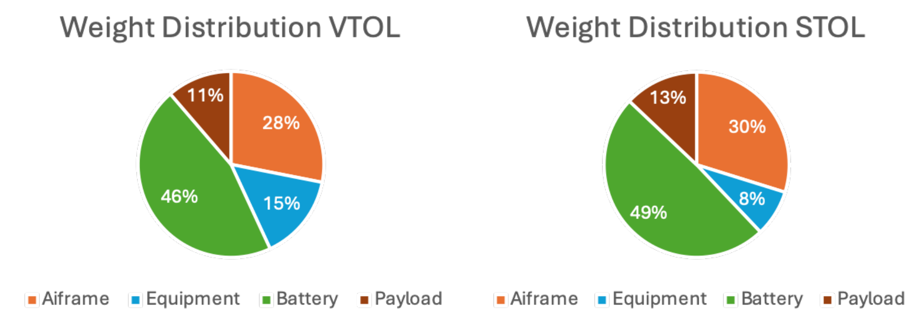

Figure 4.13 Type based Weight Distribution

4.4 Aerodynamic design - continued

Now with the location of the CG of the whole drone know it is possible to estimate the needed horizontal stabiliser size.

4.4.1 Horizontal stabiliser

The selected airfoil for horizontal stabiliser is $NACA$ 0012 with its lift polar slope being $C_{L_{\alpha_h}} = 3,083\ [1/rad]$. Some of the recommendations for stability margins. They are defined either by the distance between aerodynamic center x_{ac} and x_{cg} required to be at least 5% of b_{MAC} or $1,5 - 2$ % of l_h. First the position of the aerodynamic center needs to be estimated. For wing it is usually assumed to be in its $x_{ac_w} = 0,25\ [-]$. The aerodynamic center for wing and fuselage is calculated by this equation [27] [33]

$$\left(\frac{x_{ac}}{c}\right)_{wf} = \left(\frac{x_{ac}}{c}\right)_{w} + \frac{\Delta f_1 x_{ac}}{c} + \frac{\Delta f_2 x_{ac}}{c} \tag{4.36}$$

Where c is b_{MAC} and the last term $\frac{\Delta f_2 x_{ac}}{c}$ can be dismissed as its almost zero. Result for the second term is found by following relations

$$\frac{\Delta f_1 x_{ac}}{c} = \frac{1,8}{C_{L_{\alpha_{wf}}}} \cdot \frac{b_f \cdot h_f \cdot l_{fn}}{s \cdot b_{MAC}} \tag{4.37}$$

Which for VTOL is

$$\frac{\Delta f_1 x_{ac}}{c} = \frac{1,8}{5,499} \cdot \frac{0,15 \cdot 0,17 \cdot 0,26}{1,014 \cdot 0,2697} = -0,0079\ [-]$$

And thus

$$\left(\frac{x_{ac}}{c}\right)_{wf} = 0,25 - 0,0079 = 0,2421\ [-]$$

for STOL $(\frac{x_{ac}}{c})_{wf} = 0,2416\ [-]$. Now the exact values of the margins are (for VTOL shown)

$$\Delta_{rec} x_{ac} = 0,05 \cdot b_{MAC} = 0,05 \cdot 0,2697 = 0,0135\ [-] \tag{4.38}$$

And from l_h

$$\Delta_{sm} = 0,02 \cdot l_h = 0,02 \cdot 0,92 = 0,0184\ [-] \tag{4.39}$$

These margins will be used in further calcualtions.

Another recommendation is that l_h should be 2,5-3,5x larger than b_{MAC}, but as the l_h is already defined it is possible to check this rule straight away

$$\frac{l_h}{b_{MAC}} = \frac{0,92}{0,2697} = 3,41\ [-] \tag{4.40}$$

Based on this value our design should be at the upper limit. For further calculations a lift polar for whole aircraft with fixed control is assumed as

$$C_{L_\alpha} = 1,1 \cdot C_{L_{\alpha_{wf}}} = 1,1 \cdot 5,996 = 6,0495\ [1/rad] \tag{4.41}$$

With these values defined it is now possible to calculate needed horizontal stabiliser sizes for limit CG values.

4.4.1.1 Aft CG - stability

In this condition is explored what is the minimal needed A_h for the required longitudinal stability margin. As the l_h and b_{MAC} is known the A_h can be assumed as equal to $\frac{s_h}{s}$. The fraction between s_h and s in relation to the most aft CG is defined as

$$\frac{s_h}{s} = \frac{\frac{x_n}{c} - \left(\frac{x_{ac}}{c}\right)_{wf} + \Delta x_{sm}}{\frac{C_{L\alpha_h}}{C_{L_\alpha}} \cdot \left(1 \cdot \frac{d\epsilon}{d\alpha}\right) \cdot \frac{l_h}{c} \cdot \frac{q_h}{q}} \tag{4.42}$$

Where

- $\frac{x_n}{c} = \frac{x_{cg_{aft}}}{c} = 0,38$ most forward location for VTOL
- $\frac{q_h}{q} = 0,3\ [-]$ - flow retardation coefficient for T-tail
- $\frac{d\epsilon}{d\alpha} = 0,95\ [-]$ - down-wash effect coefficient for T-tail

So the resulting equation is

$$\left(\frac{s_h}{s}\right)_{aft} = \frac{0,3811 - 0,2421 + 0,0184}{\frac{3,083}{6.0495} \cdot (1 \cdot 0,3) \cdot 3,41 \cdot 0,95}$$

$$\frac{s_h}{s} = 0,1362\ [-]$$

For VTOL and for STOL $\frac{s_h}{s} = 0,117\ [-]$.

4.4.1.2 Fwd CG - stability

Second case deals with the up most forward CG (nose-heavy) and deals with the aircraft ability to balance it out. The equation for forward center of gravity 4.43 however requires a pitching moment coefficient c_{mac} which can be assumed based on the ΔC_l from flaps. However as the designed UAS does not utilises "classical" flaps (for take-off and landing) it will not be assumed this way and instead a coefficient of pitching moment of wing and fuselage will be used. These assumptions were done based on the supervisors recommendations.

$$\left(\frac{s_h \cdot l_h}{s \cdot c_w}\right)_{fwd} = \frac{\frac{-c_{mac}}{C_{Lmax}} + \frac{\Delta x_{cg_{fwd}} + \Delta x_{ac_{wf}} + \Delta x_{sm}}{c}}{\left(\left(1 - \frac{d\epsilon}{d\alpha}\right) \cdot \frac{C_{L\alpha_h}}{C_{L_\alpha}} - \frac{C_{L_h}}{C_{Lmax}}\right) \cdot \frac{q_h}{q}} \tag{4.43}$$

Where

- $c_{mac} = c_{m_{wf}}$ is assumed to be pitching coeff. of wing and fuselage
- $\Delta x_{sm} = 5\% b_{MAC} + 2\% l_h$ total stability margin
- C_{L_h} is minimal lift coefficient of the vertical stabiliser

The C_{L_h} can be assumed for a fixed horizontal stabiliser with aspect ratio $\lambda_h = 6\ [-]$ as

$$C_{L_h} = -0,35 \cdot \lambda_h^{1/3} = -0,35 \cdot 6^{1/3} = -0,863\ [-] \tag{4.44}$$

To keep calculation of pitching moment in stability section lets now use $c_{m_{wf}} = -0,113\ [-]$ and why it is such value will be explored in stability section.

The volume coefficient for horizontal stabiliser $A_H = \frac{s_h \cdot l_h}{s \cdot c_w}$ for fwd CG position now equals to

$$\left(\frac{s_h \cdot l_h}{s \cdot c_w}\right)_{fwd} = \frac{\frac{0,113}{1,4756} + 0,2945 - 0,2421 + 0,05 + 0,0184}{\left((1-0,3) \cdot \frac{3,083}{6,0495} - \frac{-0,863}{1,4756}\right) \cdot 0,95}$$

$$\frac{s_h}{s}_{fwd} = 0,0344\ [-]$$

For VTOL and for STOL $\frac{s_h \cdot l_h}{s \cdot c_w}_{fwd} = 0,0106\ [-]$. As both of those values are much lower than results for the first case, the first case results will be used. In the fig 4.14 is visualised the relation ship between CG position and the needed $\frac{s_h}{s}$ or A_h.

From the $\frac{s_h}{s}$ it is now possible to obtain the main horizontal stabiliser parameters, but first lets calculate the volume coefficient as it is the most common dimensionless value used for size comparison

$$A_h = \frac{s_h}{s} \cdot \frac{l_h}{b_{MAC}} = 0,136 \cdot 3,41 = 0,4646\ [-] \tag{4.45}$$

Which is right the lower end for general aviation [27]. The surface of the horizontal stabiliser now equals to

$$s_h = \frac{s_h}{s} \cdot s = 0,136 \cdot 1,0142 = 0,138\ [m^2]$$

and that is higher compared to the drones in statistics. This is the result of counting with lighter payload instead of using ballast. For the next iteration of the design a ballast approach seems more beneficial, or at least not considering a 40% lighter payload. The l_H is now

$$l_H = \lambda_h \cdot s_h = 6 \cdot 0,1382 = 0,777\ [m] \tag{4.46}$$

Also now it is possible to estimate the lift polar or the whole aircraft

$$C_{L_\alpha} = (C_{L_\alpha})_{wf} + C_{L_{\alpha_h}} \cdot \left(1 \frac{d\epsilon}{d\alpha}\right) \cdot \frac{s_h}{s} \cdot \frac{q_h}{q} \tag{4.47}$$

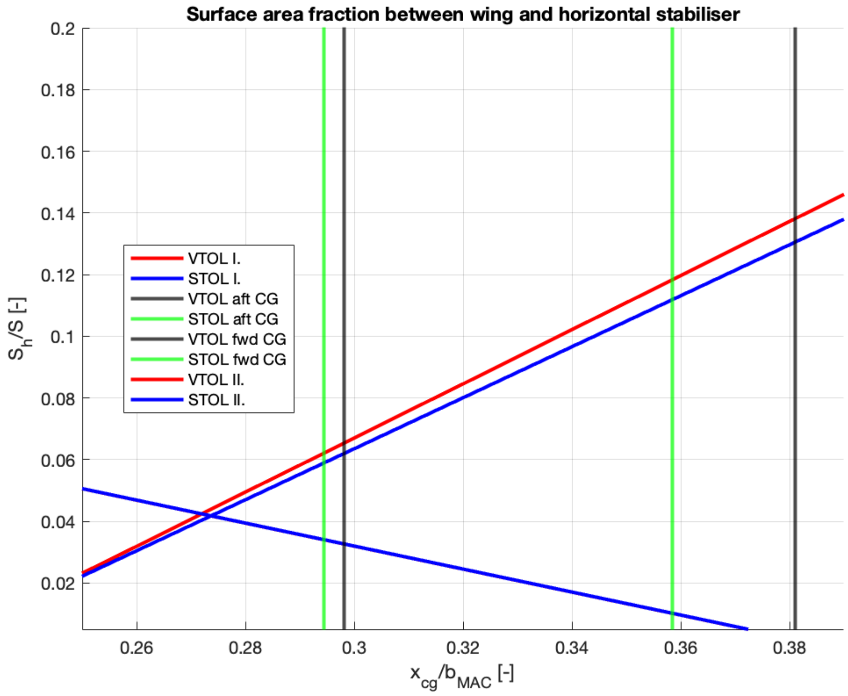

Figure 4.14 Relation of $\frac{s_h}{s}$ on CG location for both cases (II. cases are overlapping)

Resulting in

$$C_{L_\alpha} = 5,499 + 3,083 \cdot (1 + 0,3) \cdot 0.1362 \cdot 0,96 = 5,779\ [1/rad]$$

for VTOL and for STOL $C_{L_\alpha} = 5,740\ [1/rad]$. From XFLR5 the angle for $C_L = 0\ [-]$ is $\alpha_{0_w} = -4,57\ [°]$ but not to forget about wing incidence

$$\alpha_{0_{wf}} = \alpha_{0_w} - i_{w_c} = -4,57 - 1,287 = -5,857\ [°] \tag{4.48}$$

Now the coefficient of lift for $AoA = 0\ [°]$ is

$$C_{L_{0_{wf}}} = -\alpha_{0_{wf}} \cdot C_{L_\alpha} \cdot \frac{\pi}{180} = 5,857 \cdot 5,499 = 0,562\ [-] \tag{4.49}$$

Also the angle ϵ_{o_h} is equal to

$$\epsilon_{o_h} = \frac{d\epsilon}{d\alpha} \cdot \alpha_0 = 0,3 \cdot (-5,857) \cdot \frac{\pi}{180} = 0,0307\ [rad] \tag{4.50}$$

And finally coefficient of lift for $AoA = 0\ [°]$ for the whole aircraft

$$C_{L_0} = C_{L_\alpha} + C_{L_{\alpha_h}} \cdot (1 - \frac{d\epsilon}{d\alpha}) \cdot \frac{s_h}{s} \cdot \frac{q_h}{q} \cdot (i_w \cdot \frac{\pi}{180} - \epsilon_{o_h}) \tag{4.51}$$

Resulting in

$$C_{L_0} = 5,499 + 3,083 \cdot (1 - 0,3) \cdot 0,136 \cdot 0,95 \cdot (0,0225 - 0,0307) = 5,497\ [-]$$

Which can be assumed as same for both configurations (difference $0,0003\ [-]$).

4.4.2 Stability

Besides of sizing of components and aerodynamic parameters to allow aircraft fly is the ability to be passively stable and stay airborne. Besides calculating the aerodynamic center for previous section also the resulting pitching moment for the whole aircraft needs to be done and shown as declining in the operating AoA. So lets start with the aerodynamic center for whole aircraft with fixed controls which is calculated as follows

$$x_{ac_{fix}} = x_{ac_{wf}} + \frac{C_{L_{\alpha_h}}}{C_{L_\alpha}} \cdot (1 - \frac{d\epsilon}{d\alpha}) \cdot A_h \cdot \frac{q_h}{q} \tag{4.52}$$

For which we know all the values and as such

$$x_{ac_{fix}} = 0,242 + \frac{3,083}{6,0495} \cdot (1 - 0,3) \cdot 0,465 \cdot 0,95 = 0,4005$$

Now lets check if the design complies with longitudinal margin of stability previously set in 4.39

$$\Delta = x_{ac_{fix}} - x_{cg_{aft}} = 0,4005 - 0,3811 = 0,0189\ [-] \tag{4.53}$$

Yes, the margin is larger than2% of l_h.

The pitching moment coefficient c_m is generally described as

$$c_m = c_{m_0} + C_L \cdot \frac{dc_m}{dc_L}\ [-] \tag{4.54}$$

Where c_{m_0} pitching moment for $C_L = 0\ [-]$ and $\frac{dc_m}{dc_L}$ is the pitching moment coefficient slope. If we assume only linear behaviour around interested values we can create pitching moment polar based on

$$c_{m0_w} = (c_{m_{ac}})_{Basic} + \Delta_\epsilon c_{m_{ac}} \tag{4.55}$$

From the XFLR5 the measured pitching moment for the airfoil FX63-145 is $c_{m_{w_0}} = (c_{m_{ac}})_{Basic} = -0,1133\ [-]$. $\Delta_\epsilon c_{m_{ac}}$ represents the effect of wing twist (geometrical) and is calculated like this

$$c_{m0_w} = \frac{\lambda \cdot cos(\chi_{1/4})^2}{\lambda + 2 \cdot cos(\chi_{1/4})} \cdot \frac{(c_{m_{ac_r}})_{Basic} + (c_{m_{ac_t}})_{Basic}}{2} + \frac{\Delta c_{m_0}}{\epsilon_t} \cdot \epsilon_t \tag{4.56}$$

inputting values results in

$$c_{m0_w} = \frac{15 \cdot 0,9997^2}{15 + 2 \cdot 0,9997} \cdot \frac{-0,1133 - 0,1133}{2} = -0,0979$$

The slope is then defined as

$$c_{m_{C_L}} = x_{cg} - x_{ac_{wf}} \tag{4.57}$$

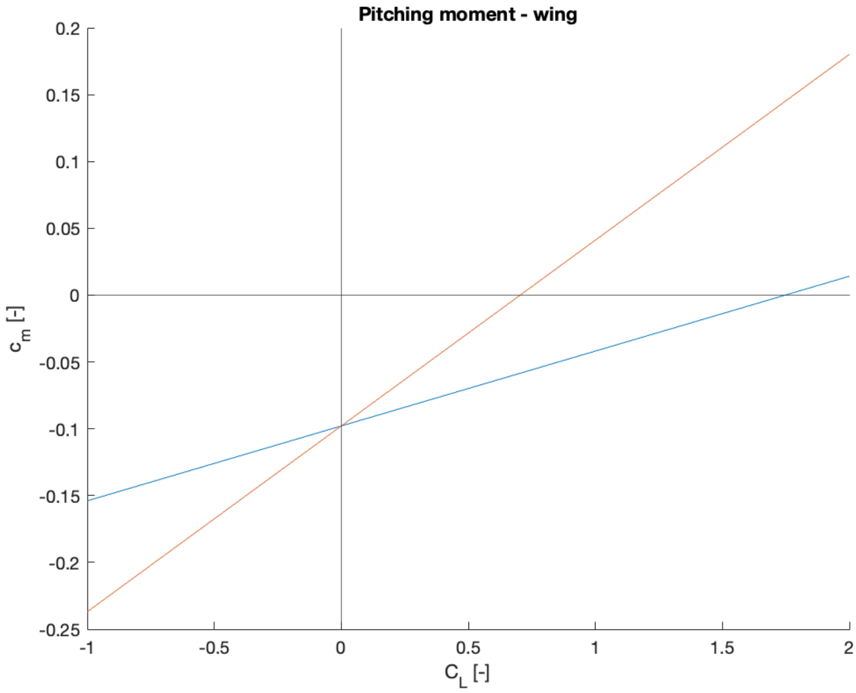

Figure 4.15 Coefficients of wing pitching moments in relation to coefficient of lift

For VTOL Aft CG

$$c_{m_{C_L}} = 0,381 - 0,2421 = 0,139\ [-]$$

And for VTOL Fwd CG

$$c_{m_{C_L}} = 0,298 - 0,2421 = 0,056\ [-]$$

Which results in these pitching moment lines c_{m_w} 4.15.
Now for the combination of fuselage and wing

$$(c_{m_{ac}})_{wf} = c_{m_{0_w}} + \Delta_f \cdot c_{m_{ac}} \tag{4.58}$$

Where $\Delta_f \cdot c_{m_{ac}}$ is the fuselage impact and is calculated via equation 4.59

$$\Delta_f \cdot c_{m_{ac}} = -1,8 \cdot (1 - \frac{2,5 \cdot b_f}{l_f}) \cdot \frac{\pi \cdot b_f \cdot h_f \cdot l_f}{4 \cdot s \cdot b_{MAC}} \cdot \frac{C_{L_{0_{wf}}}}{C_{L_{\alpha_{wf}}}} \tag{4.59}$$

For which we know all the values thus

$$\Delta_f \cdot c_{m_{ac}} = -1,8 \cdot (1 - \frac{2,5 \cdot 0,15}{1,35}) \cdot \frac{\pi \cdot 0,15 \cdot 0,17 \cdot 1,35}{4 \cdot 1,014 \cdot 0,2697} \cdot \frac{0,5622}{5,4995}$$

$$\Delta_f \cdot c_{m_{ac}} = -0,01314\ [-]$$

This is a result for VTOL, for STOL it is $\Delta_f \cdot c_{m_{ac}} = --0,01394$ $[-]$. Now it is possible to finish 4.58

$$(c_{m_0})_{wf} = -0,0979 - 0,01314 = -0,1111 \ [-]$$

And for STOL it is $(c_{m_0})_{wf} = -0,1119$ $[-]$. From which a pitch moment slope is calculated for Fwd and Aft CG as in 4.57. Resulting in 4.10

Table 4.10 Resulting $c_{m_{cL\ wf}}$

$c_{m_{wf}}$	x_{cg} Fwd [-]	x_{cg} Aft [-]
VTOL	0,0481	0,1311
STOL	0,0445	0,1085

Now for the whole aircraft it is

$$c_{m_0} = (c_{m_0})_{wf} - C_{L_{\alpha_h}} \cdot i_h \cdot A_h \frac{q_h}{q} \tag{4.60}$$

One of the parameters that need to be calculated beforehand is the horizontal stabiliser incidence (first against fuselage axis)

$$(i_h)_f = \frac{(c_{m_0})_{wf} + C_{L_{0_{wf}}} \cdot (x_{cg} - x_{ac_{wf}}}{C_{L_{\alpha_h}} \cdot A_h \cdot \frac{q_h}{q}} + \frac{\frac{d\epsilon}{d\alpha}}{C_{L_{\alpha_w}}} \cdot C_{L_{0_{wf}}} \tag{4.61}$$

Where are all the variables now known. VTOL calculated and incidence is done for Fwd CG position

$$(i_h)_f = \frac{-0,1111 + 0,5622 \cdot (0,2981 - 0,24207}{3,083 \cdot 0,4646 \cdot 0,95} + \frac{0,3}{5,4962} \cdot 0,5622$$

$$(i_h)_f = -0,0278 \ [rad] = -1,5923 \ [^\circ]$$

And for STOL it is $(i_h)_f = -1,678$ $[^\circ]$. Now the incidence in relation to the zero lift position

$$i_h = (i_h)_f - \frac{C_{L_{0_{wf}}}}{C_{L_\alpha}} = -1,5923 - \frac{0,5622}{5,4973} = -0,130 \ [rad] \tag{4.62}$$

And for the STOL it equals to $i_h = -0,132$ $[rad]$. Now the c_m for the whole aircraft can be calculated as

$$c_{m_0} = (c_{m_0})_{wf} - C_{L_{\alpha_h}} \cdot i_h \cdot A_h \cdot \frac{q_h}{h} = -0,1111 - 3,083 \cdot (-0,130) \cdot 0,4646 \cdot 0,95 = 0,0659 \ [-] \tag{4.63}$$

and also the aerodynamic center of the whole aircraft x_{ac}

$$x_{ac} = x_{ac_{wf}} + \frac{C_{L_{\alpha_h}}}{C_{L_\alpha}} \cdot (1 - \frac{d\epsilon}{d\alpha}) \cdot A_h \cdot \frac{q_h}{q} \tag{4.64}$$

that results in

$$x_{ac} = 0,2421 + \frac{3,083}{5,4973} \cdot (1 - 0,3) \cdot 0,4646 \cdot 0,95 = 0,4153$$

And the final c_m slope for all the possible configurations is in table 4.11 and is visualised in 4.16.

Table 4.11 Final $c_{m_{cL}}$ for each configuration

c_m	x_{cg} Fwd [-]	x_{cg} Aft [-]
VTOL	-0,1172	-0,0342
STOL	-0,0960	-0.0320

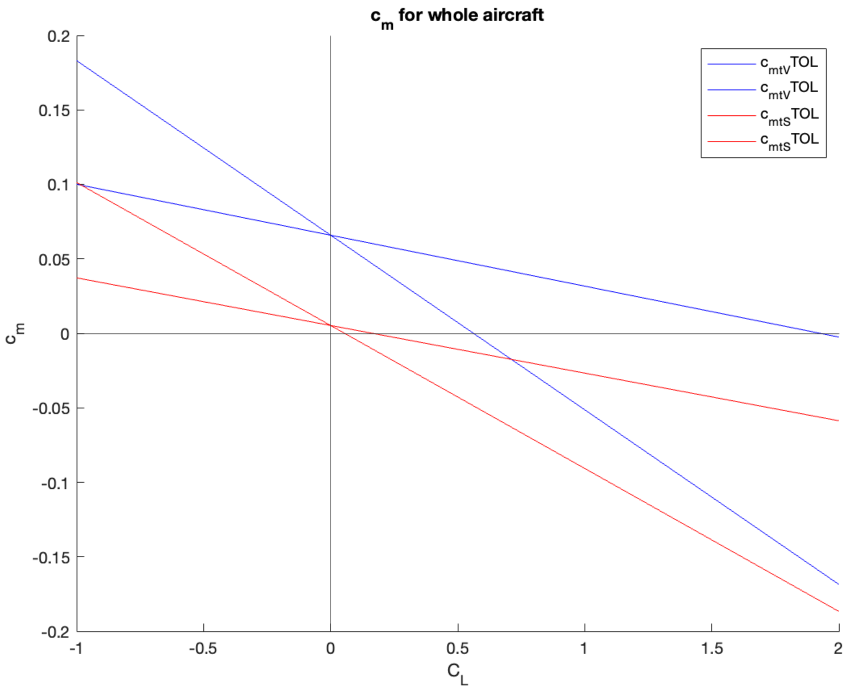

Figure 4.16 Pitching moment coefficient for whole aircraft (dimensionless [-])

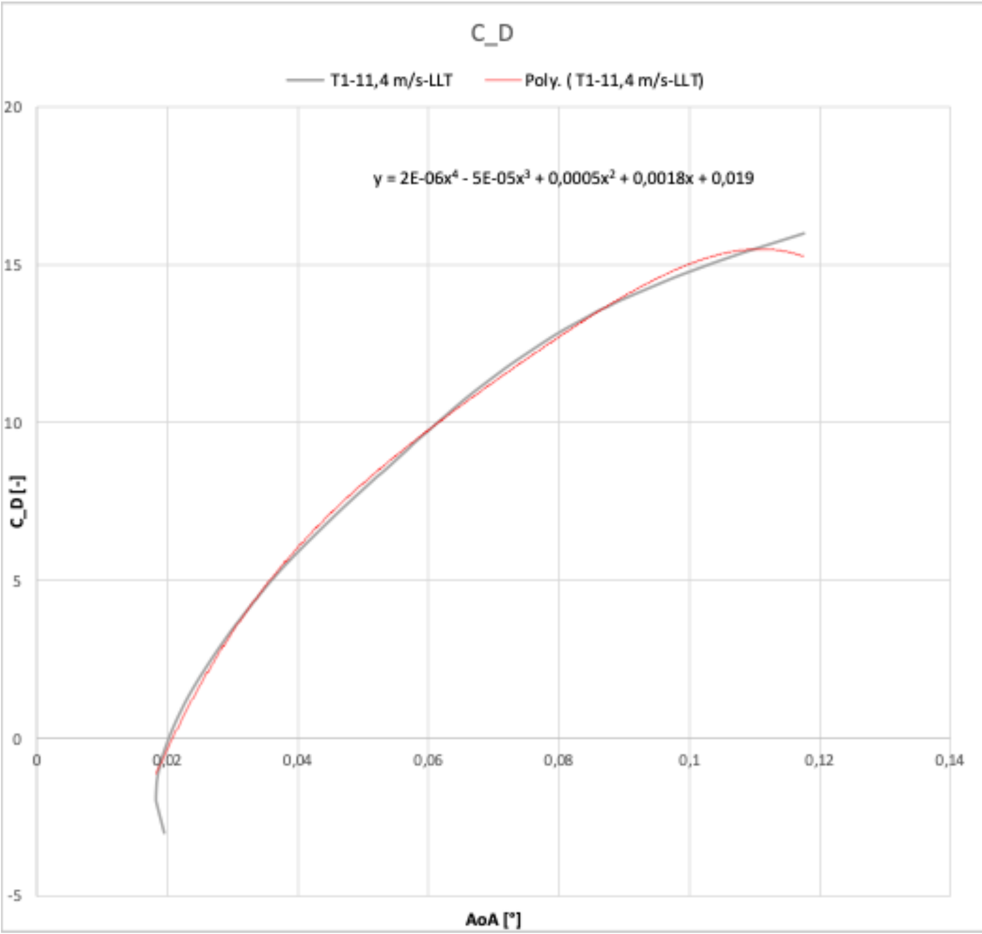

Figure 4.17 Wing Drag Polar

4.4.3 Drag

As the output of XFLR5 was also a drag polar for the whole wing it will be used as a starting point for a new more detailed drag estimation, that will be however still very much a very rough estimation. For proper drag analysis (and thus endurance tuning) a series of CFD and experimental analysis would need to be done. The drag polar from XFLR is in figure 4.17 and for the purpose of this work a trend-line was created of the 4th polynomial order 4.65.

$$C_{D_{w_{XFLR}}} = 2\cdot 10^{-6}\cdot AoA^4 - 5\cdot 10^{-5}\cdot AoA^3 + 0,0005\cdot AoA^2 + 0,0018\cdot AoA + 0,019 \quad (4.65)$$

Now an estimation of fuselage drags is

$$C_{D_f} = R_{wf}\cdot c_f\cdot (1 + \frac{60}{(l_f/d_f)^3} + 0,0025\cdot \frac{l_f}{d_f})\cdot \frac{s_{f_{wet}}}{s} \quad (4.66)$$

Where R_{wf} is from [33] a interference coefficient between wing and fuselage based on fuselage Reynolds number, which is calculated by 4.4 and is $Re = 1,43 \cdot 10^6$ $[-]$. This Re intercepts line $Mach = 0,25$ $[-]$ $and; lower$ and results in $R_w f = 1,054$. Needless to say the estimations used for fuselage should be used cautiously for this small drones as the Reynolds number for such aircraft are on the limit (or sometimes behind it) of figures in [33]. Another value acquired from the same source for fuselage was $c_f = 0,0042$ $[-]$. For these concepts a wetted area of the fuselage is assumed to be $s_{f_{wet}} = 0,1175$ $[m^2]$. From these values it is now possible to calculate the fuselage drag.

$$C_{D_f} = 1,43 \cdot 10^6 \cdot 0,0042 \cdot (1 + \frac{60}{(1,35/0,16)^3} + 0,0025 \cdot \frac{1,35}{0,16}) \frac{0,1175}{1,014} = 0,0055 \ [-]$$

Second way to estimate, very rougly, the fuselage drag is by using equations and coefficients from [38] where it looks followingly and the coefficient $c = 0,073$ $[-]$ is based purely on the shape similarity of concept fuselage and one of the example fuselages in the book.

$$C_{D_f} = 0,073 \cdot \frac{b_f \cdot h_f}{s} = 0,00184 \ [-] \tag{4.67}$$

This approach was used as the original one used on general aviation yield very low drag, however in estimating higher value it failed and as such Roskam [33] fuselage drag will be used.

Another big contribution to drag is from empennage. Lets first define the drag of horizontal stabiliser which is defined by following equation

$$C_{D_h} = R_{wf} \cdot R_{LS} \cdot c_{fw} \cdot (1 + L'(t/c) + 100 \cdot (t/c)^4) \cdot \frac{s_{h_{wet}}}{s} \tag{4.68}$$

Where friction coefficient is $c_{fw} = 0,0055$ $[-]$ [33], correcting factor for lift surface is $R_{LS} = 0,959$ $[-]$ and the chord thickness is surprisingly for $NACA$ 0012 equal to $t/c = 0,12$ $[-]$. The wetted area is assumed to be double the planform area. Lastly the $L' = 1,2$ $[-]$. Put together

$$C_{D_h} = 1,054 \cdot 0.959 \cdot 0,0055 \cdot (1 + 1,2(0,12) + 100 \cdot (0,12)^4) \cdot \frac{0,1709}{1,0142} = 0,00109 \ [-]$$

For the vertical stabiliser the equation is the same as 4.68 however the coefficients are taken from [33] based on vertical stabilisers dimensions resulting in

$$C_{D_h} = 1,054 \cdot 0.959 \cdot 0,0055 \cdot (1 + 1,2(0,12) + 100 \cdot (0,12)^4) \cdot \frac{0,068}{1,0142} = 0,0006 \ [-] \tag{4.69}$$

Other significant parts contributing to the overall drag that will be explored are payload drag and engine nacelles (for STOL one on tail and for VTOL two on wings and one on tail).

For payload two drag coefficient variants were used based on bomber turret from [38] ($C_D = 0,11$ $[-]$) and by example in [32] ($C_D = \frac{0,15}{2}$ $[-]$ for semi fared

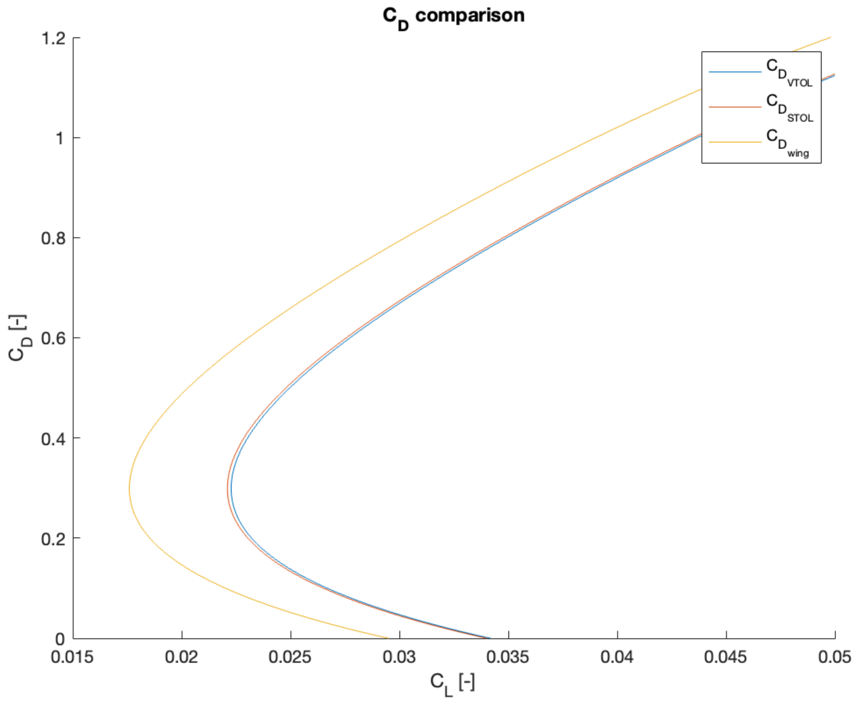

Figure 4.18 Comparison of drag polars for each configuration and for wing itself

payload. To make the coefficient of drag relative to the size of the drone the coefficients of drag were multiplied by payload cross-section to wing area ratio. The higher value was used

$$(C_{D_{payload}})_{max} = C_D \cdot \frac{s_{cs_{payload}}}{s} = 0,11 \cdot \frac{0,0088}{1,042} = 0,001\ [-] \tag{4.70}$$

And for the nacelles the coefficient was based on intermediate shaft nacelles $C_{D_n} = 0,045\ [-]$ [38] and calculated similarly to 4.70 for each cross section area (nacelles diameter was estimated to be equal to the diameters of electric motors placed in them). Example

$$c_{D_n} = 0.045 \cdot \frac{s_n}{s} = 0,0001\ [-]$$

The design of the landing was due to its size and construction neglected. The total drag is then

$$C_D = C_{D_w} + C_{D_f} + C_{D_h} + C_{D_v} + C_{D_{payload}} + C_{D_{nacelles}}\ [-] \tag{4.71}$$

The final drag polars are in 4.18.

Even with accounted landing gear, the whole drag coefficient seems very low compared to averaged real life data [33]. After a more detailed designed

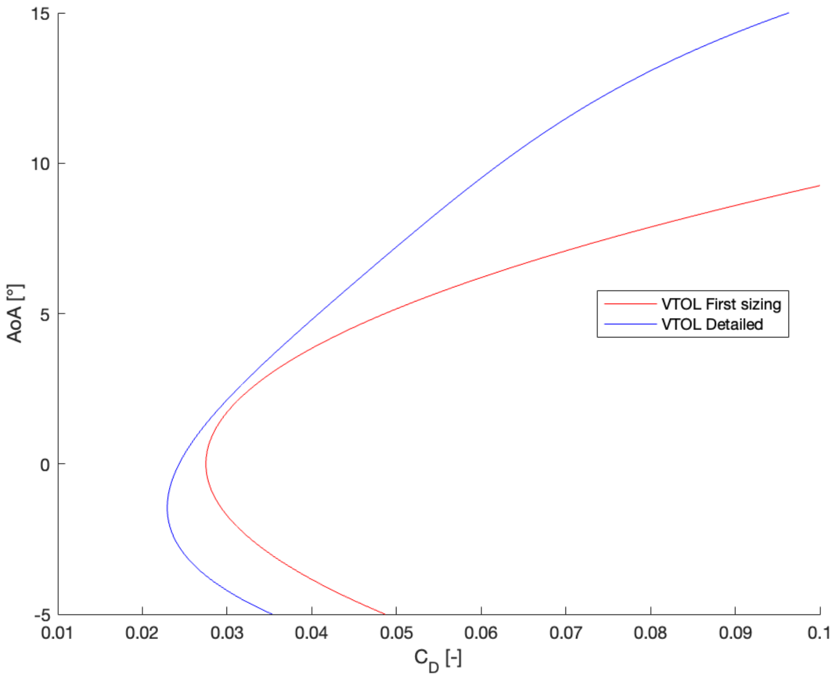

Figure 4.19 Comparison last iteration of drag polar with symmetrical drag polar from initial sizing

and fixed dimensions a more through drag definition would be needed, but that is outside of the scope of this thesis. It is noticeable how is the drag lower compared to the original symmetrical drag polar on figure 4.18.

4.5 Concepts Visualisation

Here are 3D models made in Catia V5 and Fusion 360 of concept design of VTOL and STOL. Wing and stabilisers dimensions should be ignored as the calculations and code when through number of iterations after the design and models were frozen.

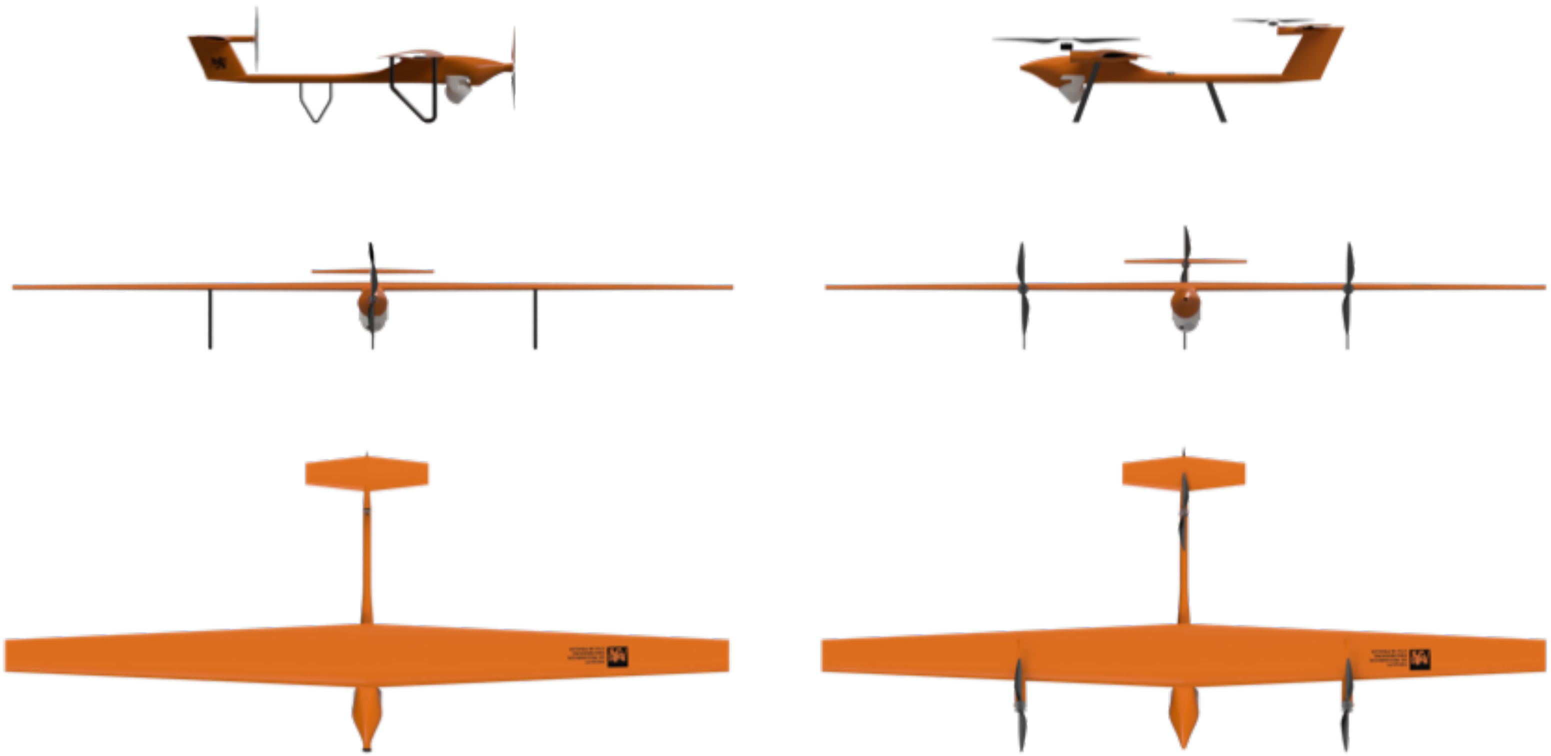

■ **Figure 4.20** 3-view of Concept Designs

Chapter 5
Preliminary Design

A selected concept which will be further developed into a more detailed design is the VTOL configuration due the not so much higher performance (can be a result of biased statistics or research) and due to the operators preference. The benefits of STOL design, respectively lack of convertiplane design, did not proof beneficial enough that the possible operator would make such a switch, if we assume its a primary multi-rotor operator.

5.1 Design

In preliminary design a further weight optimisation tight with now more precise aerodynamic performance would and performance would be appropriate, but is outside of the scope of this thesis.

At least a simple weight iteration was performed, where a series of initial MTOM, as from statistics, was inputted and compared with the MTOM based on the detailed weight calculation. Meaning that in one loop a calculation of battery sizes, Mass Fractions and each part of air-frame was done, as specified in this work. This method had some limitations as the starting geometries and other aircraft specifying parameters did not change (wing span, wing area etc.) only after the Mass Fractions was done a recalculation and only of some of this parameters. Especially the aspect ratio was through the whole process fixed.

From figure 5.2 it can be seen, that in requirements defined MTOM only a VTOL has solution (around 6,8 [kg]). On the y axis is the difference between the initial MTOM and the resulting MTOM. This can be a result of some sort of bias in the collected data as mentioned before. Another problem of this method was the fixed weight of propulsion and equipment as these would also change. As the iteration method has its flaws and would need to be expanded to be considered reliable a VTOL MTOM from concept Weight and Balance will be taken into account while further designing the Preliminary Design.

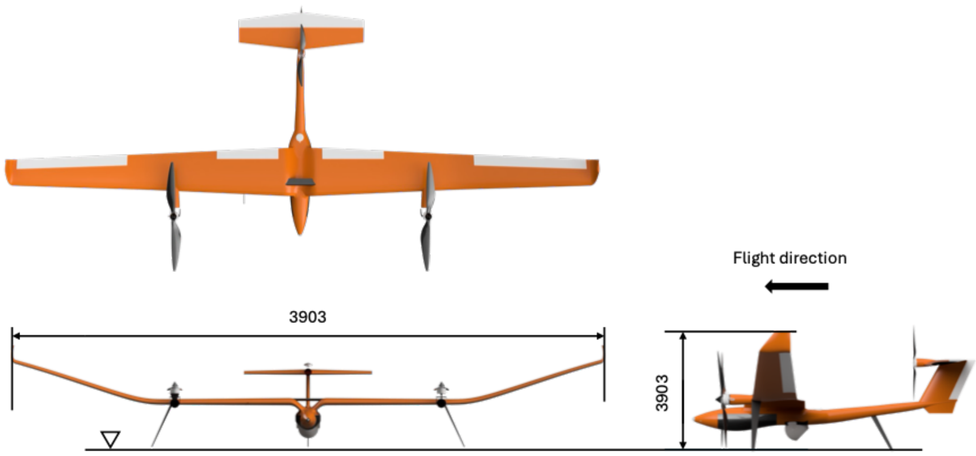

Figure 5.1 3-View of Preliminary Design

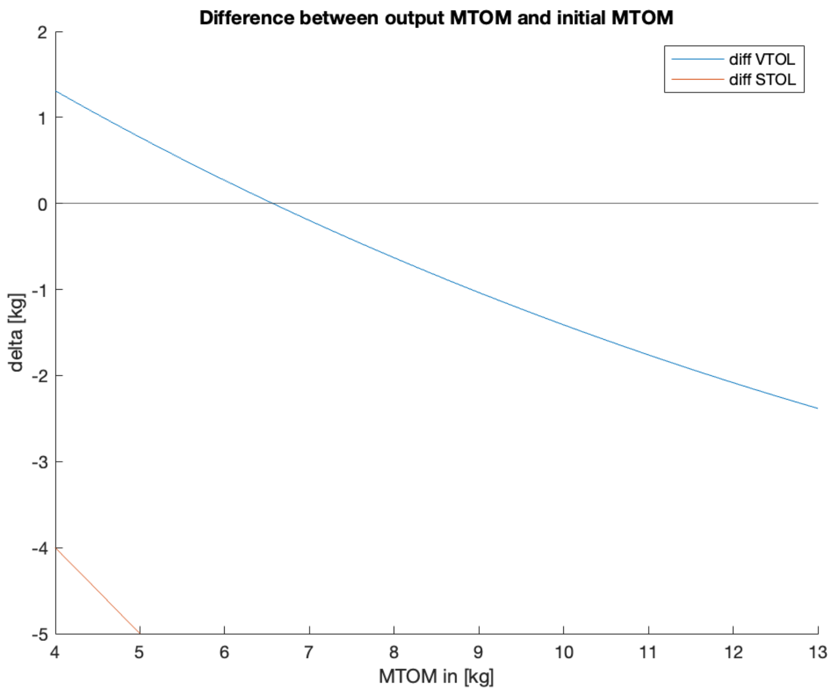

Figure 5.2 Basic iteration of MTOM

5.1.1 Wing design

Planform wing design remained unchanged from the conceptual design however winglets were added, as well as negative flaps and ailerons were visualised. Also a dihedral angle of 15 [ř] was added from the nacelles to help with the view and hover like field of view.

Wing has a unified upper spar cap, which should allow a lighter construction and can also act as a handle for ground manipulation with the drone.

A small Pitot tube is placed on the wing for airspeed and static pressure measurements.

The ailerons were designed to start at

$$\frac{l_{aileron}}{2} = \frac{0,6 \cdot l + 0,2}{2} = 1,37\ [m]$$

for VTOL which is BL=0,685. And they end at span of

$$\frac{l_{aileron}}{2} + (1 - 0.62) \cdot \frac{l}{2} = 1,91\ [m]$$

As to roughly have ailerons being 0,38 fraction of the wing span.

5.1.2 Convertiplane design

One of the trickiest parts of convertiplane design is the mechanism rotating the vector of propulsion together with the flight systems controlling the aircraft during the transition from vertical flight to horizontal. The possible mechanical rotation of motors with propellers can be done for example via proposed rails, and a fixture/control rod operated by a servomotor 5.3. This mechanism is just a placeholder and needs to be updated with more rigid mechanism and lock/fixtures at VTOL and horizontal flight regime positions.

5.1.3 Fuselage Design

The whole fuselage was reduced to limit any unused volume. The whole fuselage was also lowered as with its reduce size and payload at least partially flushed with fuselage (for lower drag) would have abysmal view angles. Another important feature was the relocation of the battery pack to the front and to the end of the fuselage. Aircraft is more impervious to the payload weight changes which results in the most aft CG being $x_{cg} = 0,349\ [-]$ (Appendix C) which results in $\frac{s_h}{s} = 0,11\ [-]$ using equations 4.42 and 4.43.

At the tip of a fuselage is also mounted a small FPV camera 5.5 for operations when no optical sensors is mounted on board and a manual control is needed.

Figure 5.3 Convertiplane mechanism proposal

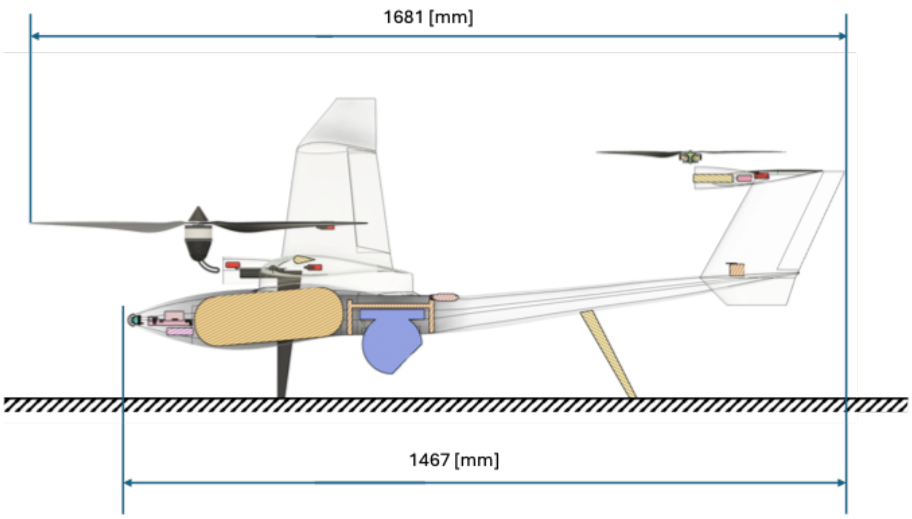

Figure 5.4 Fuselage cross section

Figure 5.5 FPV camera location

5.1.4 Payload mount

Payload is mounted on the edge of the fuselage, as such even if it is a bigger spherical electro-opctical sensors it keeps a lower drag [32]. Payload is mounted on an adjustable floor that can be moved outwards and inwards from the fuselage to allow an ideal mounting position for both ideal view and drag.

5.1.4.1 360 view features

Besides the positioning of the payload and the suspended fuselage also an angled tail was used to allow the best viewing angles while in loiter and keeping a tight circle pattern. The tail is angled 6,2 degrees to not block the view when the aircraft at loiter ($P_m in$) flight regime.

5.1.5 Battery mount

Battery is fixed behind an opening of the same size for easy swap and which also functions as avionics bay opening when battery is removed.

5.1.6 Landing gear

Will consist of three legs cut from carbon fibre desks and shaped for lower drag and minimal field of view obstruction.

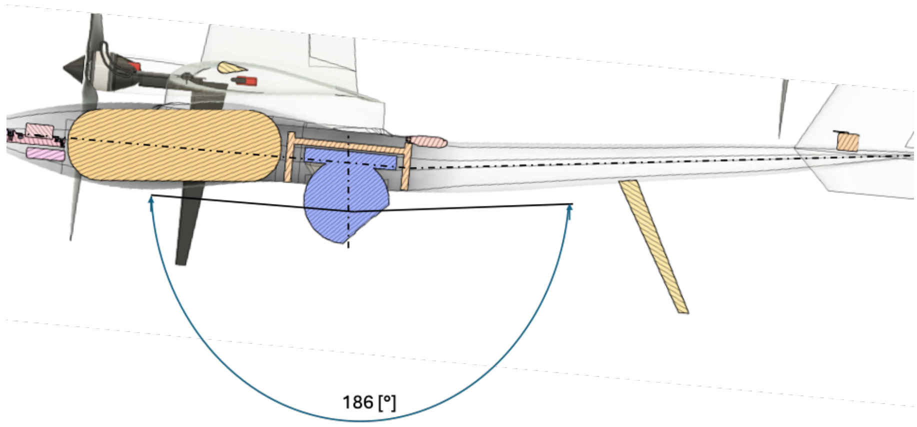

Figure 5.6 View angles at loiter flight regime

5.2 Weight and Balance

Weight and balance was done the same way as in the conceptual study and all the weights and positions are also in Appendix C. Resulting centers of gravity are

Table 5.1 CG for different configurations of Preliminary design

Config.	Nom.	VTOL	Min. Pay.	Max. Pay	Battery Pack
$x_{cg/c}$	32,39%	31,76%	29,84%	33,28%	34,97%
m [kg]	9,030	9,030	8,630	9,230	8,604

5.3 Performance

One of the key aspects of the design is calculation of the aircraft performance.

5.3.1 Speed and thrust

The available thrust decreases with speed due to the lowering efficiency and the required thrust T_p raises due to squared growth of of drag with speed. The distance between these two lines is available thrust (for climb for example).

Before drag is calculated for each speed a needed lift is calculated and from the known aircraft C_L/C_D polar a matching C_D is found. The available thrust is calculated from the trend line 3.9 created from experimental data.

Where the Thrust lines intersect, where afterwards is negative available thrust a maximal speed v_{max} is defined. Other important speeds visualised together with required and available thrust in 5.9 are minimal speed v_{min} and optimal speed v_{opt} which is defined for T_{min}. The v_{max} was calculated as

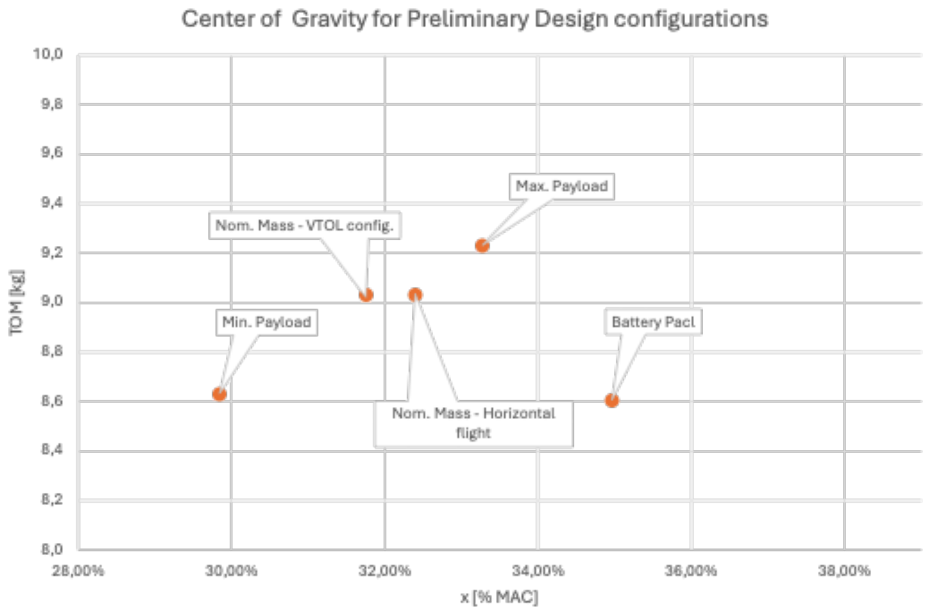

Figure 5.7 Preliminary Design Weight and Balance (notice the non existent free volume inside the fuselage)

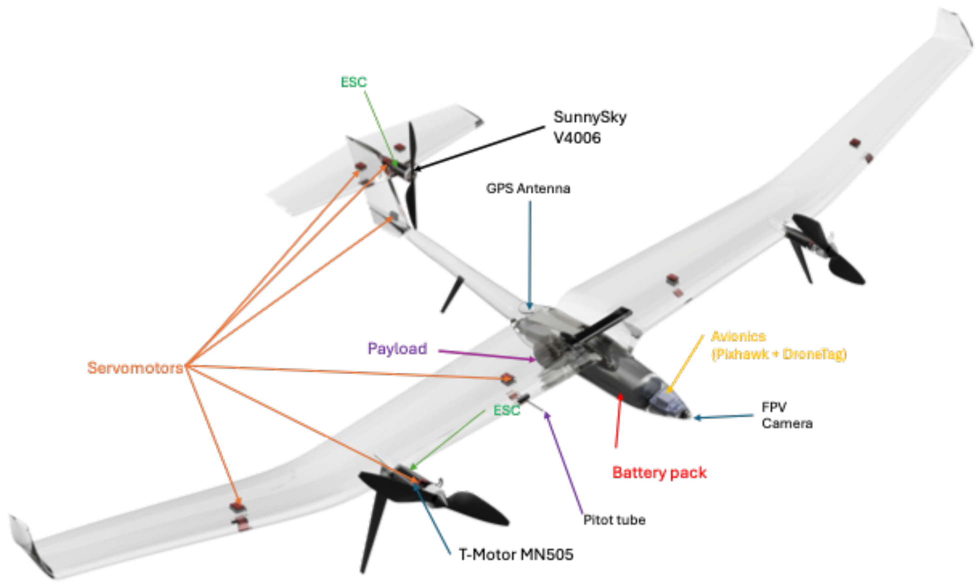

Figure 5.8 Preliminary Design with transparent (epoxy like) air-frame to showcase different parts location compared to Concept Design

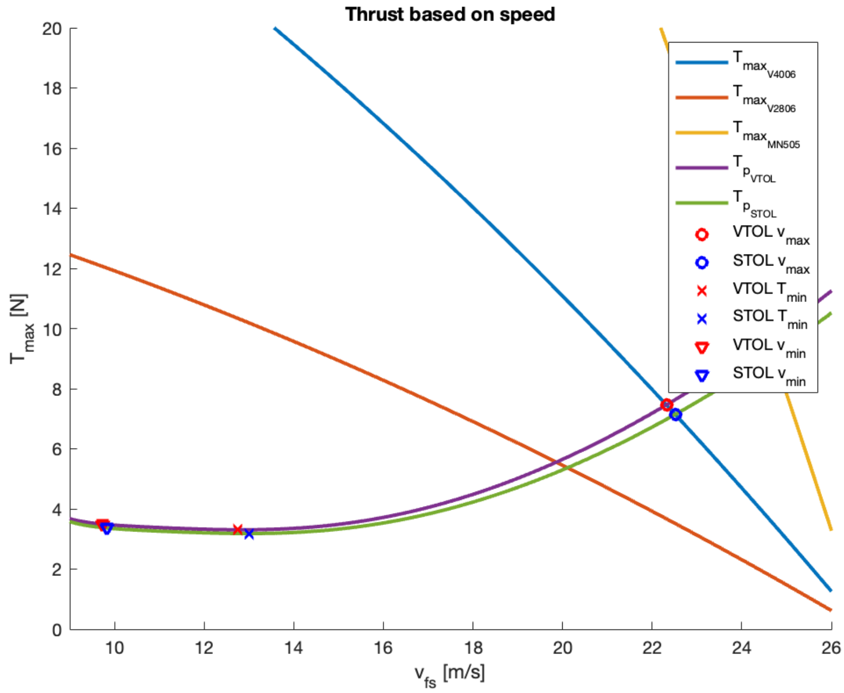

Figure 5.9 Thrust based on speed

the location of speed where the difference between T_p and T_a is closest to 0. Resulting value is $v_{max} = 22,32\ [m/s] = 80.3\ [km/h]$.

While the v_{min} was calculated by expressing the speed from lift equation 3.6 and using the wing $C_{L_{max}}$. This gives the minimal speed as $v_{min} = 9,73\ [m/s]$.

The optimal speed v_{opt} or $v_{F_{min}}$ was defined as speed for the lowest T_p which comes as $v_{opt} = 13\ [m/s]$.

If necessary a non used electric motors can be used to allow higher v_max. For more precise calculation (of all performances) an efficiency for each specific propulsion block (motor, propeller, ESC and battery) for needed range of velocities needs to be acquired/provided.

5.3.2 Climb

For operations with large terrain height differences or for some other specific missions which require longer periods of climb it would be essential to know the ideal parameters for climb (and have them stored in the autopilot logic). The resulting maximal climb speeds and ideal angles are in 5.10.

The climb speed v_z is the basically the available power divided by needed lift

$$v_{z_{climb}} = \frac{(T_{a_{V4006}} \cdot v) - (T_p \cdot v)}{MTOM \cdot g} \tag{5.1}$$

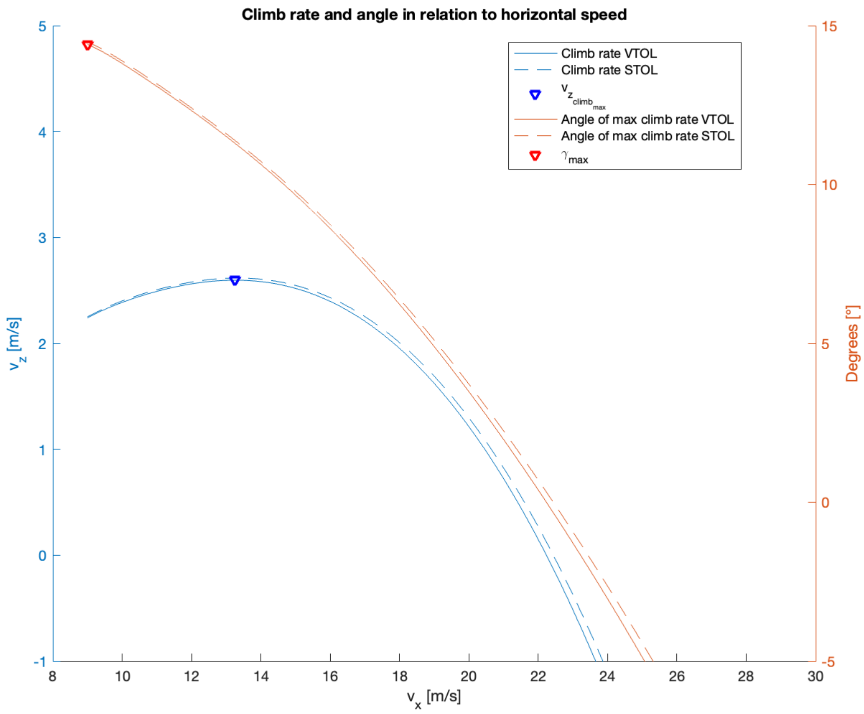

Figure 5.10 Climb performance

And the angle of climb is calculated by

$$\gamma = asin(\frac{v_{z_{climb}}}{v}) \tag{5.2}$$

The maximal values for γ or v_z were then found in the respective vortexes and also displayed in 5.10.

5.3.3 Sustained Turn

As one of the requirements which was heavily emphasised during the design was the ability to at least partially imitate hover. For that the lower the speed, roll angle and turn radius the better. Mainly the turn radius would be a limiting factor in urban areas and would raise eyebrows with the operators. The angle would however be limiting in the sense of blocking the view from the payload. The minimal turn radius being under 15 $[m]$ looks sufficient, however if it is for example compared with the design requirements for road street of being 24 $[m]$ in width in minimal, we see that this radius is still too large as the drone would not be able to "hover" (loiter) there, as also the wingspan needs to be taken into account. The diameter of an area which would the drone need for loiter is (without any reserve for drift or gust induced movement etc.).

$$d_{covered_{min}} = 2 \cdot r_{min} + 1/2 \cdot l = 2 \cdot 11,5 + 1/2 \cdot 3,9 = 24,95\ [m] \tag{5.3}$$

However if operations/missions, where the drone needs to at the same level as the monitored object, are not considered or can be executed differently then the turn radius is sufficient. Nevertheless a drone with smaller wing span would still be viewed as better as it would not be so intimidating towards people on the ground.

The following figures 5.11 were plotted from these variables that are (mostly) dependant on speed, n_{ult} (Gs) and T_a.

Minimal turn radius based on speed is calculated by this way

$$r_{min} = \frac{v^2}{g \cdot sqrtn_{ult}^2 - 1}\ [m] \tag{5.4}$$

maximal bank angle is calculated by this equation

$$\phi_{max} = acos\left(\left(\frac{v_{min}}{v}\right)^2\right)\ [rad] \tag{5.5}$$

and the time needed to perform a turn with minimal turn radius is

$$t_{r_{min}} = \frac{2 \cdot \pi \cdot r_{min}}{v}\ [s] \tag{5.6}$$

Another way a turn radius (v_{min}) can be limited is by C_L. For the whole range of C_L the v_{min} is calculated by 3.6. For the limitations by T_a a calculation of C_D for each T_a is done and based on that is found C_L for the same speed. This is then used in loads calculation

$$n = \frac{1/2 \cdot C_L \cdot \rho \cdot s \cdot v^2}{g \cdot MTOM}\ [-] \tag{5.7}$$

Which is then used in 5.4, 5.5 and 5.6 as in previous calculations.

Now it is possible to create 5.11.

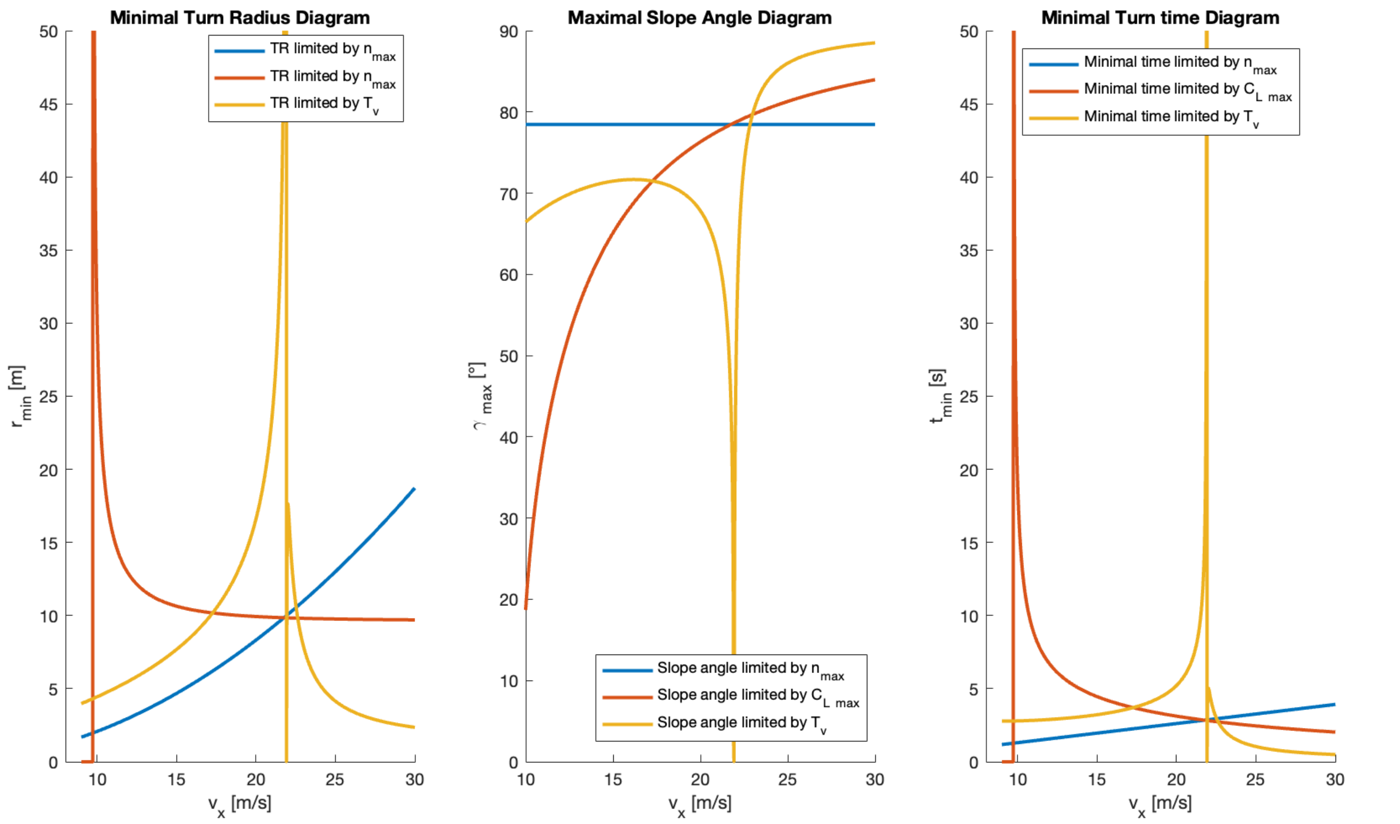

Figure 5.11 Sustained turn limitations

5.3.4 Speed polar

Another informative performance figure is the speed polar visualising the minimal vertical speed for unpowered flight and horizontal speed with the best glide ratio which is calculated as

$$K_{max} = \left(\frac{C_L}{C_D}\right)_{max} = 26,25\ [-] \tag{5.8}$$

And for this glide slope vertical v_z and v_x are found through calculating the aircraft speed v_i for each C_L/C_D by

$$v_i = \sqrt{\frac{2 \cdot g \cdot cos(\gamma)}{\rho \cdot s \cdot C_L}}\ [m/s] \tag{5.9}$$

Where γ is

$$\gamma = atan(C_D/C_L)\ [°] \tag{5.10}$$

Now it is possible to calculate descending speed as

$$v_z = -v_i \cdot sin(\gamma)\ [m/s] \tag{5.11}$$

And for the minimal value

$$v_{z_{min}} = (-v_i \cdot sin(\gamma))_{max}\ [m/s]$$

The speed v_x would be calculated similarly

$$v_x = v_i \cdot cos(\gamma)\ [m/s] \tag{5.12}$$

And from the K_{max} 5.8 the location and value of C_L can be found and based on that a value of v_i and speeds in x and z axis for this point. However results for these points were problematic and their correction did not happened in time for the thesis completions.

5.3.5 Range and Endurance

For the range and endurance calculations were used equations from the flight regime specifications for cruise and loiter. As loiter should be the regime with the highest endurance and cruise with the highest range. First a recalculation of the needed battery size was done by recalculating power consummations 3.14 in these regimes by using last C_L and C_D calculations as well as last weight definition (in 3.20 and **??**). Also speeds were for these regimes recalculated using these equations 3.22 and 3.19.

From the energy inside the new battery was subtracted energy needed for take-off and landing 3.15 (adjusted for new weight). The range was calculated by this equation (time in hours) and the power consumption was already adjusted by efficiency based on 3.9.

$$range = \frac{E_{battery_{PD}} - (t_{TO} + t_L) \cdot P_{VTOL}}{(P_{fix} + P_{cruise}) \cdot v_{cruise}} \tag{5.13}$$

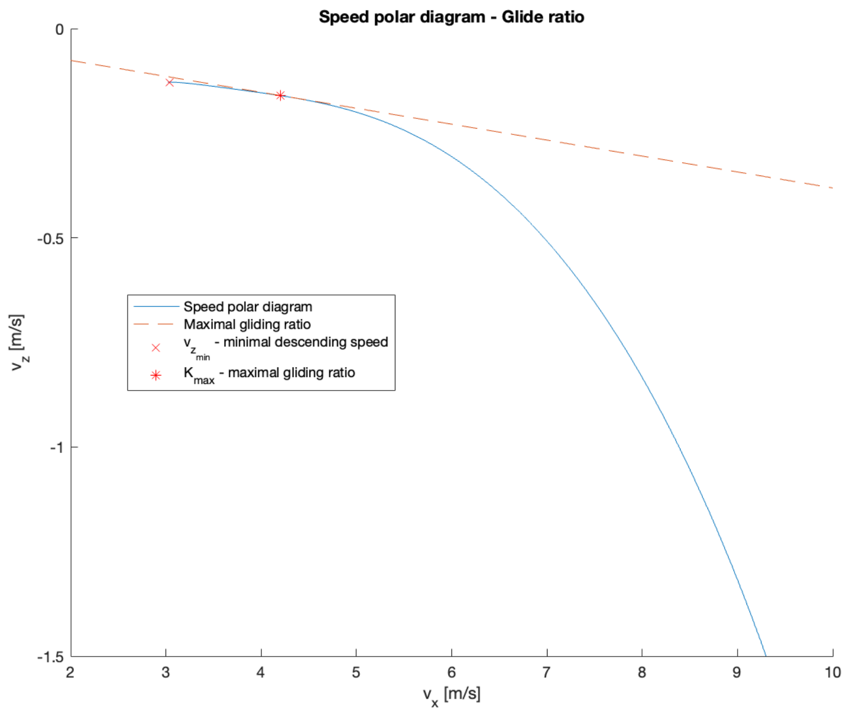

Figure 5.12 Speed polar

Which results as

$$range = \frac{957 - 0,025 \cdot 3221}{(40 + 94,1) \cdot (3,6 \cdot 14.47)} = 336\ [km] \tag{5.14}$$

and for endurance in hours

$$endurance = \frac{E_{battery_{PD}} - (t_{TO} + t_L) \cdot P_{VTOL}}{P_{fix} + P_{loiter}} \tag{5.15}$$

resulting in

$$endurance = \frac{957 - 0,025 \cdot 3221}{40 + 60,1)} = 8,65\ [hours]\ or\ 519\ [minutes] \tag{5.16}$$

Both of these values are much higher than what was recommended and part of it can be very ideal drag coefficient and also maybe inappropriate efficiency estimation.

5.4 Price Estimation

Based on experiences and consultations with subject matter experts (SME) in private following estimations were made (drone equipment prices like of avionics and motors etc. are in detailed the spreadsheet attachment). Prices

Table 5.2 Total estimated price of the project

Research and Design	Person a month	Total
Avionics and payload design, integration and testing		
4 people, 1 year	€ 3 000,00	€ 144 000,00
Air frame design and testing		
3 people, 1 year	€ 2 500,00	€ 90 000,00
Jigs and manufacturing process		
2 people, 1/2 year	€ 2 000,00	€ 24 000,00
Test bed price		€ 30 000,00
Manufacturing	Per one	
Molds (14x)	€ 2 000,00	€ 28 000,00
Equipment		€ 10 000,00
Shared Cost Total	€ 326 000,00	
Target per unit	€ 10 000,00	

used in 5.3 were estimated based on prices from research and based on how much it is probable a modification will be required, namely with the avionics - Pixhawk, due to the transition from horizontal flight to vertical and vise versa. Another level of complexity will be the loiter emulating hover for the operator.

Battery was rounded up from the most expensive battery pack as with the use of more advanced cells/pouches the price can be expected to increase but due to the higher order of cells and b2b type order the increase might not be that high.

Airfame is expected to be from composite material, probably combination of carbon and glass fiber parts. For this purpose molds out of MDF will need to be milled. Wet lamination is expected with the use of vacuum pump and unpressurised oven for latter curing. MDF is relatively cheap material for molds and as such will have tendency to degrade. Interestingly SMEs estimated the number of built airframes, before a replacement is needed, close to the number of units that need to be sold to break even.

Table 5.3 Detailed cost distribution of single aircraft

Per Aircraft [€]		
Aiframe manu.	Segment	Total
Material	100	1400
Labour	100	1400
Other labour	per hour	80 hours
Assembly	15	1200
Other admin		200
Equipment		
DroneTag		400
Modified Pixhawk		1500
Servomotors		100
Propulsion		751
Battery		1000
Other		100
Total		**8051**

Chapter 6

Thesis conclusion

During this thesis was performed thorough research on a variety of small drones and a variety of their systems, from payloads to propulsion. Customer requirements were specified and a conceptual study (aerodynamic performance, weight and balance, etc.) was made with basic performance calculations for VTOL and STOL configuration. Work finished with a rough Preliminary design proposition and concluded with financial estimations.

6.1 Design conclusion

The design is still very rough and needs a lot of optimization to truly fulfill its potential. It is also an answer to the author's original idea as to why is not such a drone done yet. In research it was observed such drones were done, but not with the endurance aspect/benefit in mind. This proved to be quite a challenging task and started with unexpectedly high-weight estimations. Design work of this depth can be a start for a true preliminary design and geometry optimization.

The combination of features to allow uninterrupted visual track of a point on the same plane as the aircraft seems efficient for its purpose, however, the resulting fuselage and wings joint might prove problematic due to the increased drag it causes, and as such this type of connection for the sole purpose of better viewing angle might/should be reconsidered.

6.2 Requirements Satisfaction

As the requirements set at the beginning were demanding and in some cases optimistic, most of them were proven to be achievable as the endurance, weight, tractability, and probably even the price points were met. However, some points are a bit more disputable as the drone ended up being quite large (with a large wing span) and heavy to be operated comfortably inside urban areas (or

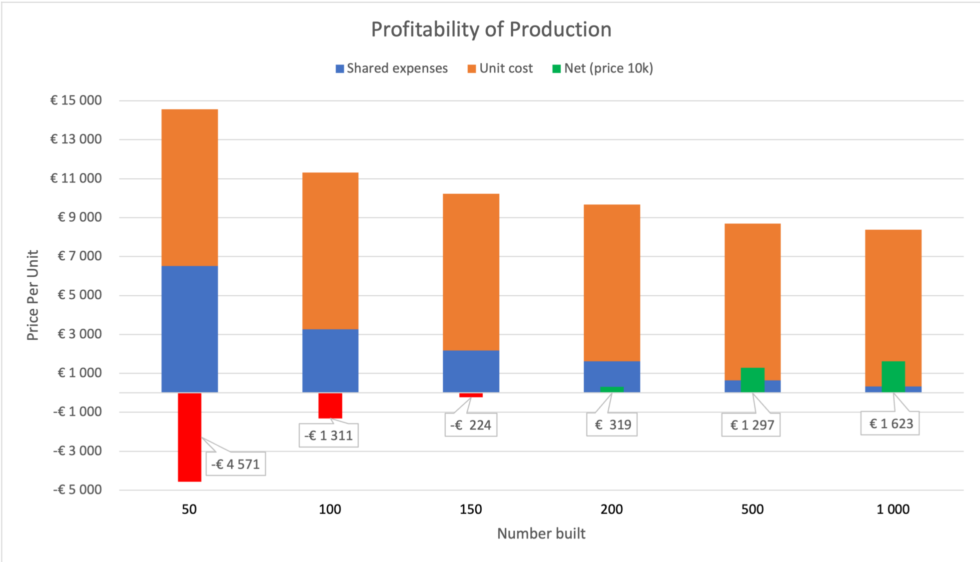

Figure 6.1 Amount of drones built to achieve profit with price under 10 000€

streets particularly), and as such the design is not able to replicate hover even if extended efforts were made to make its loiter regime as close to it as possible. This however can be further improved by further optimisation of the drone design as a whole (with aerodynamic performance and propulsion efficiencies) as just with the limited weight optimisation done in this work a probable ideal MTOM was estimated as significantly lower than the one originally (and even at the end) used. This can be a motivation for future thesis.

To compare the resulting design with the originally defined competitor, the DJi M350, the newly designed drone has several times higher endurance (45 vs 180 [min.]), higher payload (up to 1,2 compared to 0,9 [kg]) and might be around the same price. However, in space-limited areas, like streets or places with big uninvolved crowds, this design might be too. Besides the ability to loiter in a tight enough radius, the drone itself has a wingspan big enough to limit its use as it needs at least 3,9 m wide space for its wings to take off. Further design optimization would probably limit these negatives, but not sure of eliminating them.

Appendix A

Research

A.1 Electric Motors

Table A.1 Researched Electric Motors and most of the collected data [35] [34]

Name	m [g]	Max Cont. P [W]	[N/g]	$[W_{mc}/g]$	with prop	Max. T [g]	Rec. g	Max. T [N]	Rec. T [N]	[USD]	KV
T-Motor AT2303	18	100,00	0,286	5555.56	GWS8040	524		5.14	0	36	1500
SunnySky X2204	20	140,00	0,285	7142.86	GWS8040	570	135	5.59	1,32435	14	1800
SunnySky Edge Racing R2305	23	260,00	0,400	11304.35	GWS9047	937	281,1	9.19	2,757591	25	1850
SunnySky X2305 V3	23	235,00	0,324	10217.39	GWS1047	760	200	7.46	1,962	18	1620
SunnySky X2208	46	330,00	0,188	7173.91	APC6X4	880	350	8.63	3,4335	16	2600
SunnySky V2806	47	250,00	0,263	5319.15	EOLO CN12*5	1260	450	12.36	4,4145	29	650
T-Motors AT2308	47	250,00	0,218	5319.15	APC 9x6	1045	350	10.25	3,4335	30	1450
SunnySky V4004	51	310,00	0,281	6078.43	EOLO CN13*5	1460	450	14.32	4,4145	50	400
AXI 2212/34 GOLD LINE	57	115,00	0,103	2017.54	11x4,7	600	420	5886.00	4,1202	87	710
SunnySky V4006	68	560,00	0,369	8235.29	EOLO CN15*5.5	2560	800	25.11	7,848	53	740
AXI 2217/12 GOLD LINE	70	330,00	0,141	4748.20	11"x4"	1000	800	9.81	7,848	92	1380
SunnySky V3506	84	400,00	0,210	4761.90	EOLO CN15*5.5	1800	600	17658.00	5,886	38	650
SunnySky V3508	97	520,00	0,227	5360.82	EOLO CN15*5.5	2247	800	22.04	7,848	43	700
T-Motor U3	97	500,00	0,182	5154.64	13x4.4 CF	1800	600	17658.00	5,886	110	700
SunnySky V4008	105	500,00	0,228	4761.90	EOLO CN17*6.2	2440	1000	23.94	9,81	55	380
SunnySky V4010	115	725,00	0,307	6304.35	EOLO CN17*6.2	3600	1200	35316.00	11,772	60	375
T-Motor MN4110	152	770,00	0,245	5065.79	P16*5.4" prop	3800	*1266,67*	37278.00	12,426	87	400
T-Motor U5	156	850,00	0,1792212	5448.72	T-motor 16*5.4CF	2850	950	27.96	9,3195	126	400
SunnySky V4014	166	875,00	0,230	5271.08	15x5.5	3900	1300	38259.00	12,753	80	400
SunnySky XS HP X3515S	170	875,00	0,208	5147.06	15*5.5	3600	1700	35316.00	16,677	45	400
T-Motor MN501-S	170	1000,00	0,300	5882.35	P22*6.6" prop	5200	*1733,33*	51012.00	17,004	100	300
SunnySky X2826	171	900,00	0,166	5263.16	APC 13x6	2900	1800	28449.00	17,658	40	880
T-Motor MN4112	172	1210,00	0,214	7034.88	P15x5	3750	*1250*	36.79	12,2625	93	420
SunnySky V5208	175	880,00	0,269	5028.57	EOLO C20	4800	1500	47088.00	14,715	80	340
SunnySky V5210	200	1100,00	0,275	5500.00	EOLO CN22*6.2	5600	1800	54936.00	17,658	87	300
T-Motor MN4116	212	1210,00	0,222	5707.55	P16*5.4" prop	4800		47088.00		100	450
T-Motor V505	215	2500,00	0,399	11627.91	T-Motor P17x5,8	8741		85.75	0	120	260
SunnySky X S. V3 X3520 V3	219	2000,00	0,225	9132.42	APC14*7	5012	2500	49.17	24,525	60	560
T-Motor MN505-S	225	1300,00	0,291	5777.78	P22*6.6 prop	6680	*2226,67*	65.53	21,8436	110	320
SunnySky M8	232	1100,00	0,351	4741.38	29*9.5	8300	1750	81423.00	17,1675	200	100
T-Motor U8 Lite Eff.	243	1406,00	0,295	5786.01	G28x9.2 CF	7300	*2433,33*	71613.00	23,871	300	100
T-Motor MN601-S	250	1500,00	0,259	6000.00	P21*6.3" prop	6600	*2200*	64746.00	21,582	260	170
T-Motor U7	255	800,00	0,179	3137.25	CF20*6	4650	*1550*	45.62	15,2055	150	280
T-Motor U7-V2.0	255	800,00	0,179	3137.25	22x6.6 CF	4640	*1546,67*	45.52	15,1728	150	280
T-Motor U8II Lite Effi.	256	1450,00	0,349	5664.06	G28*9.2"prop	9100	*3033,33*	89271.00	29,757	310	100
T-Motor U8 Lite L Eff	282	2140,00	0,390	7588.65	G30*10.5"prop	11200	*3733,33*	109872.00	36,624	330	110
T-Motor U8 Pro Eff.	287	1450,00	0,311	5052.26	G28*9.2"prop	9100	*3033,33*	89271.00	29,757	310	100
T-Motor V602	300	2000,00	0,319	6666.67	V22x7.4	9749		95.64	0	140	180
T-Motor V605	340	3200,00	0,366	9411.76	V22x7.4	12700	*4233,33*	124587.00	41,529	150	210
T-Motor MN8012	351	1873,00	0,330	5336.18	G30x10,5	11800	*3933,33*	115758.00	38,586	270	100
SunnySky XS HP X6215S	363	1825,00	0,230	5027.55	22*6.6	8500	3000	83385.00	29,43	78	350
SunnySky XS HP X6215S	364	2675,00	0,367	7348.90		13600	4000	133416.00	39,24	78	210
T-Motor P60	373	1800,00	0,179	4825.74	P22*6.6	6800	2266,67	66708.00	22,236	108	170
T-Motor MN8014	392	2423,00	0,348	6181.12	G30x10,5	13900	*4633,33*	136359.00	45,453	280	100
T-Motors AT7215	555	5000,00	0,253	9009.01	20x10	14307	4292,1	140.35	42,105501	220	220

Appendix B
Statistics

Table B.1 Measured or collected data for geometry statistics

Name	Units	**Puma LE**	**Dragonfish S.**	**EOS**	**SpyRanger**	**Heliplane**	**Trinity Pro**	**EOS C VTOL**
Wingspan	m	4,6	2,3	3,5	3,8	2,4	2,394	5
Length	m	2,2	1,29	1,6	1,7	1,15	1,5	1,8
Heigth	m							0,45
Wing Area	m2	1,149	0,404	0,735	1,211	0,415	0,423	1,076
Hor. Stab. Area	m2	0,112	0,062	0,088	0,171	0,074	0,047	0,085
Hor. Stab. Arm	m	1,408	0,787	0,909	1,033	0,574	0,715	1,260
Propeller Diameter	m					0,356		
A_h		0,578	0,698	0,522	0,460	0,596	0,460	0,475
Lambda W	-	18,416	13,101	16,671	11,922	13,893	13,543	23,234
bAVG	m	0,223	0,166	0,170	0,273	0,175	0,175	0,213
b0	m	0,326	0,194	0,253	0,382	0,250	0,220	0,257
bk	m	0,120	0,139	0,088	0,164	0,100	0,130	0,169
bSAT	m	0,238	0,173	0,207	0,317	0,172	0,172	0,209
Eta W	-	0,368	0,716	0,347	0,429	0,400	0,591	0,658
Hor. S. b0	m	0,196	0,134	0,201	0,252	0,174	0,114	0,144
Hor. S.bk	m	0,092	0,099	0,1087	0,116	0,09	0,065	0,133
Eta Hor.S.	-	0,469	0,739	0,541	0,460	0,517	0,570	0,924
No. of motors	-	1	4	1	1	5	3	5
Payload	kg	1,001	1,5	1,1	1,2	1,001	1,001	1,1
Endurance	min	330	126	120	150	80	90	180
MTOM	kg	10,7	9	7	14,5	8	5,75	14,2
s_h/s		0,098	0,153	0,119	0,141	0,179	0,111	0,079
l_h/b_{SAT}		5,916	4,554	4,385	3,255	3,329	4,157	6,029

Appendix C

Weight and Balance

Table C.1 Weight and Balance data for both concept configurations

			VTOL		**STOL**						
		x_MAC (b_r LE)	0,0378		0,0367						
b_SAT V2	0,2697	x LE b_SAT	0,5378	0,2617	0,5367						
WnB VTOL											
x pos				**VTOL**		**Min payl.**		**Max payl.**		**Battery Pack**	
Name	**x [m]**	**m [kg]**	**Moment**	**x_VTOL**	**Arm_VTOL**	**m**	**Moment**	**m**	**Moment**	**m**	**Moment**
Batteries	0,553	4,026	2,226378	0,553	2,226	4,026	2,226378	4,026	2,226378	3,600	1,9908
Payload	0,410	1,000	0,41	0,410	0,410	0,600	0,246	1,200	0,492	1,000	0,41
Servomotors VTOL main	0,460	0,034	0,01564	0,460	0,016	0,034	0,01564	0,034	0,01564	0,034	0,01564
Servomotors VTOL tail	1,410	0,009	0,01269	1,410	0,013	0,009	0,01269	0,009	0,01269	0,009	0,01269
Wings	0,627	1,132	0,7095759	0,627	0,710	1,132	0,7095759	1,132	0,7095759	1,132	0,7095759
Fuselage	0,720	0,538	0,387144	0,720	0,387	0,538	0,387144	0,538	0,387144	0,538	0,387144
Main LG	0,490	0,150	0,0735	0,490	0,074	0,150	0,0735	0,150	0,0735	0,150	0,0735
Tail LG	1,000	0,050	0,05	1,000	0,050	0,050	0,05	0,050	0,05	0,050	0,05
Horizontal stab.	1,538	0,316	0,485239	1,538	0,485	0,316	0,485239	0,316	0,485239	0,316	0,485239
Vertical stab.	1,520	0,141	0,214016	1,520	0,214	0,141	0,214016	0,141	0,214016	0,141	0,214016
El. Motors VTOL main	0,430	0,450	0,1935	**0,400**	0,180	0,450	0,1935	0,450	0,1935	0,450	0,1935
El. Motor VTOL tail	1,380	0,068	0,09384	**1,350**	0,092	0,068	0,09384	0,068	0,09384	0,068	0,09384
Servomotors ailerons	0,640	0,018	0,01152	0,640	0,012	0,018	0,01152	0,018	0,01152	0,018	0,01152
Servomotrs rudder	1,433	0,017	0,024361	1,433	0,024	0,017	0,024361	0,017	0,024361	0,017	0,024361
Servomotrs elevator	1,542	0,017	0,026214	1,542	0,026	0,017	0,026214	0,017	0,026214	0,017	0,026214
Servomotors flaps	0,590	0,034	0,02006	0,590	0,020	0,034	0,02006	0,034	0,02006	0,034	0,02006
Propeller VTOL main	0,400	0,120	0,04816	***0,400***	0,048	0,120	0,04816	0,120	0,04816	0,120	0,04816
Propeller VTOL tail	1,350	0,021	0,02835	***1,350***	0,028	0,021	0,02835	0,021	0,02835	0,021	0,02835
ESC VTOL main	0,550	0,220	0,121	0,550	0,121	0,220	0,121	0,220	0,121	0,220	0,121
ESC VTOL tail	1,430	0,073	0,10439	1,430	0,104	0,073	0,10439	0,073	0,10439	0,073	0,10439
Avionics	0,420	0,242	0,10164	0,420	0,102	0,242	0,10164	0,242	0,10164	0,242	0,10164
Nacells Main	0,547	0,130	0,07111	0,547	0,071	0,130	0,07111	0,130	0,07111	0,130	0,07111
Nacell Tail	1,420	0,025	0,0355	1,420	0,036	0,025	0,0355	0,025	0,0355	0,025	0,0355
Other (cables, rods, antennas, lights)	0,593	0,2	0,1186	0,593	0,119	0,200	0,1186	0,200	0,1186	0,200	0,1186
Total		9,030	5,5824279	**33,48%**	5,5668879	8,630	5,4184279	9,230	5,6644279	8,604	5,3468499
x CG	0,61820222	**29,81%**	x CG VTOL	0,61648131	0,62785227	**38,11%**	0,61369085	**32,34%**	0,62143047	**35,49%**	
		delta cg VTOL	**0,28%**			Nominal	Nom. VTOL	Min payl.	Max payl.	Battery Pack	
delta cg	0,02520222			**29,81%**	**38,11%**	29,81%	38,11%	32,34%	35,49%	33,48%	
	4,1%			**8,604**	**9,230**	9,030	8,630	9,230	8,604	9,030	
				MIN	MAX						
WnB STOL						**Min payload**		**Max payload**		**Battery Pack**	
Name	**x [m]**	**m [kg]**	**Arm**			**m**	**Moment**	**m**	**Moment**	**m**	**Moment**
Batteries	0,545	3,795	2,068275			3,795	2,068275	3,795	2,068275	3,600	1,962
Payload	0,410	1	0,41			0,600	0,246	1,200	0,492	1,000	0,41
Wings	0,627	1,0484	0,6573468			1,048	0,6573468	1,048	0,6573468	1,048	0,6573468
Fuselage	0,720	0,5277	0,379944			0,528	0,379944	0,528	0,379944	0,528	0,379944
Main LG	0,410	0,250	0,1025			0,250	0,1025	0,250	0,1025	0,250	0,1025
Tail LG	1	0,05	0,05			0,050	0,05	0,050	0,05	0,050	0,05
Horizontal stab.	1,538	0,296	0,4554018			0,296	0,4554018	0,296	0,4554018	0,296	0,4554018
Vertical stab.	1,52	0,1146	0,174192			0,115	0,174192	0,115	0,174192	0,115	0,174192
El. Motor STOL main	0,25	0,068	0,017			0,068	0,017	0,068	0,017	0,068	0,017
El. Motor STOL tail	1,398	0,047	0,065706			0,047	0,065706	0,047	0,065706	0,047	0,065706
Servomotors ailerons	0,64	0,018	0,01152			0,018	0,01152	0,018	0,01152	0,018	0,01152
Servomotrs rudder	1,433	0,017	0,024361			0,017	0,024361	0,017	0,024361	0,017	0,024361
Servomotrs elevator	1,542	0,017	0,026214			0,017	0,026214	0,017	0,026214	0,017	0,026214
Servomotors flaps	0,59	0,034	0,02006			0,034	0,02006	0,034	0,02006	0,034	0,02006
Propeller STOL main	0,2225	0,021	0,0046725			0,021	0,0046725	0,021	0,0046725	0,021	0,0046725
Propeller STOL tail	1,38	0,0175	0,02415			0,018	0,02415	0,018	0,02415	0,018	0,02415
ESC STOL main	0,29	0,073	0,02117			0,073	0,02117	0,073	0,02117	0,073	0,02117
ESC STOL tail	1,43	0,073	0,10439			0,073	0,10439	0,073	0,10439	0,073	0,10439
Avionics	0,42	0,242	0,10164			0,242	0,10164	0,242	0,10164	0,242	0,10164
Other (cables, rods, antennas, lights)	0,593	0,2	0,1186			0,200	0,1186	0,200	0,1186	0,200	0,1186
Nacell Tail	1,420	0,015	0,0213			0,015	0,0213	0,015	0,0213	0,015	0,0213
Total		7,9093	4,8371431			7,509	4,6731431	8,109	4,9191431	7,714	4,7308681
x CG	0,61157664	**31,47%**			0,62231408	**35,85%**	0,60660514	**29,45%**	0,61325954	**32,16%**	
				MIN	MAX	Nominal	Min. Payload	Max. Payload	Battery pack		
delta cg	0,01857664			**29,45%**	**35,85%**	31,47%	35,85%	29,45%	32,16%		
	3,0%			**7,509**	**8,109**	7,909	7,509	8,109	7,714		

Table C.2 Weight and Balance data Preliminary Design

			VTOL								
		x_MAC (b_r LE)	0,0378								
b_SAT V2	0,2697	x LE b_SAT	0,5378								
x pos				**VTOL**		**Min payload**		**Max payload**		**Battery Pack**	
Name	**x (arm) [m]**	**m [kg]**	**Moment**	**x_VTOL**	**Arm**	**m**	**Moment**	**m**	**Moment**	**m**	**Moment**
Batteries	0,485	4,026	1,95261	0,485	1,953	4,026	1,95261	4,026	1,95261	3,600	1,746
Payload	0,735	1,000	0,735	0,735	0,735	0,600	0,441	1,200	0,882	1,000	0,735
Servomotors VTOL main	0,460	0,034	0,01564	0,460	0,016	0,034	0,01564	0,034	0,01564	0,034	0,01564
Servomotors VTOL tail	1,410	0,009	0,01269	1,410	0,013	0,009	0,01269	0,009	0,01269	0,009	0,01269
Wings	0,627	1,132	0,7095759	0,627	0,710	1,132	0,7095759	1,132	0,7095759	1,132	0,7095759
Fuselage	0,777	0,538	0,41757782	0,777	0,418	0,538	0,41757782	0,538	0,41757782	0,538	0,41757782
Main LG	0,490	0,150	0,0735	0,490	0,074	0,150	0,0735	0,150	0,0735	0,150	0,0735
Tail LG	1,000	0,050	0,05	1,000	0,050	0,050	0,05	0,050	0,05	0,050	0,05
Horizontal stab.	1,518	0,316	0,478929	1,518	0,479	0,316	0,478929	0,316	0,478929	0,316	0,478929
Vertical stab.	1,520	0,141	0,214016	1,520	0,214	0,141	0,214016	0,141	0,214016	0,141	0,214016
El. Motors VTOL main	0,430	0,450	0,1935	0,400	0,180	0,450	0,18	0,450	0,1935	0,450	0,1935
El. Motor VTOL tail	1,380	0,068	0,09384	1,350	0,092	0,068	0,0918	0,068	0,09384	0,068	0,09384
Servomotors ailerons	0,640	0,018	0,01152	0,640	0,012	0,018	0,01152	0,018	0,01152	0,018	0,01152
Servomotrs rudder	1,433	0,017	0,024361	1,433	0,024	0,017	0,024361	0,017	0,024361	0,017	0,024361
Servomotrs elevator	1,542	0,017	0,026214	1,542	0,026	0,017	0,026214	0,017	0,026214	0,017	0,026214
Servomotors flaps	0,590	0,034	0,02006	0,590	0,020	0,034	0,02006	0,034	0,02006	0,034	0,02006
Propeller VTOL main	0,400	0,120	0,04816	*0,400*	0,048	0,120	0,04816	0,120	0,04816	0,120	0,04816
Propeller VTOL tail	1,350	0,021	0,02835	*1,350*	0,028	0,021	0,02835	0,021	0,02835	0,021	0,02835
ESC VTOL main	0,600	0,220	0,132	0,600	0,132	0,220	0,132	0,220	0,132	0,220	0,132
ESC VTOL tail	1,440	0,073	0,10512	1,440	0,105	0,073	0,10512	0,073	0,10512	0,073	0,10512
Avionics	0,320	0,242	0,07744	0,320	0,077	0,242	0,07744	0,242	0,07744	0,242	0,07744
Nacells Main	0,547	0,130	0,07111	0,547	0,071	0,130	0,07111	0,130	0,07111	0,130	0,07111
Nacell Tail	1,420	0,025	0,0355	1,420	0,036	0,025	0,0355	0,025	0,0355	0,025	0,0355
Other (cables, rods, antennas, lights)	0,593	0,200	0,1186	0,593	0,119	0,200	0,1186	0,200	0,1186	0,200	0,1186
Total		9,030	5,64531372		5,62977372	8,630	5,33577372	9,230	5,79231372	8,604	5,43870372
x CG	0,62516625	**32,39%**	x CG VTOL	0,62344534	**31,76%**	**29,84%**	0,61827484	**33,28%**	0,62754615	**34,97%**	0,63210606
1/4 MAC	0,593						**Nom.**	**VTOL**	**Min. Pay.**	**Max. Pay**	**Battery Pack**
delta cg	0,03216625		delta cg VTOL	**0,28%**	**29,84%**	**34,97%**	32,39%	31,76%	29,84%	33,28%	34,97%
	5,1%				**8,604**	**9,230**	9,030	9,030	8,630	9,230	8,604
					MIN	**MAX**					

Bibliography

1. KNIGHT, Ben. *A guide to military drones* [online]. DW, 2017. Available also from: https://www.dw.com/en/a-guide-to-military-drones/a-39441185.
2. SIYUAN CHENN, Debra Laefer; MANGINA, Eleni. State of Technology Review of Civilian UAVs. *Recent Patents on Engineering*. 2016, vol. 10, no. 999. ISSN 2078-2489. Available from DOI: 10.2174/1872212110666160712230039.
3. HOWARD, Brad. *Can U.S. drone makers compete with cheap, high-quality Chinese drones?* [Available at https://www.cnbc.com/2023/10/11/can-us-drone-makers-compete-with-cheap-high-quality-chinese-drones.html (2017/02/26)]. [N.d.].
4. CORP., DJi. *DJi Enterprise Drones* [online]. DJi Corp., 2024. Available also from: https://enterprise.dji.com/.
5. EASA. *EASA - Open Category* [Available at https://www.easa.europa.eu/en/domains/civil-drones-rpas/open-category-civil-drones (2024/01)]. [N.d.].
6. EASA. *EASA - Specific Category* [Available at https://www.easa.europa.eu/en/domains/civil-drones-rpas/specific-category-civil-drones (2024/01)]. [N.d.].
7. E KARATZAS1, V Kostopoulos1; LAPPAS2, V. Preliminary weight estimation of canister based light foldable wing electric propulsion UAV, as a platform for swarm applications. *Journal of Physics: Conference Series*. 2023, vol. 2526, no. -.
8. PARAKALA, Akshara. *Janes All the World's Aircraft Unmanned*. United Kingdom: Jane's Group Limited, 2022. ISBN 9780710633989.
9. FOXTECH. *Foxtech store* [online]. Foxtech corp., 2024. Available also from: https://www.foxtechfpv.com/.
10. ROBOTICS, Autel. *Autel Robotics Website* [online]. Autel Robotics, 2024. Available also from: https://www.autelrobotics.com/.

11. CUAV TECH INC., Ltd. *CUAV Website* [online]. CUAV Tech Inc.,Ltd, 2024. Available also from: https://www.cuav.net/.

12. T-DRONES. *T-DRONES Website* [online]. T-DRONES, 2024. Available also from: https://www.t-drones.com/.

13. ENGINEERING, Trillium. *Trillium Engineering Website* [online]. Trillium Engineering, 2024. Available also from: https://www.trilliumeng.com.

14. IMAGING, Terrestrial. *Terrestrial Imaging, Website* [online]. Terrestrial Imaging, 2024. Available also from: https://www.terrestrialimaging.com/.

15. INC, AgEagle Aerial Systems. *AgEagle Website* [online]. AgEagle Aerial Systems Inc, 2024. Available also from: https://ageagle.com/drone-sensors/.

16. AEROVIRONMENT, Inc. *AeroVironment* [online]. AeroVironment, Inc, 2024. Available also from: https://www.avinc.com/uas/puma-le.

17. INC, ADS. *ADSINC* [online]. ADS inc, 2024. Available also from: https://www.adsinc.com.

18. SYSTEMS, THREOD. *THREOD SYSTEMS Website* [online]. THREOD SYSTEMS, 2024. Available also from: https://threod.com/.

19. UAV, AVIATION DESIGN. *AVIATION DESIGN UAV Website* [online]. AVIATION DESIGN UAV, 2024. Available also from: https://aviation-design-uav.fr.

20. DRONEVOLT. *Dronevolt Website* [online]. Dronevolt, 2024. Available also from: https://www.dronevolt.com/en/expert-solutions/heliplane/.

21. MEASUR. *Measur Website* [online]. Measur, 2024. Available also from: https://drones.measurusa.com/products/trinity-pro.

22. KRUS, Petter; STAACK, Ingo. *Engineering Systems Design Lecture Notes.* Linköping: Linköping University, 2022.

23. WALTER, Jiří. *The Design of Air Propeller Test Bench.* 2020. České vysoké učení technické v Praze.

24. OR D. DANTSKER Marco Caccamo, Robert W. Deters; SELIG, Michael S. Performance Testing of APC Electric Fixed-Blade UAV Propellers. *AIAA AVIATION 2022 Forum.* 2022, no. 4020. ISBN 978-1-62410-635-4.

25. GOLI, Srikanth; KURTULUŞ, Dilek Funda; ALHEMS, Luai M.; MEMON, Azhar M.; IMRAN, Imil Hamda. Experimental study on efficient propulsion system for multicopter UAV design applications. *Results in Engineering.* 2023, vol. 20, p. 101555. ISSN 2590-1230. Available from DOI: https://doi.org/10.1016/j.rineng.2023.101555.

26. O., MODEL MOTORS S. R. *AXI MODEL MOTORS Website* [online]. MODEL MOTORS S. R. O., 2024. Available also from: `https://www.modelmotors.cz`.

27. TORENBEEK, Egbert. *Synthesis of Subsonic Airplane Design*. Rotterdam: Delft University Press, 1976. ISBN 9029825057.

28. DANĚK, Vladimír. *Mechanika Letu I - Letové výkony*. Brno: CERM, 2019. ISBN 978-80-7623-014-9.

29. RAYMER, D. *Aircraft design: A conceptual approach*. Reston, Va.: American Institute of Aeronautics and Astronautics, 2006. ISBN 1563478293.

30. AIRFOILTOOL.COM. *Airfoil Tools Databse* [online]. windandwet@yahoo.com, 2024. Available also from: `http://airfoiltools.com/search/airfoils`.

31. MARK DRELA, Harold Youngren. *XFOIL 6.9 User Primer* [online]. MIT.EDU, 2001. Available also from: `https://web.mit.edu/drela/Public/web/xfoil/xfoil_doc.txt`.

32. GUNDLACH, Jay. *Designing Unmanned Aircraft Systems: A Comprehensive Approach*. Blacksburg, Virginia: American Institute of Aeronautics and Astronautics, Inc., 2012. ISBN 978-1-60086-843-6.

33. ROSKAM, Jan. *Airplane Design Part VI: Preliminary Calculation of Aerodynamic, Thrust and Power Characteristics*. Lawrence, Kan.: DARcorporation, 1997. ISBN 9781884885525.

34. USA, SunnySky. *SunnySky Motors* [online]. Shopify, 2024. Available also from: `https://sunnyskyusa.com`.

35. CORP., T-MOTOR. *T-Motors Official Store* [online]. T-Motors, 2024. Available also from: `https://store.tmotor.com`.

36. ROSKAM, Jan. *Airplane Design Part V: Component Weight Estimation*. Lawrence, Kan.: DARcorporation, 1997. ISBN 9781884885501.

37. GERARD, W. H. Prediction of Sailplane Wing Weight for Preliminary Design, *Weight Engineering*. Spring 1998, vol. A98-37633, p. 9.

38. HOERNER, Sighard F. *Fluid Dynamic Drag*. Bakersfield: the Author, 1965.

C.1 Used Software

- Matlab 2024a
- xflr5 v6,54
- Latex - Overleaf
- Microsoft Excel

- Autodesk Fusion 360
- Catia V5
- Glauert III
- ChatGPT 3.5 (Matlab and Latex editing and debugging)

Concents of the attachment

```
readme.txt ........................................ contents
├── DP Szekely .................. Excel spreadsheet - most data
├── DP Szekely ............... Matlab mlx file - most calculations
├── CAD
│   ├── igs ........................... Concept Design Surfaces
│   ├── igs ....................... Preliminary Design Surfaces
│   ├── - ................................ Concept Design Model
│   └── - ............................ Preliminary Design Model
├── Thesis
│   ├── .zip ........... Zip file with all the source codes in LaTeX format
│   └── DP FME SZ.pdf ............................ thesis in PDF
└── Drawings
    └── 3-Views .... Concept Design and Preliminary Design 3-views in PDF
```